CAPITAL UNIVERSITY OF SCIENCE AND TECHNOLOGY, ISLAMABAD

Hybrid Synchronization Control of Dynamical Networks with Uncertain Parameters

by

Nazam Siddique

A thesis submitted in partial fulfillment for the degree of Doctor of Philosophy

in the

Faculty of Engineering
Department of Electrical Engineering

2021

Hybrid Synchronization Control of Dynamical Networks with Uncertain Parameters

By

Nazam Siddique

(PE-123003)

Dr. Hang-Fang Zhao, Professor

Zhejiang University, China

(Foreign Evaluator 1)

Dr. Muhammad Nasiruddin Mahyuddin, Associate Professor

University of Sains Malaysia, Malaysia

(Foreign Evaluator 2)

Supervisor Name

(Dr. Fazal ur Rehman)

Dr. Noor Muhammad Khan

(Head, Department of Electrical Engineering)

Dr. Imtiaz Ahmad Taj

(Dean, Faculty of Engineering)

DEPARTMENT OF ELECTRICAL ENGINEERING

CAPITAL UNIVERSITY OF SCIENCE AND TECHNOLOGY

ISLAMABAD

2021

Dedicated to my late father Muhammad Siddique Chughtai, my inspiration my mother, my wife, My brother Asjad Javaid Chughtai, cute daughter Manhal Fatima, my sons Abdullah and Abdul Moeed.

CAPITAL UNIVERSITY OF SCIENCE & TECHNOLOGY ISLAMABAD

Expressway, Kahuta Road, Zone-V, Islamabad
Phone:+92-51-111-555-666 Fax: +92-51-4486705
Email: info@cust.edu.pk Website: https://www.cust.edu.pk

CERTIFICATE OF APPROVAL

This is to certify that the research work presented in the thesis, entitled "**Hybrid Synchronization Control of Dynamical Networks with Uncertain Parameters**" was conducted under the supervision of **Dr. Fazal ur Rehman**. No part of this thesis has been submitted anywhere else for any other degree. This thesis is submitted to the **Department of Electrical Engineering, Capital University of Science and Technology** in partial fulfillment of the requirements for the degree of Doctor in Philosophy in the field of **Electrical Engineering.** The open defence of the thesis was conducted on **June 22, 2021.**

Student Name : Nazam Siddique (PE-123003)

The Examination Committee unanimously agrees to award PhD degree in the mentioned field.

Examination Committee :

(a) External Examiner 1: Dr. Nisar Ahmed
Professor
GIKI, Topi, Swabi, KPK

(b) External Examiner 2: Dr. Suheel Abdullah Malik
Associate Professor
IIU, Islamabad

(c) Internal Examiner : Dr. Aamer Iqbal Bhatti
Professor
CUST, Islamabad

Supervisor Name : Dr. Fazal ur Rehman
Professor
CUST, Islamabad

Name of HoD : Dr. Noor Muhammad Khan
Professor
CUST, Islamabad

Name of Dean : Dr. Imtiaz Ahmad Taj
Professor
CUST, Islamabad

AUTHOR'S DECLARATION

I, **Nazam Siddique (Registration No. PE-123003)**, hereby state that my PhD thesis titled, "**Hybrid Synchronization Control of Dynamical Networks with Uncertain Parameters**" is my own work and has not been submitted previously by me for taking any degree from Capital University of Science and Technology, Islamabad or anywhere else in the country/ world.

At any time, if my statement is found to be incorrect even after my graduation, the University has the right to withdraw my PhD Degree.

(**Nazam Siddique**)

Dated: June, 2021

Registration No : PE-123003

PLAGIARISM UNDERTAKING

I solemnly declare that research work presented in the thesis titled "**Hybrid Synchronization Control of Dynamical Networks with Uncertain Parameters**" is solely my research work with no significant contribution from any other person. Small contribution/ help wherever taken has been duly acknowledged and that complete thesis has been written by me.

I understand the zero tolerance policy of the HEC and Capital University of Science and Technology towards plagiarism. Therefore, I as an author of the above titled thesis declare that no portion of my thesis has been plagiarized and any material used as reference is properly referred/ cited.

I undertake that if I am found guilty of any formal plagiarism in the above titled thesis even after award of PhD Degree, the University reserves the right to withdraw/ revoke my PhD degree and that HEC and the University have the right to publish my name on the HEC/ University Website on which names of students are placed who submitted plagiarized thesis.

(**Nazam Siddique**)

Dated: June, 2021

Registration No : PE-123003

List of Publications

It is certified that following publication(s) have been made out of the research work that has been carried out for this thesis:-

1. **Nazam Siddique** and Fazal ur Rehman. "Parameter Identification and Hybrid Synchronization in An Array of Coupled Chaotic Systems with Ring Connection: An Adaptive Integral Sliding Mode Approach." Mathematical Problems in Engineering, pp. 1-15, 2018.

2. **Nazam Siddique** and Fazal ur Rehman. "Hybrid Synchronization and Parameter Estimation of Complex Chaotic Network of Permanent Magnet Synchronous Motors using Adaptive Integral Sliding Mode Control.", Bulletin of the Polish Academy of Sciences, vol. 69(3), pp. 1-9, 2021.

(Nazam Siddique)

Registration No: PE-123003

Acknowledgement

In the name of Allah, The Most Gracious, The Most Beneficent. All praise is due to Allah alone, Who granted me the opportunity and abilities to pursue my post-graduate research and study. All respect is due to the Holy Prophet Muhammad (P.B.U.H), the last messenger of Allah, whose whole life is the perfect model for all human beings and Whose teachings are the source of guidance in all disciplines of practical life.

I am especially indebted to my research adviser, Dr. Fazal ur Rehman, for his valuable counselling, strong encouragement and kind support towards my research and study. His strong mathematical background, clear concepts of systems and control theory have always been the foremost sources of motivation and inspiration for my research. In fact, pursuing research in control systems would not have been realized without Dr. Rehman's continued motivation, guidance, and advice. I would like to thank all the teachers of Electrical Engineering Department at CUST, with special mention of Dr. Aamer Iqbal Bhatti, Dr. Raza Samar, Dr Muhammad Ashraf and Dr Muhammad Sajjad for imparting up-to-date and state-of-the-art knowledge, with devotion and sincerity, to all who come to CUST to seek education and carry out research.

Special thanks are due to Dr. Muhammad Mansoor Ahmad whose clear vision, great leadership, and endless efforts made CUST an excellent center for postgraduate research and study in the country.

Many thanks go to my research colleagues Dr. Ibrahim Shah Dr. Waseem Abbasi, Dr. Muhammad Sarfraz and Sami Uddin for technical discussion, encouraging remarks and fruitful suggestions. Sincere gratitude is due to Usama and Umair of FPGA and Microelectronics Lab for their sincere advice and uttermost assistance.

Most special and profound thanks go to Mian Najeeb Ullah Wilana, who motivated me to go for higher education and to play my positive role in the development of the society. I think without his continuous counseling and guidance it would be quite difficult for me to be on the track of Higher education.

Above all, I am highly grateful to my lovely family, especially my wife, for their encouragement, for letting me ignore the many beautiful moments of life enjoying with them and for letting me ignore them when they needed me to be with them at many many occasions during all this process of long research.

(Nazam Siddique)

Abstract

Hybrid synchronization control of dynamical networks with uncertain parameters has increasing importance for the last two decades. A key motivation for this research comes from the fact that chaotic systems pose challenging circumstances for control design engineers. Chaotic systems are very sensitive to their initial conditions, a slight perturbation in the initial conditions leads to a very significant variation in the steady-state response of these systems. The hybrid synchronization of these kinds of systems in an interconnected network is of significant interest from a control point of view.

In this thesis, the hybrid synchronization control problem of the dynamical networks in the presence of uncertain parameters is investigated using adaptive integral sliding mode control (ISMC) and smooth super twisting algorithm (SSTA). To apply the adaptive ISMC, the error system is transformed into a special arrangement comprising of a nominal portion and a few unknown items. The unknown items are gauged adaptively. The error system is stabilized using ISMC. The designed controller for the error system comprises of both the nominal and compensatory control. Lyapunov stability theorem is employed to derive the adapted laws and compensator controllers.

The first part of the thesis deals with the hybrid synchronization control of a dynamical network of non-identical and identical chaotic systems connected in the ring topology by assuming the unknown parameters. The proposed control algorithm is employed onto a network of three different chaotic systems and then it is applied to a dynamical network of four identical dynamical systems. In the second part of this thesis, hybrid synchronization control is investigated for the dynamical network of complex chaotic systems connected in a ring topology. The proposed control algorithm is employed onto complex chaotic permanent magnet synchronous motors. In the last part of this thesis, Hybrid synchronization control is investigated for neural networks by assuming the uncertain parameters. The proposed control algorithm is applied to a 3-cell cellular neural network.

This dissertation primarily focuses on the design and application of adaptive ISMC and SSTA to investigate hybrid synchronization of dynamical networks of chaotic systems in the presence of unknown parameters. For this purpose, control laws are formulated using Lyapunov stability analysis. In all the cases, errors dynamics are converging to zero. The convergence of error dynamics to zero yields the convergence of systems states i.e the states of all the chaotic systems connected in the network are synchronized for synchronization scenario and are anti-synchronized for the anti-synchronization scenario. Moreover, the uncertain parameters are converging to their true values. Numerical simulations results support the validation of the proposed control algorithms.

Contents

List of Figures

Abbreviations

APS	Anti phase synchronization
AS	Anti-synchronization
CNN	Cellular Nonlinear network
CS	Complete synchronization
DN	Dynamical network
FPS	Function projective synchronization
GS	Generalized Synchronization
HS	Hybrid synchronization
ISMC	Integral sliding mode control
LE	Lyapunov exponent
PMSM	Permanent magnet synchronous motor
PS	Phase synchronization
SMC	Sliding mode control
SOSMC	Second order sliding mode control
SS	Sliding Surface
SSTA	Smooth super twisting algorithm

Symbols

a, b, c, d, e	constant parameters
D_o	diagonal matrix
e_r,	error system
$f(x), F(x), \digamma(x)$	functions of system states
g	order of unknown parametrs
k, κ	constant coefficients
M, N	order of the system states
t	time
v	compensator term
V	Lyapunov function
x, y	system states
z	integral term
μ	control term
σ	Sliding surface
θ, Θ	constant parameters vector representations

Chapter 1

Introduction

In this chapter, an introduction of the research work carried out in this dissertation is described. After discussing the background, motivation for this work is developed. The research problem and objectives are clearly defined and then the novel contribution of this dissertation is presented. Finally, a brief overview of this dissertation is presented.

1.1 Background and Motivation

The Newtonian philosophy states that the future can be determined by the present state of the universe. The belief in Newtons philosophy is stated by Laplace: We ought to regard the present state of the universe as the effect of the past and the cause of the future. This opinion is supported by Newton's state of the art equations of motion, which claims that initial conditions play a major role in finding the solutions for future and past.

The works presented by Birkhoff [1, 2], Poincare [3], Smalle and others, have stated that many beliefs on natural phenomena are erroneous. The analysis of the equations of motions presented by Newton predicts the future behavior of dynamical systems. There are several natural systems which exhibit a strong dependency on their initial conditions; orbits of typical points in close proximity go far away

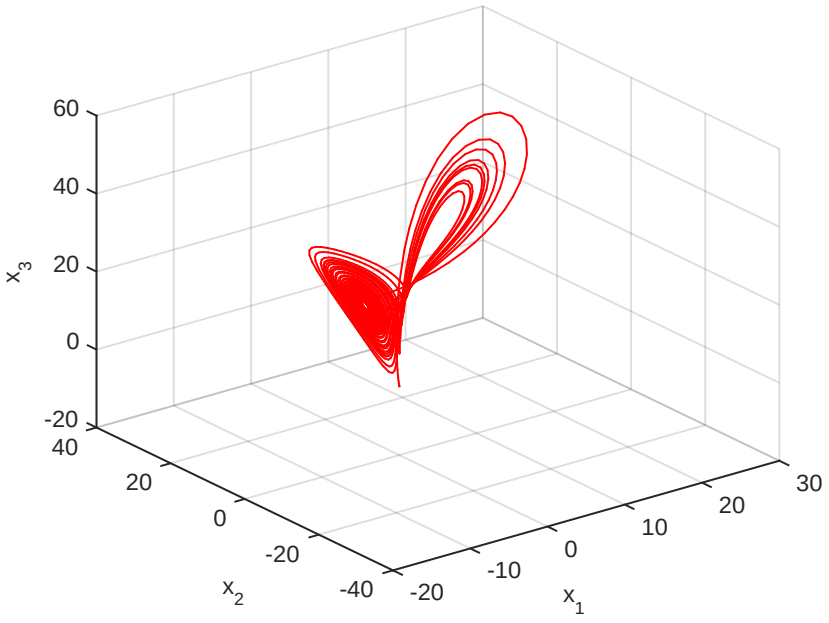

FIGURE 1.1: Phase portrait of Lorenz attractor

under the influence of system dynamics. Consequently, future dynamics cannot be predicted for a large time span. Such dynamical aggression characterizes deterministic chaos. Chaotic phenomena have been widely investigated in numerous fields of physical sciences [4, 5], economy [6], ecology [7] and applied engineering [8]. A non-linear system is chaotic if it comprises of following characteristics: boundedness, infinite recurrence and sensitive dependency on initial conditions [9]. As an example, a Lorenz chaotic attractor on phase portrait is depicted in Fig.1.1. Chaotic systems are different as compared to uncertain systems. Uncertain systems mean the systems with uncertain parameters. A dynamic system is said to be uncertain if there are some external disturbances being occured due to noise and other undesirable circumstances which are making the parameters of the system uncertain.

In practice, all physical systems are naturally considered as nonlinear systems. To get a better concept of non-linear system behaviors, it is important to analyze synchronization between two non-linear systems. Synchronization is a natural phenomenon which appears in almost every field of science, social science and

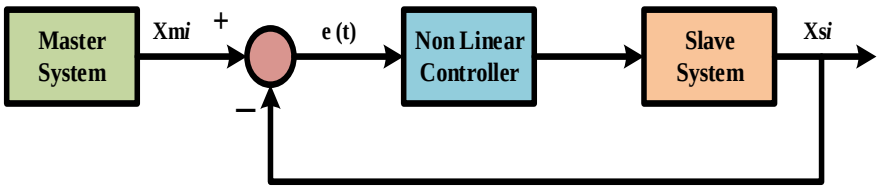

FIGURE 1.2: Block diagram representation of synchronization concept

engineering. In this phenomenon, the dynamic states of one system converges to the dynamic states of the other systems. In this process, one is acting as master and the other is acting slave. Figure 1.2 shows a basic block diagram of Master/Slave type synchronization and Fig 1.3 shows the state-level concept of synchronization.

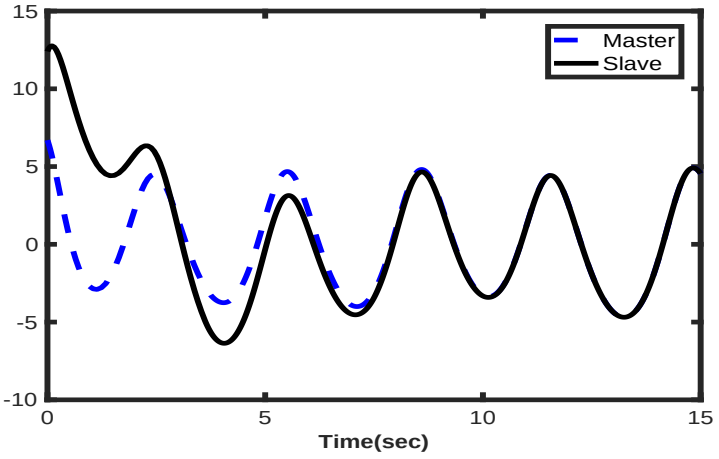

FIGURE 1.3: Synchronization between master and slave systems

Fujisaka and Yamada [10], presented, for the first time, the concept of synchronization amongst the coupled systems. Subsequently, some artistic works were presented by Pecora and Carrol [11] on synchronization between coupled chaotic systems. As time passed on, the interest in analyzing the synchronization phenomena amongst coupled chaotic systems keep rising exponentially. Currently, the concern is complete synchronization (CS), where the state variables of the individual system converge towards each other. As for as the difficulty level is concerned CS is difficult than phase synchronization (PS) [12]. In nature, however, some

interacting dynamic systems form small and large networks in a typical coupling topology e.g. neural networks. Astonishingly, although chaotic systems own exponential divergent characteristics of close by trajectories, they observe synchronization [11, 13]. The synchronization phenomena between interacting systems are relatively frequent phenomena being found in many branches of science [14–16], neuroscience [17, 18], and lasers [19, 20].

Since the artistic work of Poincare [21] on the three-body problem, the study of non-linear phenomena has attracted several researchers of many fields, that made the non-linear dynamics a subject of values. The valuable efforts made in this field provided a new angle to the control engineers, the recent interests are analyzing and designing new control laws for dynamical networks. The invention of such electronic circuits which shows chaotic behavior set up the new standards for non-linear dynamics to tackle with. The works of Chua et.al [22] and Pecora et.al [23] opened new dimensions to the chaos. It not only gives brand new behavior for signal processing but also new processing engines that can be within sizable systems. For the processing of unique patterns from arrays with defined connections between cells, cellular neural networks have become a standard for complexity. Currently, the CNNs engines are designed on the CNN-universal machine architecture are serving as visual processing machines. this have empowered real-time employment like unmanned aerial vehicles, video-based vigilance etc. In addition, CNNs furnishes the sufficient capability of analysis and design due to its complex dynamics. Artificial neural networks exhibit chaos [24, 25], that is why, synchronization of chaotic neural networks have achieved significant importance in the previous decade [26, 27].

Several unique synchronization techniques for chaotic systems were reported [28–32]. Among these schemes, hybrid synchronization (HS) [33, 34] is currently a topic of interest in which synchronized and anti-synchronized appears together. Due to its practical importance, HS has been the subject of many research works. Among these works: study of synchronization/anti synchronization of PMSMs coupled in ring topology [33], function projective synchronization [35], complete synchronization (CS) [36], and many other works reported in literature [34, 37]. Study of HS

which involves multiple chaotic systems like complete, adaptive, global, projective and anti-synchronization (AS) [38, 39], and synchronization in multiple coupled complex networks [40, 41]. Currently, hybrid synchronization (HS) of several coupled chaotic systems is an interesting area of research [42, 43].

All the techniques mentioned above are mainly designed for synchronization of two or more complex systems, where usually one is drive system, as well as the other, is respond system. The purpose of these kinds of techniques is that the dynamic states of one system follow the trajectories of the other system. Instead of using the simple techniques, the synchronization technique for multiple coupled complex chaotic systems can better improve the protection of message signal in secure communication and also has a bright future in the communication field. Consequently, many researchers are attracted and are spending their efforts to analyze multiple coupled systems.

The motivation of this thesis is to investigate hybrid synchronization (HS) control of dynamical networks with coupled nodes and uncertain parameters. Three different kinds of networks are selected as test cases, the dynamical network of non-identical and identical coupled chaotic systems, a dynamical network of complex chaotic systems and the dynamical cellular nonlinear network. The design of control laws for these kinds of networks is a challenging task in the presence of uncertain parameters.

1.2 Problem Statement

Hybrid synchronization (HS) has increasing theoretical and practical importance in the field of engineering and science especially in secure communication and crypto-systems. Co-existence of synchronization and anti-synchronization (AS) makes it a difficult job for the control design engineers to design a single controller to control HS amongst several coupled chaotic systems forming a complex network. Plenty of research has been carried out to investigate HS in chaotic systems but less work is done for chaotic systems connected in a network. Up till now, several

control algorithms are tested to investigate HS in a dynamical network of chaotic systems. Some of them were system-oriented and not generalized and some of them investigated HS with some error bound. To our best knowledge hybrid synchronization (HS) control problem is still open and needs maturity particularly for the ring connected network[33, 44].

1.3 Research Objectives

The core research objective of this work is to investigate, by applying adaptive ISMC theory and smooth twisting algorithm, a comprehensive and robust control design framework for hybrid synchronization (HS) control of dynamical networks. Moreover, in the existence of uncertain parameters and co-existence of synchronization and anti-synchronization (AS) the controller design will be a much more difficult job. The proposed control framework is generalized and applicable to all identical and non-identical chaotic systems coupled in a dynamical network. Finally, the proposed methodology is applied to the following benchmark dynamical networks:

- Dynamical network of non-identical and identical chaotic systems.
- Dynamical network of complex chaotic systems.
- Dynamical network of 3-cell cellular nonlinear network.

1.4 Research Contributions

The core contributions of this dissertation are as follows:
i) A novel hybrid synchronization (HS) control scheme for dynamical networks of non-identical and identical chaotic systems, based on adaptive ISMC, is provided in this dissertation. This synchronization control scheme is advantageous

compared to conventional active control scheme used to achieve hybrid synchronization (HS). This control technique is robust against the parameter uncertainties and is easy to implement [45].

ii) A novel hybrid synchronization (HS) control scheme for a dynamical network of complex natured, chaotic, PMSM systems coupled in the ring topology, based on adaptive ISMC, is provided in this thesis. The application of ISMC for hybrid synchronization (HS) of the complex chaotic network of PMSM systems with uncertain parameters is proposed for the first time up to our best knowledge [46].

iii) A novel Hybrid synchronization (HS) control scheme for a 3-cell cellular nonlinear network using master/slave type environment, using the SSTA, is provided in this thesis. The application of SSTA for achieving hybrid synchronization in CNNs with uncertain parameters is considered for the first time up to our best knowledge.

1.5 Research Scope

In pursuance of the research carried out in this thesis following assumptions are made:

- It is assumed that there are no delays in synchronization between the systems coupled in the dynamical network.
- It is also assumed that the coupling between the systems is constant.

1.6 Organization of Dissertation

This thesis comprises of seven chapters. The major focus of this thesis is to give novel solutions to the HS control problem of dynamical networks. in order to organize a self-descriptive text on HS of dynamical networks, the nonlinear feedback control method is being reviewed to highlight the significance of HS

control problem in the presence of uncertain parameters. Finally, the framework is presented in a detailed fashion and numerical results are being examined.

The chapter-wise description is given below:

- **Chapter 2, Literature Survey:** This chapter presents a comprehensive study about the synchronization and hybrid synchronization (HS) control of DNs. The chapter summarized the findings of limitations and research contributions of various synchronization methods. The research gap in the literature helped to formulate the problem statement and finding the solution for hybrid synchronization (HS) control problem of DNs.

- **Chapter 3, Preliminaries:** In this chapter some preliminaries are presented to understand the hybrid synchronization (HS) control of DNs. This chapter presents the base for Chapter 4, Chapter 5 and Chapter 6.

- **Chapter 4, Hybrid Synchronization (HS) in a Dynamical Network of Non-identical and Identical Chaotic Systems:** In this chapter adaptive ISMC is proposed to investigate hybrid synchronization (HS) of DNs in the existence of uncertain parameters. in the first part of this chapter, a dynamical ring type network of nonidentical chaotic systems is considered. In the second part, a DN of identical chaotic systems is examined. The simulation results given in the end of this chapter justifies the validity of the proposed solution.

- **Chapter 5, Hybrid Synchronization (HS) in a Dynamical Network of Complex Chaotic PMSM Systems:** In this chapter adaptive ISMC is proposed to examine the hybrid synchronization (HS) control problem in a DN of complex chaotic PMSM systems. The simulation results given in the end, justifies the validity of the proposed solution.

- **Chapter 6, Hybrid synchronization (HS) in a 3-cell cellular nonlinear network:** In this chapter SSTA which is a variant of SOSM control is

proposed to investigate the hybrid synchronization control problem for cellular nonlinear networks. Finallyafafaza, simulation results are given, which validates the effectiveness of the proposed methodology.

- **Chapter 7, Conclusion and Future Work:** This chapter summarizes the overall thesis and draws conclusions along with the recommendations and claims. The importance of the proposed research is emphasized. Future directions have also been proposed for further research.

1.7 Summary

This chapter presents the motivation and background of this research. On the basis of overview and motivation from the existing literature, problem statement and research goals are defined. The research contributions based on the objectives are presented and finally, the organization of the thesis is discussed.

Chapter 2

Literature Review

2.1 Introduction

Synchronization emerges in coupled chaotic systems and can be stable if the coupling strength is above a threshold value. There are many synchronization types reported in the literature for different coupling thresholds. For large coupling strengths, complete synchronization and anti-synchronization regimes are suggested, where the phase as well as amplitudes of states of the coupled systems become identical and opposite respectively as $t \to \infty$. Both these kinds of synchronization are possible for identical dynamic systems. For non-identical dynamic systems which commonly appears in nature, other types of synchronization are investigated e.g. Lag synchronization, phase synchronization, generalized synchronization. Following is a brief description of these synchronization schemes.

2.2 Synchronization

In the mid of 17th century investigation of synchronization between dynamic systems was started when Christiaan Huygens firstly revealed that two similar pendulums hanging over a single rod synchronized either in-phase or anti-phase [47].

A couple of similar kind of cases reported in the literature, for example: properties of arrangement of organ pipes [48] and twinkling of glowworms in conjunction [49]. Several paradigms of synchronization reported like: cardio-respiratory synchronization [50], crowd synchronization [51, 52], and bacterial quorum sensing [53]. From the last couple of decades, chaos synchronization has grasp significant attention. As described earlier a chaotic system is sensitive to its initial conditions,i.e. two similar chaotic systems starting from two nearby initial conditions produce dissimilar response. Due to this property it was generally considered that two similar kind of chaotic systems can not be synchronized. Ultimately, Fujisaka and Yamada [13] revealed that two chaotic systems can be synchronized after that some artistic work presented by Pecora and Carroll [11].

As an elementary definition of synchronization of chaos, it is seen as a procedure in which two or more chaotic systems adopt a motion to develop a common attitude because of coupling or forcing [54, 55]. Interestingly, for identical systems, the coupled systems maintain their isolated dynamics once the synchronization is established after the initial transients.

The synchronization has been investigated in different field of science, physics, chemistry and biology and engineering. In the field of physics, synchronization can be found in electronic circuit [56], laser [57], and plasma [58]. In the field of chemistry, there are examples of chemical reactions [59] where many coherent patterns were observed. Many synchronization phenomena were also reported in chemical [60] and electrochemical systems [61]. In biology, the list of examples is too long, but prominent works are the issues related to cardio-respiratory interaction [62] and brain function [63] where the process of synchronization plays key role in useful functional behaviors. In spreading of epidemics [64] and ecological systems too [65], synchrony is present: different species show synchrony [66]. Synchronization is thus ubiquitous in nature.

Two or many dynamical systems can interact through coupling in two significant ways, either unidirectional or bidirectional. In case of unidirectional coupling, a drive-response (or master-slave) configuration is realized [67]. In Master-Slave

configuration, one which moves freely is called master system and the other which follows the trajectory of Master is called slave system. In simple words the master system drives the slave system. This master-slave configuration of the interacting dynamical systems is a potential candidate for secure communications and showed promising results [68].

On the other hand, the bidirectional coupling presents a different scenario, here the interacting systems mutually influence each other. The coupling parameter convinces their rhythms onto a common synchronization behavior; the interacting systems come into a state of synchronization or develop a common rhythm.

There are several types of synchronization reported in the last two decades, namely, complete synchronization (CS) [11], phase synchronization (PS) [68, 69], anti-synchronization (AS) [67, 70, 71], antiphase synchronization (APS) [70, 72], lag synchronization (LS) [73], generalized synchronization (GS) [74, 75] and mixed synchronization [70].

In recent years, several different other forms of coupling were also considered in studies of synchronization, instantaneous or delay coupling [55], synaptic coupling [76]. The information exchange may happen between the interacting systems either instantaneously or delayed in time. In all the cases, of course, the unidirectional or bidirectional concept is considered. In most of these cases, a scalar type coupling suffices the condition of stable synchronization when the coupling is made through one or a few of the state variables. Sometimes, the interacting systems interact via all the state variables which are known as vector coupling and it is necessary for the stability of synchronization in particular cases. On the other hand, the synaptic coupling is relevant in the context of neuronal systems [77]. The synaptic coupling is a special type of coupling form [78]. However, the gap junction type coupling [79] in case of neuron is diffusive linear type. This coupling form is not utilized in the thesis.

In contrary to studies using diffusive coupling or synaptic coupling where the coupling form is known a priori, an alternative approach of designing coupling is given importance to realize a targeted synchronization [80] or desired coherent

pattern [81] where the coupling is assumed unknown a priori. It is designed for a given dynamical system and a desired synchronization state to realize between the oscillators based on selected stability criteria.

Time has significant importance and plays a vital role as for as physical systems are concerned. Since the physical systems are dynamic so their peculiar movement changes with time. Even there are a lot physical systems which need a rigorous timing between oscillators for actual working. Synchronization is such a phenomenon in which a precise timing is given between two oscillators [11, 13, 54, 82, 83]. There are a lot of synchronization types which depend on the nature and coupling properties between the oscillators. Let x_1 and x_2 be the two oscillators, If these are appropriately coupled then it is possible to attain CS i.e. both behaves similarly:

$$\lim_{t\to\infty} ||\chi_1 - \chi_2|| = 0 \tag{2.1}$$

Generally, CS is meant for identical oscillators. If, however, they present a mismatch parameter the states can be close $\chi_1 \approx \chi_2$, but not equal.

2.3 Types of Synchronization

2.3.1 Complete Synchronization (CS)

The CS is more artificial since it is true for identical systems only, which is actually not a practical assumption. However, using the idealistic case, complete synchronization is investigated in computer simulations as well as verified in experimental setup for closely similar systems. The interacting dynamical systems become almost identical even if they start from any initial point for the coupling strength greater than some critical value. The complete synchronization was first investigated in [13, 84]. Pecora and Carrol investigated synchronization in an experimental set up where a chaotic oscillator, which was considered to be the drive system, was coupled unidirectionally to its subsystem. The signature of CS

was recognized by the presence of negative lyapunov exponents [82, 85] of the subsystem.

2.3.2 Anti Synchronization (AS)

In the 17th century, Huygens for the first time investigated anti synchronization between pendulums hanging on a single beam [47, 86]. He reported that two identical pendulums hanged on a single beam oscillate with same frequency but having 180 degree phase shift. Recently, the phenomenon of complete synchronization and anti synchronization between two coupled pendulums was investigated in [87]. Anti synchronization appears frequently in nature just like complete synchronization but APS is much likely to be occur in nature [88]. In APS the phases of coupled oscillators are 180 degree out of phase but their amplitudes are totally uncorrelated. The anti synchronization can be defined as: $\lim t \to \infty ||\omega(t) + \chi(t)|| = 0$: where $\omega(t)$ and $\chi(t)$ are two possible states of chaotic systems. Anti synchronization is normally observed in van der pol system with cubic nonlinearity under the diffusive coupling [89].

2.3.3 Phase Synchronization (PS)

Rosenblum et. al. [68, 73] was the pioneer who reported the phase synchronization (PS) among dynamical systems for the first time. PS is generally similar to phase lock loop in periodic oscillators. Phase synchronization (PS) means that the phases of the two connected chaotic systems are locked and is normally observed in non-identical systems for weak coupling strength. In [68], phase is considered to be a fickle which corresponds to the zero LE of a system that has chaotic response. Estimation of phase is discussed in detail for chaotic systems in [90–92]. Phase synchronization is observed in several laboratory results and natural phenomena like electrically connected neurons also in networks of complex systems connected to each other in ring topology. Phase synchronization in electronic circuits is discussed in [93–95].

2.3.4 Generalized Synchronization (GS)

The generalized synchronization can be defined like this: $\omega(t) = \Xi[\chi(t)]$ where $\chi(\chi \in C^n)$ is dynamic variable of driving system, $\omega(\omega \in B^n)$ is the dynamic variable of respond system and Ξ is transformation. If the trajectories in C transforms to the trajectories in B space through the transformation function Ξ, then it is possible to say that both variables χ and ω are synchronized. The transformation may be of complex nature but it develops a functional relation between both variables which is called generalized synchronization [96, 97]. When this transformation function is set equal to unity function then the synchronization amongst the master and slave system is called complete synchronization. GS has very vast applications in electronic circuits, communication etc [75, 98].

2.3.5 Lag Synchronization

Lag synchronization happens in weak coupling strength. Lag synchronization can be defined as $\omega(t) = \chi(t - \tau)$ where both variables χ and ω are almost similar but are shifted in time. There is another particular case of lag synchronization called anticipatory synchronization $\lim t \to \infty ||\omega(t) - \chi(t + \tau)|| = 0$ in which the responding system forecast the trajectory of driving system. In both the lag synchronization and anticipatory synchronization the delaying factor τ is assumed to be positive $\tau > 0$. The anticipation time can be maximized by connecting the chaotic systems in a ring topology or array [91, 99, 100].

2.3.6 Projective Synchronization

In projective synchronization [101–104], the master and slave chaotic systems are synchronized under the influence of a constant scaling term. The projective synchronization is defined as:

$$\begin{aligned} \dot{\chi} &= F(\chi) \\ \dot{\omega} &= g(\omega) + \mu(\chi, \omega) \end{aligned} \tag{2.2}$$

Where $\chi \in R^n$ are the dynamic states of the master system and $\omega \in R^n$ are the dynamic states of slave system, $F \in R^n$, $g \in R^n$ are differentiable functions and $\mu(\chi, \omega)$ represents the input control term. The synchronization error is described as:

$$\epsilon = \chi - \alpha\omega \tag{2.3}$$

Where α is a constant scaling factor up to which the synchronization yields.

2.3.7 Function Projective Synchronization

Function projective synchronization (FPS) [105–108] is slightly different than the projective synchronization. In FPS, instead of constant scaling factor, synchronization occurs for a time dependent scaling function $\alpha(t)$. The FPS is defined as:

$$\begin{aligned} \dot{\chi} &= F(\chi) \\ \dot{\omega} &= g(\omega) + \mu(\chi, \omega) \end{aligned} \tag{2.4}$$

Where $\chi \in R^n$ are the dynamic states of master system and $\omega \in R^n$ are the dynamic states of the slave system, $F \in R^n$, $g \in R^n$ are differentiable functions and $\mu(\chi, \omega)$ represents input control term. The synchronization error for FPS is described as: $\epsilon = \chi - \alpha(t)\omega$, where $\alpha(t)$ is a scaling function up to which the synchronization yields.

2.3.8 Hybrid Synchronization (HS)

The HS for chaotic systems [45, 101, 109–115] coupled in a network is defined as:

$$\begin{aligned} \dot{x_1} &= f_1(x_1) + F_1(x_1)\theta_1 + D_1(x_M - x_1) \\ \dot{x_2} &= f_2(x_2) + F_2(x_2)\theta_2 + D_2(x_1 - x_2) + \mu_1 \\ &\vdots \\ \dot{x_M} &= f_M(x_M) + F_M(x_M)\theta_M + D_M(x_{M-1} - x_M) + \mu_{M-1} \end{aligned} \tag{2.5}$$

Definition: For system Eqn.(2.5), it is defined that it exhibits hybrid synchronization if controllers $u_o, o = 1, 2, 3, 4, ...M-1$ exist such that all trajectories $x_1(t), x_2(t), \cdots, x_M(t)$ for initial conditions $x_1(0), x_2(0), \cdots, x_M(0)$ satisfy:
(1) For the AS errors $e_{ro} = (e_{ro1}, e_{ro2}, ..., e_{rom})^T, o = 1, 2, 3, 4, ...,$
$M-1$, yields:

$$\lim_{t\to\infty} ||e_{ro}|| = \lim_{t\to\infty} ||x_o(t) + x_{o+1}(t)|| = 0, o = 1, 2, 3, 4, ..., M-1 \tag{2.6}$$

(2) For Synchronization the error $e_{rp} = (e_{rp1}, e_{rp2}, ..., e_{rpm})^T$ and $e_{rq} = (e_{rq1}, e_{rq2}, ...,$ $e_{rqm})^T$ if $M(M \geqslant 3)$ is odd, then e_{rp} and e_{rq} satisfy:

$$\begin{aligned} \lim_{t\to\infty} ||e_{rp}|| &= \lim_{t\to\infty} ||x_{p+2}(t) - x_p(t)|| = 0, p = 1, 3, 5, 7, 9, ..., M-2 \\ \lim_{t\to\infty} ||e_{rq}|| &= \lim_{t\to\infty} ||x_{q+2}(t) - x_q(t)|| = 0, q = 2, 4, 6, 8, 10, ..., M-3 \end{aligned} \tag{2.7}$$

and if $M(M \geqslant 4)$ is even, the e_{rp}, e_{rq} satisfy:

$$\begin{aligned} \lim_{t\to\infty} ||e_{rp}|| &= \lim_{t\to\infty} ||x_{p+2}(t) - x_p(t)|| = 0, p = 1, 3, 5, 7, 9, ..., M-3 \\ \lim_{t\to\infty} ||e_{rq}|| &= \lim_{t\to\infty} ||x_{q+2}(t) - x_q(t)|| = 0, q = 2, 4, 6, 8, 10, ..., M-2 \end{aligned} \tag{2.8}$$

it is clear from Eqns.(2.6) - (2.8) that e_{ro}, e_{rp}, e_{rq} are globally and asymptotically stable. So, to achieve HS, the controllers must be designed in such a way that it make e_{ro}, e_{rp}, e_{rq} converge to zero.

2.3.9 Mixed Synchronization

This is a very interesting scheme of synchronization. In this scheme a couple of states in a dynamical system are synchronized and the other couple of states are AS in the coupling mode. For Lorenz systems, this type of synchronization for scalar coupling is investigated in [67, 71]. Mixed synchronization is investigated through many control techniques, like, Layapunov stability theory [116], nonlinear feedback control method [117], pinning control [118] etc. Mixed synchronization is also studied in hyper chaotic [119] systems and complex networks [120].

2.4 Control Techniques

Several control techniques are investigated in the literature. In this section, some of the mostly widely used control techniques are discussed.

2.4.1 Active Control Technique

In active control technique [121, 122] the synchronization amongst the master and slave chaotic systems is possible to attain by simply designing the control terms directly for the error systems. As an example the active control method is employed for synchronization in master-slave configuration between two Lorenz chaotic systems [123], the master system is defined as:

$$\begin{aligned} \dot{\chi_1} &= \sigma(\omega_1 - \chi_1) \\ \dot{\omega_1} &= r\chi_1 - \omega_1 - \chi_1\zeta_1 \\ \dot{\zeta_1} &= \chi_1\omega_1 - b\zeta_1 \end{aligned} \tag{2.9}$$

and the slave system is defined as:

$$\begin{aligned} \dot{\chi_2} &= \sigma(\omega_2 - \chi_2) + u_a \\ \dot{\omega_2} &= r\chi_2 - \omega_2 - \chi_2\zeta_2 + u_b \\ \dot{\zeta_2} &= \chi_2\omega_2 - b\zeta_2 + u_c \end{aligned} \tag{2.10}$$

where u_a, u_b, u_c are control inputs. Subtracting the Eqn. (2.8) from Eqn. (2.9) following error dynamical system yields:

$$\begin{aligned} \dot{\chi_3} &= \sigma(\omega_3 - \chi_3) + u_a \\ \dot{\omega_3} &= r\chi_3 - \omega_3 - \chi_2\zeta_2 + \chi_1\zeta_1 + u_b \\ \dot{\zeta_3} &= \chi_2\omega_2 - \chi_1\omega_1 - b\zeta_3 + u_c \end{aligned} \tag{2.11}$$

Now the only job is to design u_a, u_b, u_c to converge the error dynamics to zero. The active control technique [124–127] is widely used in the master/slave environment and is very effective.

2.4.2 Direct Design Method

Chen et al. [44] presented the direct control method to get the hybrid synchronization of multiple chaotic systems connected in an array. This method of controlling synchronization has some advantages like (i) this provides a very simple and easy procedure for designing the controllers to get synchronization (ii) the implementation of controllers is very easy. The proposed problem of hybrid synchronization reads as:

$$\begin{aligned} \dot{x_1} &= \beta_1 x_1 + \Phi_1(x_1)\theta_1 + A_1(x_M - x_1) \\ \dot{x_2} &= \beta_2 x_2 + \Phi_2(x_2)\theta_2 + A_2(x_1 - x_2) + u_1 \\ &\vdots \\ \dot{x_M} &= \beta_M x_M + \Phi_M(x_M)\theta_M + A_M(x_{M-1} - x_M) + u_{M-1} \end{aligned} \tag{2.12}$$

to achieve hybrid synchronization, the error system for anti synchronization and synchronization are defined same like in Eqn. (2.6) and Eqs. (2.7)(2.8) respectively. The direct design method [128–134] of synchronization for chaotic systems has wide spread of applications and is very effective when there are no perturbations.

2.4.3 Adaptive Control Technique

In [135], adaptive control technique is applied to study the synchronization between several coupled chaotic systems. They have considered the following model to investigate adaptive synchronization:

$$\begin{aligned} \dot{\chi_1} &= f_1(\chi_1) + F_1(\chi_1(t))\hat{\Theta}_1 \\ \dot{\chi_2} &= f_2(\chi_2) + F_2(\chi_2(t))\hat{\Theta}_2 + \mu_1 \\ \dot{\chi_3} &= f_3(\chi_3) + F_3(\chi_3(t))\hat{\Theta}_3 + \mu_2 \\ \dot{\chi_4} &= f_4(\chi_4) + F_4(\chi_4(t))\hat{\Theta}_4 + \mu_3 \\ &\vdots \\ \dot{\chi_M} &= f_M(\chi_M) + F_M(\chi_M(t))\hat{\Theta}_M + \mu_{M-1} \end{aligned} \tag{2.13}$$

The adaptive control technique [30, 136–144] of synchronization between chaotic systems is very popular and most widely used when the system parameters are unknown.

2.4.4 Active Backstepping

Runzi et al. [145] studied combination synchronization for three benchmark systems like Lu system, Lorentz system and Chen system using back-stepping approach. Lorentz system and Chen system are used as a master system and Lu system is used as a slave system. The effectiveness of the proposed technique established through the simulation results. Backstepping control [146–149] technique comprised of a repeated algorithm amalgamating the option of Lyapunov function theory for designing the active control. Particularly, this method provides flexibility in building up the control law.

2.4.5 Sliding Mode Control

Hou et al. [150] presented the chaotic system synchronization by means of SMC. For the error dynamics in sliding motion a proportional integral controller is designed and after this SMC is designed to get the chaos synchronization in master slave fashion. The justification of the proposed technique validated by the simulation results. SMC [146, 151–157] is a very effective non-linear control method. It is very popular due to its robust characteristics against the perturbations and widely used technique. The main demerit of the SMC approach is the introduction of chattering characteristics which is unwanted.

2.4.6 State Feedback Control

In [158] chaos synchronization and hyper-chaotification of systems is discussed. To get hyper-chaotification of the dynamic systems state feedback control is used and to get synchronization active controllers are designed. State feedback control

[159–163] is a very effective to regulate the response of the dynamic systems and is very useful in synchronization of chaotic systems.

2.4.7 Robust Synchronization using Active SMC

Naseh et al. [164] discussed the robust synchronization in the presence of uncertainties using active SMC which is very effective technique to synchronize chaotic systems. An algorithm is proposed to select most excellent control parameters so that less control effort is required for synchronization. Robust control technique [165–168] is very effective when there are external disturbances. It is assumed in this type of control that the disturbances are bounded.

2.5 Findings of the Literature Review

The literature reviewed in this chapter directs towards two streams, one is the type of synchronizations and the other is the control techniques used by many researchers to reach the goal. The types of synchronizations are classified mainly in two classes, the CS and AS. In all most all the literature surveyed in this chapter, the Master-Slave type formation of synchronization is considered. In this type of formation, if the slave system is in phase with the master then it is said its complete synchronization and if all states of slave are 180 degree out of phase then it is called anti-synchronization. The control techniques used in the literature to reach synchronization is of the direct design type and a few work investigated SMC for chaos synchronization. The bulk of the literature reviewed emphasis on the investigation of different control approaches to address synchronization problem of chaotic systems which helps us to contribute in this field of research. In this emerging field of research, researchers are striving for new techniques and exploring new areas. Furthermore, hybrid synchronization in dynamical network is also being investigated. Following are some points or research gap in the existing literature, which helps us to clarify the research goals and objectives for this dissertation:

- Most of the literature is about the synchronization or anti-synchronization by considering two chaotic systems in master/slave formation. A very less work is reported in the literature which addresses the co-existence of synchronization and anti-synchronization problem for more than two systems forming a DN.

- The HS control problem for coupled chaotic systems in a ring network investigated in the literature is assumption based and do not consider the robustness property.

2.6 Summary

In this chapter, synchronization and HS control problem of chaotic systems is presented to find the research gap in the existing literature. Regardless of particular types of control technique, a wast range of control methods are available which has their own merits and demerits discussed above. While reviewing the survey about the HS of chaotic systems coupled in the ring type DN, certain assumptions are assumed. The control techniques used to investigate hybrid synchronization are direct design type which do not provide the robustness. Consequently, based on the literature review, a comprehensive framework is in dire need to cope with these issues so that HS in CNNs and DN of identical,non-identical and complex systems could be achieved.

Chapter 3

Preliminaries

In this chapter, some preliminaries are presented regarding the hybrid synchronization of dynamical networks by employing adaptive ISMC and SSTA. A preliminary mathematical description is presented to understand the technique used to achieve hybrid synchronization in the presence of uncertainties.

3.1 Dynamical Networks (DNs)

The word networks refer to graphs with non-trivial topological characteristics. This section presents a brief introduction on the network theory, the terms used, and about some network structures [169–173]. Main components of the network are nodes, which are connected with small paths providing ease of going from node to another. These types of dynamical networks are called, small-world networks e.g. neural networks, networks of movies stars and the networks of electric power substations [172].

Erdos and Rnyi [171] introduced the small-world networks model for the first time in detailed. Unluckily, this model was not realistic in sense that it does address many real network features. The small-world network, discussed in [172] is more realistic and has both characteristics i.e. nodes are well connected to each

other and you can go to any other node with limited steps, and meanwhile a high clustering coefficient.

3.1.1 Mathematical Description

A dynamical network comprises of some nodes which can be denoted by N and some links L connecting these nodes. There is a discrimination between a directed network and undirected networks. As the name explains the link in directed network is unidirectional and points from one node to another, whereas, in undirected network the link is bidirectional. In a dynamical network, it is necessary to study the adjacency matrix to know the complete linkages between the nodes. An adjacency matrix can be defined as:

$$A_{ij} = \begin{cases} 1, & \text{if node } j \text{ has a link to node } i \\ 0, & \text{otherwise} \end{cases}$$

The above matrix A is helpful in explaining network properties and provides a nice description for unweighted networks. However, most of the real world networks have links with different strengths. In distinction, the coupling matrix in a dynamical network is quite different. The term Ξ_{ij} of the coupling matrix Ξ expresses a link from one node to another node by having some weight Ξ_{ij}.The relationship between the adjacency matrix and coupling matrix is defined in the following equation:

$$A_{ij} = \mathcal{H}\Xi_{ij} \tag{3.1}$$

where

$$\mathcal{H}(a) = \begin{cases} 1, & if a > 0 \\ 0, & if a \leq 0 \end{cases}$$

The matrices are symmetric for undirected dynamical networks and unsymmetrical for directed dynamical networks. A ring connected dynamical network is a network in which all the nodes are connected in a chain formation, moreover, the last and first node are also connected in ring type arrangement.

3.1.2 Types of Coupling

As mentioned above, there are mainly two types of interactions that are commonly found in natural systems, unidirectional exchange of information as mathematically expressed below. Consider the following coupled system,

$$Master : \dot{\chi} = F(\chi) \tag{3.2}$$

$$Slave : \dot{\omega} = F(\omega) + \mu(\chi, \omega) \tag{3.3}$$

Where $\chi, \omega \in \mathbb{R}^n$ and $\mu(\chi, \omega) \in \mathbb{R}^{n*n}$ is the coupling function. This system Eq. 3.2 is called the master and the system Eq. 3.3 is the slave system. The coupling function is considered usually as a diffusive term as $\mu(\chi, \omega) = \kappa(\chi - \omega)$ which may be defined as a difference of potential or ion concentration of the two interacting system represented by the state variables and κ is rate of transfer of ions or of current that is defined as the coupling strength. The mutual bidirectional diffusive coupling is considered as written, in a similar fashion,

$$\begin{aligned} \dot{\chi} &= F(\chi) + \kappa(\omega - \chi) \\ \dot{\omega} &= F(\omega) + \kappa(\chi - \omega) \end{aligned} \tag{3.4}$$

A very basic assumption in the above definition of coupling is that the coupling is instantaneous and constant in time and, known as a priori coupling. The interacting systems exchange information between then instantaneously, i.e., the information reaching to each dynamical system without any delay. Keeping the fact in mind, this interaction can be delayed and the coupling can be time varying. The delay couling in unidirectional mode is

$$\begin{aligned} \dot{\chi} &= F(\chi) \\ \dot{\omega} &= F(\omega) + \xi(\chi(t - \tau) - \omega) \end{aligned} \tag{3.5}$$

Where $\chi(t - \tau)$ is the delayed version of the driving signal. Such delay coupling can be mutual too. For time varying coupling, the coupling constant ξ becomes a time dependent $\xi(t)$ function, otherwise the conditions remains same.

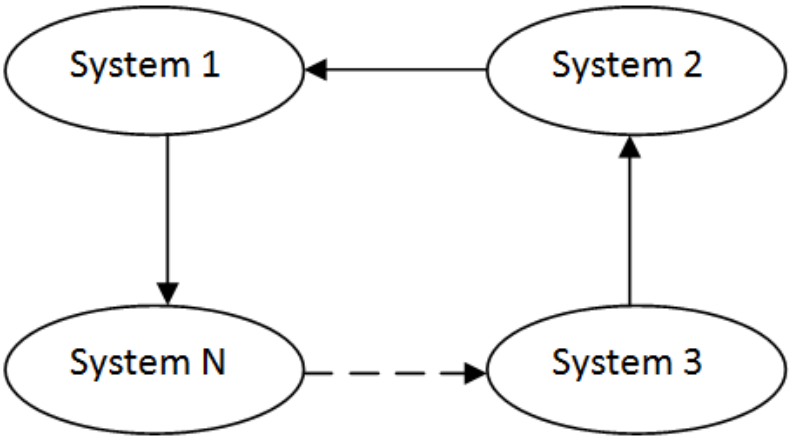

FIGURE 3.1: Dynamical network of systems connected in a ring topology.

3.1.3 Network Topologies

In real world, most of the networks have random connections between their nodes. However, there are some networks which comprises some noticeable characteristics e.g. small path lengths and high degree nodes. To represent topological features, many models have been developed and analyzed in the literature like small world model, scale free network random network models etc. Some commonly used network topologies are given below.

3.1.3.1 Circular Networks

Figure 3.1 represents a ring type network with all the systems linked to each other. This type of network is very interesting because it displays chimera states under some particular conditions [174, 175]. Chimera states means that the network exhibits the co-existence of state synchronization and anti-synchronization (AS). Unidirectional type ring network is a special type of circulant network which is taken for this thesis. A circulant matrix C can be defined as:

$$C = \begin{bmatrix} c_0 & c_1 & c_2 & c_3 & \cdots & c_{N-1} \\ c_{N-1} & c_0 & c_1 & c_2 & \cdots & c_{N-2} \\ \vdots & \vdots & \vdots & \vdots & \ddots & \vdots \\ c_1 & c_2 & c_3 & c_4 & \cdots & c_0 \end{bmatrix} \tag{3.6}$$

The circulant matrix for unidirectional ring is defined as

$$C = \begin{bmatrix} 0 & 1 & 0 & \cdots & 0 \\ 0 & 0 & 1 & \cdots & 0 \\ \vdots & \vdots & \vdots & \ddots & \vdots \\ 1 & 0 & 0 & \cdots & 0 \end{bmatrix} \tag{3.7}$$

3.1.3.2 Random Networks

In mathematics, random networks are of particular interest as for as the probability distributions over networks are concerned. Random networks are characterized by a probability distribution which makes them. The concept of random networks describes the co-existence of network theory and probability theory. Mathematically, random networks describes the properties of typical networks. Its experimental applications are found in all areas in which complex networks need to be modeled. In a mathematical context, random network refers almost exclusively to the ErdosRenyi [171, 176] random graph model.

3.1.3.3 Small World Networks

In small-world network [177], all nodes may not be directly coupled to each other, but they can be accessed to each other by going through the small paths.A class of small-world networks were classified as a random network by Watts and Strogatz [172]. They found that networks can be categorized according to the two features, clustering coefficient, and average node-node distance. They also found that several physical networks contains these features.

3.1.3.4 Scale Free Networks

Scale-free networks [178] are those networks which preserve a power distribution law for a node to originate links with other nodes. These networks are created by adding nodes and making links with the nodes which are already present in the

network. Practically there exist several examples of scale free networks e.g. the network of movies stars with the co-stars, the network of power grids, substations, and distribution lines e.t.c.

Moreover, there are some practical implications with the network models presented by many researchers, e.g the small world network model produced by Erdos and Renyi [171] did not presented topological information. In fact, many real network models are neither completely regular nor completely random. The small world network model presented by Watts and Strogatz [172] has high degree of clustering as in regular networks and small average distance among the connected systems as in the random networks. The connectivity distribution of the network peaks at an average value and decays exponentially which is common in both Watts and Strogatz model and Erdos and Renyi. Coupling delays, coupling strength, uncertainty about the topological structures are common practical implication in the mathematical networks presented in the literature.

3.2 Dynamics of Ring Connected Network

In practice, the complexity of a DN con not be examined by only considering its physical structure. The nodes, which are dynamical systems and are connected through links, must be given full attention to describe the level of complexity a DN has. As an example, laser, which can be a node in a DN, interact with other lasers through its light [179]. Another example of DNs are neural networks. The nodes in the neural networks are the neural models and the links are the interaction between the neurons [180, 181]. Moreover, many researchers investigated the interaction of dynamical nodes and the networks in terms of synchronization [44, 182]. The dynamics of a ring connected network in [44] are defined in Eq. (3.8), Where $x_1, x_2, x_3, x_4, ..., x_M$ are vectors, $f_o : \mathbb{R}^m \rightarrow \mathbb{R}^m, o = 1, 2, 3, 4, ..., M$ are the nonlinear continuous function, $\theta_o \in \mathbb{R}^g$ are unknown parameters. $F_o(x_o) \in \mathbb{R}^{m*g}$ are matrices, $D_o = diag\{d_{o1}, d_{o2}, d_{o3} \cdots, d_{oM}\}$ are m dimensional diagonal matrices, and $d_{op} \geq 0$ is a diagonal matrix. If $f_o(.) \neq f_p(.), o = 1, 2, 3, 4, \cdots, M$, then the

arrangement Eq. (3.8) has non-identical systems.

$$\begin{aligned} \dot{x_1} &= f_1(x_1) + F_1(x_1)\theta_1 + D_1(x_M - x_1) \\ &\vdots \\ \dot{x_M} &= f_M(x_M) + F_M(x_M)\theta_M + D_M(x_{M-1} - x_M) \end{aligned} \tag{3.8}$$

Remark 3.1. in Eq. (3.8), ring coupling topology [45] is applied, in which 1^{st} system is connected with M^{th}, and 2^{nd} system is connected with 1^{st}; and so on, finally the M^{th} system is connected with $M - 1^{th}$ system.

3.3 Sliding Mode Control (SMC)

Among the state of the art non-linear control techniques, SMC has attained a reasonable attention in the previous decades. It provides remarkable features like accuracy, robustness and easy tuning capability and implementation. The control design process in SMC can be divided into two parts.

i. Design of SS in such a manner that the desired response of the system is accomplished.

ii. Selection of suitable control law, such that in the existence of external disturbances and matched uncertainties, it drags the sliding variable to zero.

Design of the SS is established by keeping in view the design specifications of sliding motion. After designing the SS, a suitable law is needed, to engage the system states to the switching surface. Closed loop response in SMC consists of the following phases:

i. A reaching phase in which plant trajectories are driven to the sliding manifold.

ii. A sliding phase in which plant trajectories slides to the origin.

3.3.1 Reaching Phase in SMC

Figure 3.2 shows the operation of SMC. In this figure a reaching phase is shown. In this phase controllers will drive the trajectories to sliding manifold σ regardless

of any initial condition. This is guaranteed by the hitting condition as explained in [183].

3.3.2 Sliding Phase in SMC

As shown in 3.2, as the system trajectory hits the SS σ it stays on it due to the control action and after hitting the SS the system is now in sliding phase. In the sliding phase the system trajectory is derived to equilibrium by the control action and finally it settle at the origin [183].

3.3.3 Practical Limitations in SMC

Ideally, SMC assumed to be an infinite frequency controller, but practically, it has some limitations. These limitations includes the bandwidth, switching delays, saturation, etc., limits the performance of the SM controllers. This deviated behavior of SM controller is called chattering [184] as shown in Fig. 3.2. These practical limitations makes the SMC a quasi SMC. In chattering behavior the system trajectory oscillates at high frequency around the sliding manifold resulting in steady state error.

3.3.4 Advantages of SMC

The principle benefit of SMC is that it offers robustness to external disturbances and parameter variations. To stabilize the system, the gain must be more than the norm of external disturbances and parametric variations. The switching nature produces unwanted characteristics known as chattering in SMC. Different HOSM control techniques are also adopted for the elimination of the chattering. However, in situations where system dynamics are unknown, an observer-based SMC law is constructed to stabilize the system dynamics. The first main advantage of SMC is its dynamic behavior, which is due to the suitable selection of the sliding function. Secondly, for some particular uncertainties, closed-loop system response becomes

insensitive. The principle of Sliding Mode (SM) can be extended to the model which has disturbances, parameter uncertainties, and bounded nonlinearities. The control strategies such as SMC of uncertain systems were briefly discussed in [87].

3.3.5 Design of SMC Algorithm

Consider a system given in the following:

$$\dot{x} = F(x) + g(x)\mu \tag{3.9}$$

where $x \in \Re^n$ is the state vector, $F(x) \in \Re^n$ and $g(x) \in \Re^n$ are the vector

fields, where $\mu \in \Re$ is the input control vector field. The SS $\sigma(x)$ is designed as $\sigma(x) = C^T x$, where $C \in R^n$ is constant vector field. The first derivative of the SS is taken as:

$$\dot{\sigma}(x) = C^T \dot{x} \tag{3.10}$$

The reaching condition for Eq. 3.10 is described in such a manner that it guarantees the inception of sliding mode.

$$\dot{\sigma}(x) = -M\,\mathrm{sign}(\sigma(x)) \tag{3.11}$$

The positive constant M is selected greater than the magnitude of the disturbances. Equation 3.10 can be rewritten as:

$$\dot{\sigma}(x) = C^T F(x) + C^T g(x)\mu \tag{3.12}$$

The control law for Eq. 3.26 can be designed as:

$$\mu = -[C^T g(x)]^{-1}[C^T F(x) + M\,\mathrm{sign}(\sigma(x))] \tag{3.13}$$

The control law designed in Eq. 3.13 comprises two components one is discontinuous and the other is equivalent control. Discontinuous part of the control law rejects the disturbances incurred in the system, this shows the robustness of the

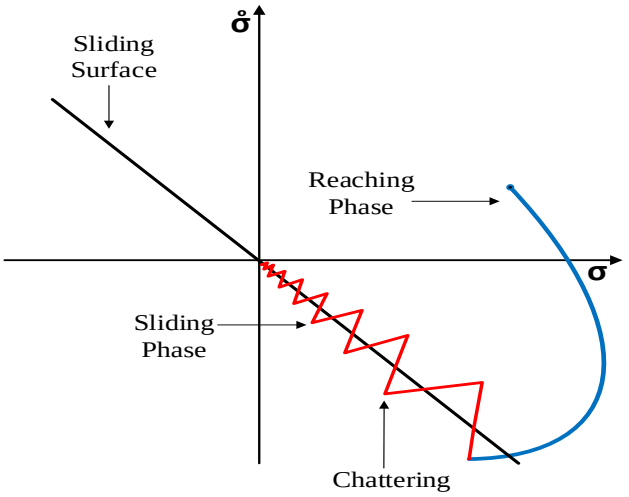

FIGURE 3.2: Sliding surface(SS)

control scheme. Figure 3.2 shows the complete framework of SMC by showing the reaching phase and the sliding phase. The dangerous chattering characteristics which is the major drawback of this scheme is also shown in the Fig. 3.2. There are many solutions available in the literature to eliminate this drawback of SMC [185–187].

3.3.6 Integral Sliding Mode Control (ISMC)

A modified form of SMC is ISMC. In ISMC the reaching phase is eradicated while maintaining the robustness property of the conventional SMC [45, 188–191] . The ISMC consists of the nominal control input to stabilizes the nominal system and a discontinuous control input to reject the uncertainties. Consider the following nonlinear system:

$$\dot{x} = f(x) + \beta\mu + h(x,t) \tag{3.14}$$

where $x \in R^n$ are system states, $\mu \in R^m$ is the input vector, $\beta \in R^{n*m}$ behaves as input gain, $f(x)$ is nonlinear function and the term $h(x,t)$ is a bounded matched uncertainty. To implement ISMC the following two part controller is defined in (3.15) where $\mu_0 \in R^m$ is the nominal control part and the second part μ_1 is further divided in two parts $\mu_1 = \mu_{1eq} + \mu_{1disc}$ where μ_{1eq} rejects the matched uncertainties

and the other part can be defined as μ_{1disc}.

$$\mu = \mu_0 + \mu_1 \tag{3.15}$$

By replacing the controller defined in Eq. 3.15, the Eq. 3.14 is rewritten as:

$$\dot{x} = f(x) + \beta\mu_0 + \beta\mu_1 + h(x,t) \tag{3.16}$$

The sliding surface for Eq. 3.16 is described as:

$$\sigma = \sigma_0(x) + z \tag{3.17}$$

where $z \in R^m$ is integral term defined in a manner that $z(0) = -\sigma_0(0)$. The 1^{st} derivative of SS defined in Eq. 3.17 is taken as:

$$\dot{\sigma} = \frac{\partial\sigma(0)}{\partial x}[f(x) + \beta\mu_0 + \beta\mu_1 + h(x,t)] + \dot{z} \tag{3.18}$$

To reach ISMC the nominal trajectory $x_0(t)$ should converge to ISMC trajectory $x(t)$ i.e. $x_0(t) = x(t)$. To achieve this the equivalent control is defined as:

$$\beta\mu_{1eq}(t) = -h(x,t) \tag{3.19}$$

By replacing Eq. 3.19 in Eq. 3.18 the integral term can be calculated in the following:

$$0 = \frac{\partial\sigma(0)}{\partial x}[f(x) + \beta\mu_0] + \dot{z} \tag{3.20}$$

The initial value of $z(0)$ must be defined in such a way that it ensure $\sigma = 0$ and the sliding mode exists right from the starting. The dynamics of the system in ISMC look like this: $\dot{x} = f(x) + \beta\mu_0$ which clearly shows that there are no disturbances.

3.3.7 Second Order Sliding Mode Control (SOSMC)

The SOSMC control reduces the dangeraous chattering characteristics [192–195]. In conventional or standard SMC the 1^{st} derivative of the SS is discontinuous

where as, in SOSM the second derivative of SS is discontinuous. The chattering phenomenon is reduced in SOSM by making a trade-off between the controller gain and disturbance rejection.

3.3.8 Super Twisting Algorithm (STA)

The STA [196–200] is a particular form of SOSM that gives

finite time convergence. The twisting algorithm can be written as:

$$\begin{aligned} \mu &= -\lambda_1 |\sigma|^{\frac{1}{2}} \operatorname{sign}(\sigma) + w \\ \dot{w} &= -\lambda_2 \operatorname{sign}(\sigma) \end{aligned} \tag{3.21}$$

3.3.9 Smooth Super Twisting Algoritm (SSTA)

The SSTA [201–203] smoothens the chattering effect and does not need information regarding derivative of SS. SSTA can be written as:

$$\begin{aligned} \mu &= -\lambda_1 |\sigma|^{\frac{\rho-1}{\rho}} \operatorname{sign}(\sigma) + w \\ \dot{w} &= -\lambda_2 |\sigma|^{\frac{\rho-2}{\rho}} \operatorname{sign}(\sigma) \end{aligned} \tag{3.22}$$

3.4 Hybrid Synchronization of Dynamical Networks (DNs) and Adaptive Integral Sliding Mode Control

As a general case a dynamical network(DN) connected in a ring topology is shown in Fig. 3.1. Considering that all the parameters of all the nodes connected in this network are uncertain, the general mathematical structure of network is defined in Eq. (2.5). In practice, the design of control law is essentially based on the mathematical description of the network to be synchronized. There always exist discrepancies between the actual network model and its mathematical model.

These discrepancies arise due to external disturbances, unmodeled/neglected dynamics and parametric uncertainties. To get the required closed loop performance for plants operating in the existence of disturbances/uncertainties, the controller must be robust against the external disturbances and model uncertainties. However, designing robust controllers is a difficult task. SMC is a very successful robust control approach for high order nonlinear complex networks operating in the existence of uncertainties. The ISMC, a special type of SMC, ensures the robustness [204] by eliminating the reaching-phase [190, 191]. The ISMC includes the nominal and the discontinuous control. To reach hybrid synchronization and estimation of uncertain parameters the adaptive ISMC approach for system Eq. (3.8) is as follows:

For the anti synchronization, the error vectors are:

$$e_{r1} = x_2 + x_1,\ e_{r2} = x_3 + x_2, \cdots, e_{M-1} = x_M + x_{M-1} \tag{3.23}$$

Let $\hat{\theta}_o$ is the estimate of θ_o and let $\tilde{\theta}_o = \theta_o - \hat{\theta}_o$ are the errors while estimating $\theta_o, o = 1, 2, 3, 4, \cdots, M$. To employ the integral sliding mode control, following nominal system is defined for the error dynamics as:

$$\begin{aligned}
\dot{e}_{r1} &= e_{r2} \\
\dot{e}_{r2} &= e_{r3} \\
\dot{e}_{r3} &= e_{r4} \\
\dot{e}_{r4} &= e_{r5} \\
\dot{e}_{r5} &= e_{r6} \\
&\vdots \\
\dot{e}_{rM-2} &= e_{rM-1} \\
\dot{e}_{rM-1} &= v_0
\end{aligned} \tag{3.24}$$

To stabilize the system Eq. (3.10), the Hurwitz SS for system Eq. (3.10) is as follows:

$$\sigma_0 = (1 + \frac{d}{dt})^{M-2} e_{r1} = e_{r1} + c_1 e_{r2} + c_2 e_{r3} + \cdots + c_{M-3} e_{rM-2} + e_{rM-1} \tag{3.25}$$

Then the over all sliding surface for the error dynamics including all terms can be defined as:

$$\sigma = \sigma_0 + z \tag{3.26}$$

where z is an integral term. The first derivative of Eq. (3.26) yields following:

$$\dot{\sigma} = \dot{\sigma_0} + \dot{z} \tag{3.27}$$

For Eq. (3.13) the following Lyapunove stability function is designed.

$$V = \frac{1}{2}\{\sigma^T\sigma + \tilde{\theta}_1^T\tilde{\theta}_1 + \tilde{\theta}_2^T\tilde{\theta}_2 + \sum_{o}^{M-1}\tilde{\theta}_{o+2}^T\tilde{\theta}_{o+2} + \tilde{\theta}_{M-1}^T\tilde{\theta}_{M-1} + \tilde{\theta}_M^T\tilde{\theta}_M\} \tag{3.28}$$

The first derivative of Eq. (3.14) yields:

$$\dot{V} = \sigma^T\dot{\sigma} + \tilde{\theta}_1^T\dot{\tilde{\theta}}_1 + \tilde{\theta}_2^T\dot{\tilde{\theta}}_2 + \sum_{o=3}^{M-4}\tilde{\theta}_{o+2}^T\dot{\tilde{\theta}}_{o+2} + \tilde{\theta}_{M-1}^T\dot{\tilde{\theta}}_{M-1} + \tilde{\theta}_M^T\dot{\tilde{\theta}}_M \tag{3.29}$$

by designing adaptive laws and $\dot{z}$ Eq. (3.29) becomes as following:

$$\dot{V} = -\kappa\sigma^2 - \sum_{o=1}^{M}\kappa_o\tilde{\theta}_o^T\tilde{\theta}_o \tag{3.30}$$

From Eq. (3.30) it is clear that $\dot{V} < 0$ for $\kappa > 0$ so, $\sigma, \tilde{\theta}_o \to 0$ therefore $e_o \to 0, o = 1, 2, 3, \cdots, M-1$. Thus anti synchronization achieved. The controllers designed for the anti synchronization can be used for complete synchronization by considering the cases discussed in Eqs. (2.6)-(2.8). The complete detail is discussed in the upcoming Section 4.3.

3.5 Summary

This chapter presents the mathematical model, types of coupling and different types of DNs. The concept of ISMC is presented in brief and a coherent way of establishing interest to employ this technique for HS of DN of coupled chaotic systms. This chapter laid the foundation of upcoming chapters of this thesis.

Chapter 4

Hybrid Synchronization in a Dynamical Network (DN) of Non-identical and Identical chaotic Systems

4.1 Introduction

This chapter presents the HS of chaotic systems which are coupled as shown in Fig. 3.1. This type of coupling was studied in [44] where all the constant parameters of the systems were assumed to be known. We extend this work in [45] and assumed that due to uncertain situations all the constant parameters are uncertain. To achieve HS for this kind of arrangement, adaptive ISMC method is utilized. By using this technique, the error systems is converted to a particular format through a transformation. The transformed structure has a nominal part and few un-known terms. The un-known terms are figured out adaptively. Then the error system is stabilized by employing ISMC. The designed controller for the error system consists of both the nominal and the compensator control. Lyapunov stability theory is used to drive the adaptive laws and compensator control.

4.2 Problem Formulation

4.2.1 System Description and Mathematical Model

The structure of a DN of chaotic systems connected in the ring topology is described in sec (3.2) and in Eq. (3.8) is defined as:

$$\begin{aligned} \dot{x_1} &= f_1(x_1) + F_1(x_1)\theta_1 + D_1(x_M - x_1) \\ \dot{x_2} &= f_2(x_2) + F_2(x_2)\theta_2 + D_2(x_1 - x_2) \\ &\vdots \\ \dot{x_M} &= f_M(x_M) + F_M(x_M)\theta_M + D_M(x_{M-1} - x_M) \end{aligned} \tag{4.1}$$

4.2.2 Problem Statement

$$\begin{aligned} \dot{x_1} &= f_1(x_1) + F_1(x_1)\theta_1 + D_1(x_M - x_1) \\ \dot{x_2} &= f_2(x_2) + F_2(x_2)\theta_2 + D_2(x_1 - x_2) + \mu_1 \\ &\vdots \\ \dot{x_M} &= f_M(x_M) + F_M(x_M)\theta_M + D_M(x_{M-1} - x_M) + \mu_{M-1} \end{aligned} \tag{4.2}$$

Definition: For system Eq. (4.2), it is defined that it exhibits hybrid synchronization if controllers $u_o, o = 1, 2, 3, 4, ...M - 1$ exist such that all trajectories $x_1(t), x_2(t), x_3(t), x_4(t), ..., x_M(t)$ for any starting point $x_1(0), x_2(0), x_3(0), x_4(0)$, $..., x_M(0)$ satisfy Eqs. (2.6) - (2.8).

4.3 The Proposed Control Algorithm

For the anti synchronization, the error vectors are:

$$e_{r1} = x_2 + x_1, e_{r2} = x_3 + x_2, \cdots, e_{M-1} = x_M + x_{M-1} \tag{4.3}$$

Let $\hat{\theta}_o$ be the estimate of θ_o and let $\tilde{\theta}_o = \theta_o - \hat{\theta}_o$ be the errors while estimating $\theta_o, o = 1, 2, 3, 4, \cdots, M$ then the derivative of Eq. (4.3) leads to the following:

$$
\begin{aligned}
\dot{e_{r1}} &= \dot{x_2} + \dot{x_1} = f_2(x_2) + F_2(x_2)\hat{\theta}_2 + F_2(x_2)\tilde{\theta}_2 + D_2(x_1 - x_2) + \mu_1 \\
&\quad + f_1(x_1) + F_1(x_1)\hat{\theta}_1 + F_1(x_1)\tilde{\theta}_1 + D_1(x_M - x_1) \\
\\
\dot{e_{r2}} &= \dot{x_3} + \dot{x_2} = f_3(x_3) + F_3(x_3)\hat{\theta}_3 + F_3(x_3)\tilde{\theta}_3 + D_3(x_2 - x_3) + \mu_2 \\
&\quad + f_2(x_2) + F_2(x_2)\hat{\theta}_2 + F_2(x_2)\tilde{\theta}_2 + D_2(x_1 - x_2) + \mu_1 \\
&\quad \vdots \\
\dot{e_{rM-1}} &= \dot{x_M} + \dot{x_{M-1}} = f_M(x_M) + F_M(x_M)\hat{\theta}_M + F_M(x_M)\tilde{\theta}_M + D_M(x_{M-1} - x_M) \\
&\quad + \mu_{M-1} f_{M-1}(x_{M-1}) + F_{M-1}(x_{M-1})\hat{\theta}_{M-1} + F_{M-1}(x_{M-1})\tilde{\theta}_{M-1} \\
&\quad + D_{M-1}(x_{M-2} - x_{M-1}) + \mu_{M-2}
\end{aligned}
\tag{4.4}
$$

Equation (4.4) can be written in matrix form as:

$$
\begin{bmatrix} \dot{e}_{r1} \\ \dot{e}_{r2} \\ \vdots \\ \dot{e}_{rM-1} \end{bmatrix} = \begin{bmatrix} f_2(x_2) + F_2(x_2)\hat{\theta}_2 + D_2(x_1 - x_2) + f_1(x_1) + F_1(x_1)\hat{\theta}_1 + D_1(x_M - x_1) \\ f_3(x_3) + F_3(x_3)\hat{\theta}_3 + D_3(x_2 - x_3) + f_2(x_2) + F_2(x_2)\hat{\theta}_2 + D_2(x_1 - x_2) \\ \vdots \\ f_M(x_M) + F_M(x_M)\hat{\theta}_M + f_{M-1}(x_{M-1}) + F_{M-1}(x_{M-1})\hat{\theta}_{M-1} \\ +D_M(x_{M-1} - x_M) + D_{M-1}(x_{M-2} - x_{M-1}) \end{bmatrix}
$$
$$
+ \begin{bmatrix} F_2(x_2)\tilde{\theta}_2 + F_1(x_1)\tilde{\theta}_1 \\ F_3(x_3)\tilde{\theta}_3 + F_2(x_3)\tilde{\theta}_2 \\ \vdots \\ F_M(x_M)\tilde{\theta}_M + F_{M-1}(x_{M-1})\tilde{\theta}_{M-1} \end{bmatrix} + \begin{bmatrix} 1 & 0 & 0 & \cdots & 0 \\ 1 & 1 & 0 & \cdots & 0 \\ \vdots & \vdots & \vdots & \vdots & \vdots \\ 0 & 0 & \cdots & 1 & 1 \end{bmatrix} \begin{bmatrix} \mu_1 \\ \mu_2 \\ \vdots \\ \mu_{M-1} \end{bmatrix}
\tag{4.5}
$$

by defining the controllers in the following way:

$$
\begin{bmatrix} \mu_1 \\ \mu_2 \\ \vdots \\ \mu_{M-1} \end{bmatrix} = \begin{bmatrix} 1 & 0 & 0 & \cdots & 0 \\ 1 & 1 & 0 & \cdots & 0 \\ \vdots & \vdots & \vdots & \vdots & \vdots \\ 0 & 0 & \cdots & 1 & 1 \end{bmatrix}^{-1} \left\{ \begin{bmatrix} e_{r2} \\ e_{r3} \\ \vdots \\ e_{rM-1} \\ v \end{bmatrix} - \mathbb{A} \right\}
\tag{4.6}
$$

Where, the term v is new input vector and

$$\mathbb{A} = \begin{bmatrix} f_2(x_2) + F_2(x_2)\hat{\theta}_2 + D_2(x_1 - x_2) + f_1(x_1) + F_1(x_1)\hat{\theta}_1 + D_1(x_M - x_1) \\ f_3(x_3) + F_3(x_3)\hat{\theta}_3 + D_3(x_2 - x_3) + f_2(x_2) + F_2(x_2)\hat{\theta}_2 + D_2(x_1 - x_2) \\ \vdots \\ f_M(x_M) + F_M(x_M)\hat{\theta}_M + f_{M-1}(x_{M-1}) + F_{M-1}(x_{M-1})\hat{\theta}_{M-1} \\ +D_M(x_{M-1} - x_M) + D_{M-1}(x_{M-2} - x_{M-1}) \end{bmatrix} \tag{4.7}$$

then Eq. (4.5) becomes:

$$\begin{aligned} \dot{e}_{r1} &= e_{r2} + F_2(x_2)\tilde{\theta}_2 + F_1(x_1)\tilde{\theta}_1 \\ \dot{e}_{r2} &= e_{r3} + F_3(x_3)\tilde{\theta}_3 + F_2(x_2)\tilde{\theta}_2 \\ &\vdots \\ \dot{e}_{rM-1} &= v + F_M(x_M)\tilde{\theta}_M + F_{M-1}(x_{M-1})\tilde{\theta}_{M-1} \end{aligned} \tag{4.8}$$

To employ the integral sliding mode control, following nominal system is defined for Eq. (4.8) as:

$$\begin{aligned} \dot{e}_{r1} &= e_{r2} \\ \dot{e}_{r2} &= e_{r3} \\ \dot{e}_{r3} &= e_{r4} \\ &\vdots \\ \dot{e}_{rM-2} &= e_{rM-1} \\ \dot{e}_{rM-1} &= v_0 \end{aligned} \tag{4.9}$$

To stabilize the system (4.9), the Hurwitz sliding surface for system (4.9) is as following:

$$\sigma_0 = (1 + \frac{d}{dt})^{M-2} e_{r1} = e_{r1} + c_1 e_{r2} + c_2 e_{r3} + \cdots + c_{M-3} e_{rM-2} + e_{rM-1} \tag{4.10}$$

where the coefficients c_o are choosen in a manner that σ_0 becomes Hurwitz polynomial. The first derivative of Eq. (4.10) is taken to be as: $\dot{\sigma}_0 = e_{r2} + c_1 e_{r3} + c_2 e_{r4} + \cdots + c_{M-3} e_{rM-1} + v_0$. By defining $v_0 = -e_{r2} - c_1 e_{r3} - c_2 e_{r4} - \cdots - c_{M-3} e_{rM-1} - \kappa\sigma_0 -$

$\kappa sign(\sigma_0), \kappa > 0$ yields $\dot{\sigma}_0 = -\kappa\sigma_0 - \kappa sign(\sigma_0)$, therefore $\sigma_0 \to 0$ consequently $e_{r1}, e_{r2}, e_{r3}, \cdots, e_{rM-1} \to 0$. Therefore, system (4.9) becomes asymptotically stable.The sliding surfaces for system (4.8) is $\sigma = \sigma_0 + z$. The term z in the sliding surface is an integral term to be calculated later in this section. To avert the reaching phase, choosing $z(0)$ such that $\sigma(0) = 0$. By choosing $v = v_0 + v_s$, where the first term v_0, is the nominal input vector and the second term v_s is compensator which will be calculated later. Then the first derivative of the SS becomes as:

$$\begin{aligned}\dot{\sigma} &= \dot{\sigma}_0 + \dot{z} = \dot{e}_{r1} + c_1\dot{e}_{r2} + c_2\dot{e}_{r3} + c_3\dot{e}_{r4} + \cdots + c_{M-3}\dot{e}_{M-2} + \dot{e}_{M-1} + \dot{z} \\ &= e_{r2} + c_1 e_{r3} + c_2 e_{r4} + \cdots + c_{M-3}e_{rM-1} + v_0 + v_s + F_1(x_1)\tilde{\theta}_1 + (1+c_1)F_2(x_2)\tilde{\theta}_2 \\ &+ (c_1+c_2)F_3(x_3)\tilde{\theta}_3 + (c_2+c_3)F_4(x_4)\tilde{\theta}_4 + \cdots + (c_{M-4}+c_{M-3})F_{M-2}(x_{M-2})\tilde{\theta}_{M-2} \\ &+ (c_{M-3}+1)F_{M-1}(x_{M-1})\tilde{\theta}_{M-1} + F_M(x_M)\tilde{\theta}_M\dot{z}\end{aligned} \tag{4.11}$$

For Eq. (4.11) the following Lyapunove stability function is designed:

$$V = \frac{1}{2}\{\sigma^T\sigma + \tilde{\theta}_1^T\tilde{\theta}_1 + \tilde{\theta}_2^T\tilde{\theta}_2 + \sum_{o}^{M-1}\tilde{\theta}_{o+2}^T\tilde{\theta}_{o+2} + \tilde{\theta}_{M-1}^T\tilde{\theta}_{M-1} + \tilde{\theta}_M^T\tilde{\theta}_M\} \tag{4.12}$$

from Eq. (4.12) designing the adaptive laws $\hat{\theta}_o, \tilde{\theta}_o, o = 1, 2, 3, \cdots, M$ and computing v_s in such a way that the derivative of Eq. (4.12) becomes $\dot{V} < 0$.

Theorem 4.1. *Consider the Layapunov equation of the form Eq.* (4.12)*, then to get* $\dot{V} < 0$ *the following values of* $v_s, \dot{z}$ *are derived as* $\dot{z} = -e_{r2} - \sum_{0=3}^{M-1} c_{o-2}e_{ro} - v_0$, $v_s = -\kappa\sigma$ *and adaptive laws for* $\hat{\theta}_o, \tilde{\theta}_o, o = 1, 2, 3, \cdots, M$ *are derived as:*

$$\dot{\tilde{\theta}}_1 = -F_1^T(x_1)\sigma - \kappa_1\tilde{\theta}_1, \dot{\hat{\theta}}_1 = -\dot{\tilde{\theta}}_1 \tag{4.13a}$$

$$\dot{\tilde{\theta}}_2 = -(1+c_1)F_2^T(x_2)\sigma - \kappa_2\tilde{\theta}_2, \dot{\hat{\theta}}_2 = -\dot{\tilde{\theta}}_2 \tag{4.13b}$$

$$\dot{\tilde{\theta}}_{o+2} = -(c_o + c_{o+1})F_{o+2}^T(x_{o+2})\sigma - \kappa_{o+2}\tilde{\theta}_{o+2} \tag{4.13c}$$

$$\dot{\hat{\theta}}_{o+2} = -\dot{\tilde{\theta}}_{o+2}, o = 1, 2, 3, \cdots, M-4 \tag{4.13d}$$

$$\dot{\tilde{\theta}}_{M-1} = -(c_{M-3}+1)F_{M-1}^T(x_{M-1})\sigma - \kappa_{M-1}\tilde{\theta}_{M-1}, \tag{4.13e}$$

$$\dot{\hat{\theta}}_{M-1} = -\dot{\tilde{\theta}}_{M-1} \tag{4.13f}$$

$$\dot{\tilde{\theta}}_M = -F_M^T(x_M)\sigma - \kappa_M\tilde{\theta}_M, \dot{\hat{\theta}}_M = -\dot{\tilde{\theta}}_M \tag{4.13g}$$

Proof. since

$$\begin{aligned}\dot{V} &= \sigma^T\dot{\sigma} + \tilde{\theta}_1^T\dot{\tilde{\theta}}_1 + \tilde{\theta}_2^T\dot{\tilde{\theta}}_2 + \sum_{o=3}^{M-4}\tilde{\theta}_{o+2}^T\dot{\tilde{\theta}}_{o+2} + \tilde{\theta}_{M-1}^T\dot{\tilde{\theta}}_{M-1} + \tilde{\theta}_M^T\dot{\tilde{\theta}}_M \\ &= \sigma^T\{e_{r2} + \sum_{0=3}^{M-1} c_{o-2}e_{ro} + v_0 + v_s + \dot{z}\} + \tilde{\theta}_1^T\{\dot{\tilde{\theta}}_1 + F_1^T(x_1)\sigma\} \\ &+ \tilde{\theta}_2^T\{\dot{\tilde{\theta}}_2 + (1+c_1)F_2^T(x_2)\sigma\} + \sum_{o=1}^{M-4}\tilde{\theta}_{o+2}^T\{\dot{\tilde{\theta}}_{o+2} + (c_o + c_{o+1})F_{o+2}^T(x_{o+2})\sigma\} \\ &+ \tilde{\theta}_{M-1}^T\{\dot{\tilde{\theta}}_{M-1} + (c_{M-3}+1)F_{M-1}^T(x_{M-1})\sigma\} + \tilde{\theta}_M^T\{\dot{\tilde{\theta}}_M + F_M^T(x_M)\sigma\}\end{aligned} \tag{4.14}$$

by replacing adaptive laws and the values of $v_s, \dot{z}$ designed in Eq. (4.13) into Eq. (4.14) gives following.

$$\dot{V} = -\kappa\sigma^2 - \sum_{o=1}^{M}\kappa_o\tilde{\theta}_o^T\tilde{\theta}_o \tag{4.15}$$

Equation (4.15) shows that $\dot{V} < 0$ for $\kappa > 0$ consequently $\sigma, \tilde{\theta}_o \to 0$, since $\sigma \to 0$, therefore $e_o \to 0, o = 1, 2, 3, \cdots, M-1$. Thus anti synchronization achieved. The designed controllers which are used to achieve the anti-synchronization are employed to get CS. Following are two cases considered to illustrate the entire procedure.

case (1): For odd number of systems and $M(M \geq 3)$, synchronization error is defined in Eq. (2.6).

case (2): For even number of systems and $M(M \geq 4)$, synchronization error is defined in Eq. (2.7).

4.4 Application Examples

4.4.1 Dynamical Network(DN) of Non-identical Systems

In this section HS in a DN of non-identical chaotic systems connected in ring topology is discussed. To examine hybrid synchronization, three non-identical

chaotic systems are considered with uncertain parameters. As an example, chen , Lorenz, and Lu chaotic system are selected which are expressed as following:

$$\begin{aligned} \dot{x_{11}} &= -35x_{11} + 35x_{12} + d_{11}(x_{31} - x_{11}) \\ \dot{x_{12}} &= -7x_{11} + 28x_{12} + x_{11}x_{13} + d_{12}(x_{32} - x_{12}) \\ \dot{x_{13}} &= -3x_{13} + x_{11}x_{12} + d_{13}(x_{33} - x_{13}) \end{aligned} \tag{4.16}$$

$$\begin{aligned} \dot{x_{21}} &= -36x_{21} + 36x_{22} + d_{21}(x_{11} - x_{21}) + u_{11} \\ \dot{x_{22}} &= 20x_{22} - x_{21}x_{23} + d_{22}(x_{12} - x_{22}) + u_{12} \\ \dot{x_{23}} &= -3x_{23} + x_{21}x_{22} + d_{23}(x_{13} - x_{23}) + u_{13} \end{aligned} \tag{4.17}$$

$$\begin{aligned} \dot{x_{31}} &= -10x_{31} + 10x_{32} + d_{31}(x_{21} - x_{31}) + u_{21} \\ \dot{x_{32}} &= 28x_{31} - x_{32} - x_{31}x_{33} + d_{32}(x_{22} - x_{32}) + u_{22} \\ \dot{x_{33}} &= \frac{-8}{3}x_{33} + x_{31}x_{32} + d_{33}(x_{23} - x_{33}) + u_{23} \end{aligned} \tag{4.18}$$

In Eqs. (4.16),(4.17),(4.18) all the constant parameters are there by values, these equations with unknown parameters can be rewritten as:

$$\begin{aligned} \dot{x_{11}} &= a_1x_{11} + b_1x_{12} + d_{11}(x_{31} - x_{11}) \\ \dot{x_{12}} &= c_1x_{11} + d_1x_{12} - x_{11}x_{13} + d_{12}(x_{32} - x_{12}) \\ \dot{x_{13}} &= e_1x_{13} + x_{11}x_{12} + d_{13}(x_{33} - x_{13}) \end{aligned} \tag{4.19}$$

$$\begin{aligned} \dot{x_{21}} &= a_2x_{21} + b_2x_{22} + d_{21}(x_{11} - x_{21}) + u_{11} \\ \dot{x_{22}} &= c_2x_{22} - x_{21}x_{23} + d_{22}(x_{12} - x_{22}) + u_{12} \\ \dot{x_{23}} &= e_2x_{23} + x_{21}x_{22} + d_{23}(x_{13} - x_{23}) + u_{13} \end{aligned} \tag{4.20}$$

$$\begin{aligned} \dot{x_{31}} &= a_3x_{31} + b_3x_{32} + d_{31}(x_{21} - x_{31}) + u_{21} \\ \dot{x_{32}} &= c_3x_{31} - x_{32} - x_{31}x_{33} + d_{32}(x_{22} - x_{32}) + u_{22} \\ \dot{x_{33}} &= e_3x_{33} + x_{31}x_{32} + d_{33}(x_{23} - x_{33}) + u_{23} \end{aligned} \tag{4.21}$$

Let $\hat{a}_o, \hat{b}_o, \hat{c}_o, \hat{e}_o, \hat{d}_1, o = 1, 2, 3$ be estimates of $a_o, b_o, c_o, e_o, d_1, o = 1, 2, 3$ respectively and let $\tilde{a}_o = a_o - \hat{a}_o, \tilde{b}_o = b_o - \hat{b}_o, \tilde{c}_o = c_o - \hat{c}_o \tilde{e}_o = e_o - \hat{e}_o, \tilde{d}_1 = d_1 - \hat{d}_1, o = 1, 2, 3$ be errors in estimation of $a_o, b_o, c_o, e_o, d_1, o = 1, 2, 3$, respectively.

Defining:

$$x_1 = \begin{bmatrix} x_{11} \\ x_{12} \\ x_{13} \end{bmatrix}, x_2 = \begin{bmatrix} x_{21} \\ x_{22} \\ x_{23} \end{bmatrix}, x_3 = \begin{bmatrix} x_{31} \\ x_{32} \\ x_{33} \end{bmatrix}, u_1 = \begin{bmatrix} u_{11} \\ u_{12} \\ u_{13} \end{bmatrix}, u_2 = \begin{bmatrix} u_{21} \\ u_{22} \\ u_{23} \end{bmatrix},$$
$$\hat{\theta} = \begin{bmatrix} \hat{a} \\ \hat{b} \\ \hat{c} \\ \hat{d} \\ \hat{e} \end{bmatrix}, \tilde{\theta} = \begin{bmatrix} \tilde{a} \\ \tilde{b} \\ \tilde{c} \\ \tilde{d} \\ \tilde{e} \end{bmatrix} \tag{4.22}$$

Then the Eqs. (4.19),(4.20),(4.21) in vector form are written as:

$$\begin{aligned} \dot{x}_1 &= f_1(x_1) + F_1(x_1)\hat{\theta}_1 + F_1(x_1)\tilde{\theta}_1 \\ \dot{x}_2 &= f_2(x_2) + F_2(x_2)\hat{\theta}_2 + F_2(x_2)\tilde{\theta}_2 + u_1 \\ \dot{x}_3 &= f_3(x_3) + F_3(x_3)\hat{\theta}_3 + F_3(x_3)\tilde{\theta}_3 + u_2 \end{aligned} \tag{4.23}$$

Where,

$$\hat{\theta}_1 = \begin{bmatrix} \hat{a_1} & \hat{b_1} & \hat{c_1} & \hat{d_1} & \hat{e_1} \end{bmatrix}^T, \tilde{\theta}_1 = \begin{bmatrix} \tilde{a_1} & \tilde{b_1} & \tilde{c_1} & \tilde{d_1} & \tilde{e_1} \end{bmatrix}^T, \hat{\theta}_2 = \begin{bmatrix} \hat{a_2} & \hat{b_2} & \hat{c_2} & \hat{d_2} & \hat{e_2} \end{bmatrix}^T,$$
$$\tilde{\theta}_2 = \begin{bmatrix} \tilde{a_2} & \tilde{b_2} & \tilde{c_2} & \tilde{d_2} & \tilde{e_2} \end{bmatrix}^T, \hat{\theta}_3 = \begin{bmatrix} \hat{a_3} & \hat{b_3} & \hat{c_3} & \hat{d_3} & \hat{e_3} \end{bmatrix}^T, \tilde{\theta}_3 = \begin{bmatrix} \tilde{a_3} & \tilde{b_3} & \tilde{c_3} & \tilde{d_3} & \tilde{e_3} \end{bmatrix}^T,$$
$$f_1(x_1) = \begin{bmatrix} d_{11}(x_{31} - x_{11}) \\ x_{11}x_{13} + d_{12}(x_{32} - x_{12}) \\ x_{11}x_{12} + d_{13}(x_{33} - x_{13}) \end{bmatrix}, F_1(x_1) = \begin{bmatrix} x_{11} & x_{12} & 0 & 0 & 0 \\ 0 & 0 & x_{11} & x_{12} & 0 \\ 0 & 0 & 0 & 0 & x_{13} \end{bmatrix},$$
$$f_2(x_2) = \begin{bmatrix} d_{21}(x_{11} - x_{21}) \\ -x_{21}x_{23} + d_{22}(x_{12} - x_{22}) \\ x_{21}x_{22} + d_{23}(x_{13} - x_{23}) \end{bmatrix}, F_2(x_2) = \begin{bmatrix} x_{21} & x_{22} & 0 & 0 & 0 \\ 0 & 0 & 0 & x_{22} & 0 \\ 0 & 0 & 0 & 0 & x_{23} \end{bmatrix},$$
$$f_3(x_3) = \begin{bmatrix} d_{31}(x_{21} - x_{31}) \\ -x_{32} - x_{31}x_{33} + d_{22}(x_{22} - x_{32}) \\ x_{31}x_{32} + d_{33}(x_{23} - x_{33}) \end{bmatrix}, F_3(x_3) = \begin{bmatrix} x_{31} & x_{32} & 0 & 0 & 0 \\ 0 & 0 & 0 & x_{31} & 0 \\ 0 & 0 & 0 & 0 & x_{33} \end{bmatrix} \tag{4.24}$$

For the anti-synchronization, the errors $e_{r1} = \begin{bmatrix} e_{r11} & e_{r12} & e_{r13} \end{bmatrix}^T$, $e_{r2} = \begin{bmatrix} e_{r21} & e_{r22} & e_{r23} \end{bmatrix}^T$ are: $e_{r1} = x_2 + x_1$, $e_{r2} = x_3 + x_2$. Therefore,

$$\begin{bmatrix} \dot{e_{r1}} \\ \dot{e_{r2}} \end{bmatrix} = \begin{bmatrix} f_2(x_2) + F_2(x_2)\hat{\theta}_2 + f_1(x_1) + F_1(x_1)\hat{\theta}_1 \\ F_2(x_2)\hat{\theta}_2 + f_3(x_3) + F_3(x_3)\hat{\theta}_3 \end{bmatrix} + \begin{bmatrix} F_2(x_2)\tilde{\theta}_2 + F_1(x_1)\tilde{\theta}_1 \\ F_2(x_2)\tilde{\theta}_2 + F_3(x_3)\tilde{\theta}_3 \end{bmatrix} + \begin{bmatrix} 1 & 0 \\ 1 & 1 \end{bmatrix} \begin{bmatrix} u_1 \\ u_2 \end{bmatrix} \tag{4.25}$$

by choosing

$$\begin{bmatrix} u_1 \\ u_2 \end{bmatrix} = \begin{bmatrix} 1 & 0 \\ 1 & 1 \end{bmatrix}^{-1} \left\{ - \begin{bmatrix} f_2(x_2) + F_2(x_2)\hat{\theta}_2 + f_1(x_1) + F_1(x_1)\hat{\theta}_1 \\ F_2(x_2)\hat{\theta}_2 + f_3(x_3) + F_3(x_3)\hat{\theta}_3 \end{bmatrix} + \begin{bmatrix} e_{r2} \\ v \end{bmatrix} \right\} \tag{4.26}$$

where $v = \begin{bmatrix} v_1 & v_2 & v_3 \end{bmatrix}^T$ is the new input vector, then system (4.25) becomes:

$$\begin{aligned} \dot{e_{r1}} &= e_{r2} + F_2(x_2)\tilde{\theta}_2 + F_1(x_1)\tilde{\theta}_1 \\ \dot{e_{r2}} &= v + F_3(x_3)\tilde{\theta}_3 + F_2(x_2)\tilde{\theta}_2 \end{aligned} \tag{4.27}$$

The nominal system for Eq. (4.27) is:

$$\begin{aligned} \dot{e_{r1}} &= e_2 \\ \dot{e_{r2}} &= v_0 \end{aligned} \tag{4.28}$$

where, $v_0 = \begin{bmatrix} v_{01} & v_{02} & v_{03} \end{bmatrix}^T$ is the nominal input vector. The SS for Eq. (4.28) is defined as:$\sigma_0 = e_{r1} + e_{r2}$, i.e.,

$$\begin{bmatrix} \sigma_{01} \\ \sigma_{02} \\ \sigma_{03} \end{bmatrix} = \begin{bmatrix} e_{r11} + e_{r21} \\ e_{r12} + e_{r22} \\ e_{r13} + e_{r23} \end{bmatrix} \tag{4.29}$$

The nominal system Eq. (4.29) is asymptotically stable if $v_0 = -e_{r2} - k\sigma_0 - k\,\mathrm{sign}(\sigma_0), k > 0$. The SS for Eq. (4.27) is $\sigma = \sigma_0 + z = e_{r1} + e_{r2} + z$, where,

$z = \begin{bmatrix} z_1 & z_2 & z_3 \end{bmatrix}^T$ is the integral term and z(0) is chosen in such a manner that $\sigma(0) = 0$. Defining $v = v_0 + v_s$, where, $v_s = \begin{bmatrix} v_{s1} & v_{s2} & v_{s3} \end{bmatrix}^T$ is compensator. Then system (4.27) can be rewritten as:

$$\begin{aligned}
\dot{e}_{r11} &= e_{r21} + \tilde{a_2}x_{21} + \tilde{b_2}x_{22} + \tilde{a_1}x_{11} + \tilde{b_1}x_{12} \\
\dot{e}_{r12} &= e_{r22} + \tilde{c_2}x_{22} + \tilde{c_1}x_{11} + \tilde{d_1}x_{12} \\
\dot{e}_{r13} &= e_{r23} + \tilde{e_2}x_{23} + \tilde{e_1}x_{13} \\
\dot{e}_{r21} &= v_1 + \tilde{a_3}x_{31} + \tilde{b_3}x_{32} + \tilde{a_2}x_{21} + \tilde{b_2}x_{22} \\
\dot{e}_{r22} &= v_2 + \tilde{c_3}x_{31} + \tilde{c_2}x_{22} \\
\dot{e}_{r23} &= v_3 + \tilde{e_3}x_{33} + \tilde{e_2}x_{23}
\end{aligned} \tag{4.30}$$

Then $\dot{\sigma} = \dot{e_{r1}} + \dot{e_{r2}} + \dot{z}$ gives:

$$\begin{aligned}
\dot{\sigma_1} &= e_{r21} + v_{01} + v_{s1} + \dot{z_1} + \tilde{a_1}x_{11} + \tilde{b_1}x_{12} + 2\tilde{a_2}x_{21} + 2\tilde{b_2}x_{22} + \tilde{a_3}x_{31} + \tilde{b_3}x_{32} \\
\dot{\sigma_2} &= e_{r22} + v_{02} + v_{s2} + \dot{z_2} + \tilde{c_1}x_{11} + \tilde{d_1}x_{12} + 2\tilde{c_2}x_{22} + \tilde{c_3}x_{31} \\
\dot{\sigma_3} &= e_{r23} + v_{03} + v_{s3} + \dot{z_3} + 2\tilde{e_2}x_{23} + \tilde{e_1}x_{13} + \tilde{e_3}x_{33}
\end{aligned} \tag{4.31}$$

By taking a Lyapunov equation of the following form:

$$\begin{aligned}
V = \frac{1}{2}\{&\sigma_1^2 + \sigma_2^2 + \sigma_3^2 + \tilde{a}_1^2 + \tilde{a}_2^2 + \tilde{a}_3^2 + \tilde{b}_1^2 + \tilde{b}_2^2 + \tilde{b}_3^2 + \tilde{c}_1^2 + \tilde{c}_2^2 + \tilde{c}_3^2 + \tilde{e}_1^2 + \tilde{e}_2^2 \\
&+ \tilde{e}_3^2 + \tilde{d}_1^2\}
\end{aligned} \tag{4.32}$$

Then $\dot{V} < 0$ if the adaptive laws for $\tilde{a}_o, \hat{a}_o, \tilde{b}_o, \hat{b}_o, \tilde{c}_o, \hat{c}_o, \tilde{e}_o, \hat{e}_o, \tilde{d}_1, \hat{d}_1$ and the values of $v_{ro}, o = 1, 2, 3$ are chosen as:

$$\begin{aligned}
&\dot{z}_1 = -e_{r21} - v_{01}, v_{s1} = -k_1\sigma_1, \dot{z}_2 = -e_{r22} - v_{02}, v_{s2} = -k_2\sigma_2 \\
&\dot{z}_3 = -e_{r23} - v_{03}, v_{s3} = -k_3\sigma_3, \dot{\tilde{a}_1} = -\sigma_1 x_{11} - k_4\tilde{a}_1, \dot{\hat{a}}_1 = -\dot{\tilde{a}}_1 \\
&\dot{\tilde{a}}_2 = -2\sigma_1 x_{21} - k_5\tilde{a}_2, \dot{\hat{a}}_2 = -\dot{\tilde{a}}_2, \dot{\tilde{a}}_3 = -\sigma_1 x_{31} - k_6\tilde{a}_3, \dot{\hat{a}}_3 = -\dot{\tilde{a}}_3 \\
&\dot{\tilde{b}}_1 = -\sigma_1 x_{12} - k_7\tilde{b}_1, \dot{\hat{b}}_1 = -\dot{\tilde{b}}_1, \dot{\tilde{b}}_2 = -2\sigma_1 x_{22} - k_8\tilde{b}_2, \dot{\hat{b}}_2 = -\dot{\tilde{b}}_2 \\
&\dot{\tilde{b}}_3 = -\sigma_1 x_{31} - k_9\tilde{b}_3, \dot{\hat{b}}_3 = -\dot{\tilde{b}}_3
\end{aligned}$$

$$\begin{aligned}
\dot{\tilde{c}}_1 &= -\sigma_2 x_{11} - k_{10}\tilde{c}_1, \dot{\hat{c}}_1 = -\dot{\tilde{c}}_1 \\
\dot{\tilde{c}}_2 &= -2\sigma_2 x_{22} - k_{11}\tilde{c}_2, \dot{\hat{c}}_2 = -\dot{\tilde{c}}_2 \\
\dot{\tilde{c}}_3 &= -\sigma_1 x_{31} - k_{12}\tilde{c}_3, \dot{\hat{c}}_3 = -\dot{\tilde{c}}_3 \\
\dot{\tilde{e}}_1 &= -\sigma_3 x_{13} - k_{13}\tilde{e}_1, \dot{\hat{e}}_1 = -\dot{\tilde{e}}_1 \\
\dot{\tilde{e}}_2 &= -2\sigma_3 x_{23} - k_{14}\tilde{e}_2, \dot{\hat{e}}_2 = -\dot{\tilde{e}}_2 \\
\dot{\tilde{e}}_3 &= -\sigma_3 x_{33} - k_{15}\tilde{e}_3, \dot{\hat{e}}_3 = -\dot{\tilde{e}}_3 \\
\dot{\tilde{d}}_1 &= -\sigma_2 x_{12} - k_{16}\tilde{d}_1, \dot{\hat{d}}_1 = -\dot{\tilde{d}}_1, k_o > 0, o = 1, 2, ..., 16
\end{aligned} \tag{4.33}$$

By incorporating the Eq. (4.33) in the derivative of Eq. (4.32) it yields:

$$\begin{aligned}
\dot{V} = &-k_2{\sigma_1}^2 - k_2{\sigma_2}^2 - k_3{\sigma_3}^2 - k_4\tilde{a}_1^2 - k_5\tilde{a}_2^2 - k_6\tilde{a}_3^2 - k_7\tilde{b}_1^2 - k_8\tilde{b}_2^2 - k_9\tilde{b}_3^2 - k_{10}\tilde{c}_1^2 \\
&- k_{11}\tilde{c}_2^2 - k_{12}\tilde{c}_3^2 - k_{13}\tilde{e}_1^2 - k_{14}\tilde{e}_2^2 - k_{15}\tilde{e}_3^2 - k_{16}\tilde{d}_1^2
\end{aligned} \tag{4.34}$$

From this it is clear that $\sigma_o, \tilde{e}_o, \tilde{d}_1, \tilde{a}_o, \tilde{b}_o.\tilde{c}_o \to 0$ where $o = 1, 2, 3$. Therefor, anti-synchronization is achieved. For CS, the error is $e_{r3} = x_3 - x_1 = x_3 + x_2 - x_2 + x_1 = e_{r2} - e_{r1}$. As $e_{r1}, e_{r2} \to 0$ therefore $e_{r3} \to 0$. Thus complete synchronization is achieved.

4.4.1.1 Performance Analysis

The work presented in this chapter can be compared with the work presented in [44, 205]. There are many differences like the network model presented in [44] is different as compared to network model presented in Eq.(4.1) it consist of an additional parameter . The error dynamics defined in Eq.(4.7) and the controller defined in Eq.(4.9) are entirely different. The proposed control methodology is integral sliding mode control whereas direct design control technique is employed in [44]. The proposed control technique presented in this chapter is advantageous in sense that it provides fast response and robustness to uncertainties. The work presented in this chapter is more practical because it considers the effect of uncertainties. Lyapunove stability function defined in Eq.(4.15) is much more different

than [44] as it justifies the adaptive laws as well. Moreover, estimating the unknown parameters is another valuable difference.

Figures 4.1 - 4.5 displays simulation results for Sec. 4.4.1 with M=3. The initial (starting point) conditions are chosen as $(x_{11}(0) = 10, x_{12}(0) = 20, x_{13}(0) = 30)$, $(x_{21}(0) = -5.8, x_{22}(0) = 8, x_{23}(0) = 10)$ and $(x_{31}(0) = 11, x_{32}(0) = 15, x_{33}(0) = 26)$. The coupling parameters are chosen as $d_{11} = d_{21} = d_{13} = d_{23} = d_{31} = d_{33} = 0, d_{12} = 10, d_{22} = 11$ and $d_{32} = 1$. Figure 4.1(a) shows the errors e_{r11}, e_{r12}, e_{r13}, e_{r21}, e_{r22}, and e_{r23} asymptotically goes to zero. Figure 4.1(b) displays the errors $e`_{r31}, e`_{r32}$, and $e`_{r33}$, converging to origin. Figure 4.2(a) shows system states x_{11}, x_{21}, x_{31}, Figure 4.2(b) shows system states x_{12}, x_{22}, and x_{32} and Fig. 4.2(c) shows system states x_{13}, x_{23}, and x_{33}.

From these figures it can be seen that systems $x_1(t)$ and $x_2(t)$, and systems $x_2(t)$ and $x_3(t)$ achieve the AS, and systems $x_1(t)$ and $x_3(t)$ attain CS and therefore milestone attained i.e. hybrid synchronization. Figure 4.3 shows the adaptive estimation of parameters a, b, c, d, and e_r for the three systems. Figure 4.3(a) shows the estimation of a_1, b_1, c_1, d_1,and e_{r1}, the parameters of the first system, which converge to their true values of $-35, 35, -7, 28$, and -3 respectively. Figure 4.3(b) shows the estimation of a_2, b_2, c_2, d_2,and e_{r2}, and the parameters of the second system, which converges to their actual values of $-36, 36, 20$, and 3 respectively. Figure 4.3(c) shows the estimation of a_3, b_3, c_3, d_3,and e_{r3}, the parameters of the third system, which converges to their actual values $-10, 10, 28$, and $-8/3$ respectively. Figures 4.4 and 4.5 depicts the control effort exerted to achieve hybrid synchronization.

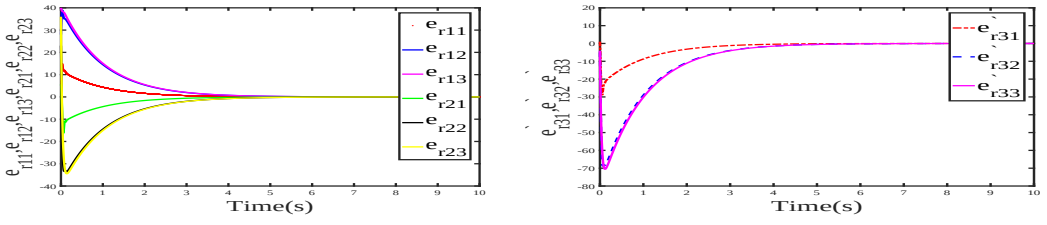

(a) (b)

FIGURE 4.1: Convergence of error system (a) $e_{r11}, e_{r12}, e_{r13}, e_{r21}, e_{r22}, e_{r23}$ (b) $e_{r31}, e_{r32}, e_{r33}$

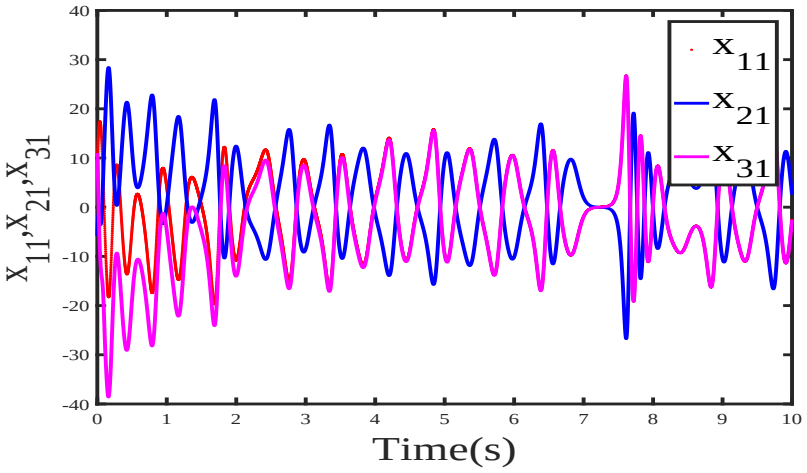

(a)

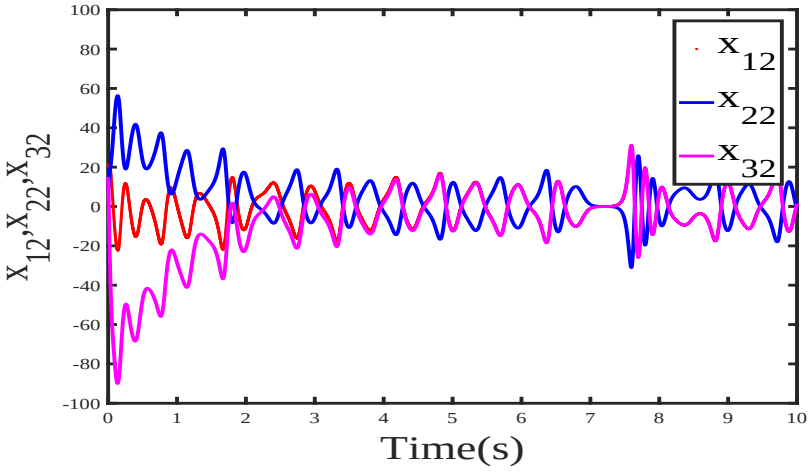

(b)

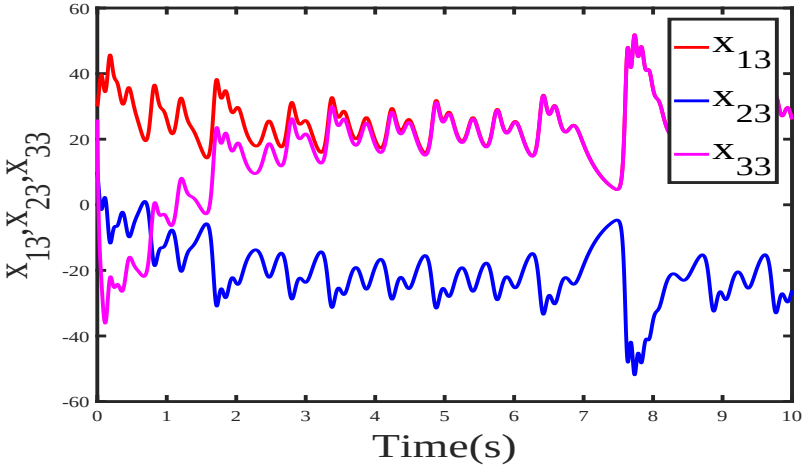

(c)

FIGURE 4.2: Time history of system states (a) x_{11}, x_{21}, x_{31} (b) x_{12}, x_{22}, x_{32} (c) x_{13}, x_{23}, x_{33}

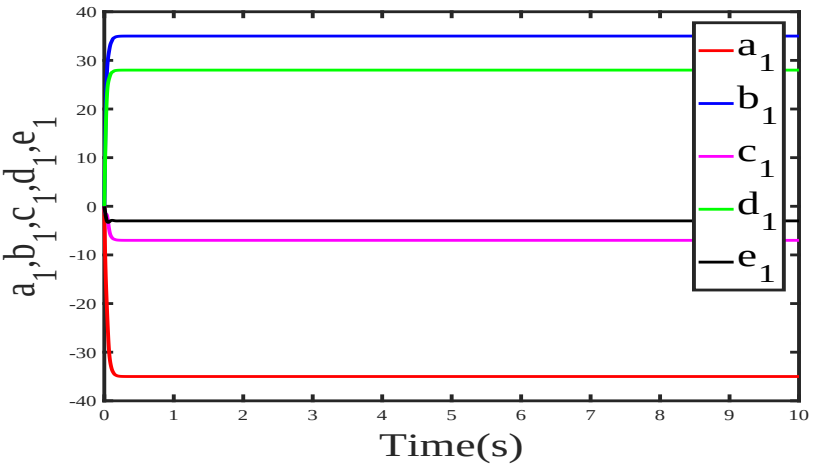

(a)

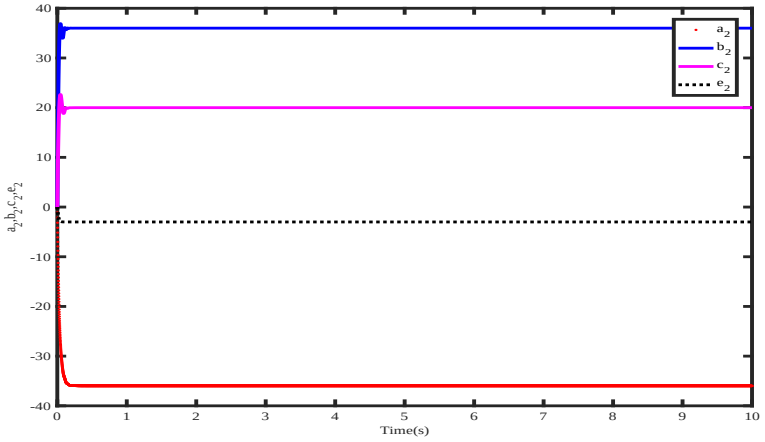

(b)

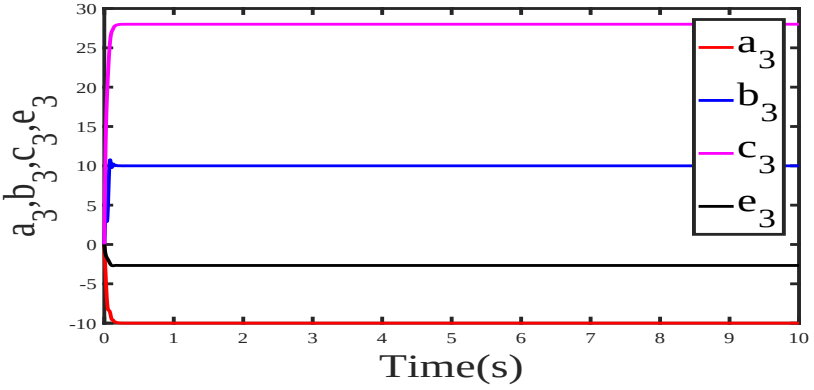

(c)

FIGURE 4.3: Parameter estimation (a) $a_1, b_1, c_1, d_1, e_{r1}$ (b) a_2, b_2, c_2, e_{r2} (c) a_3, b_3, c_3, e_{r3}

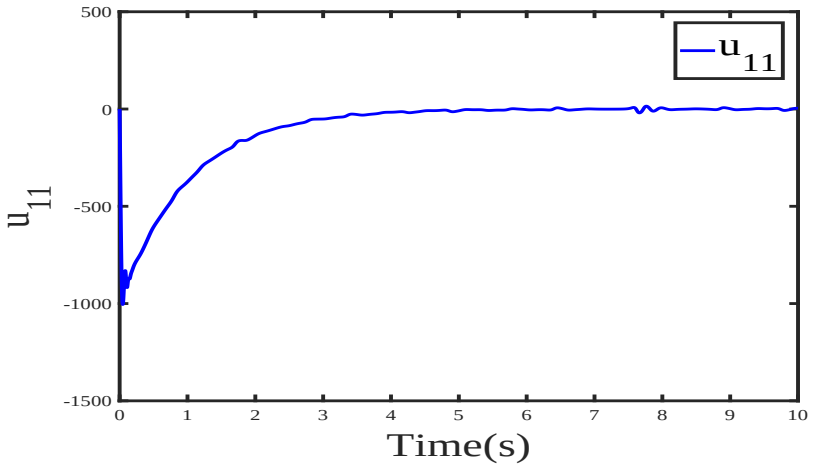

(a)

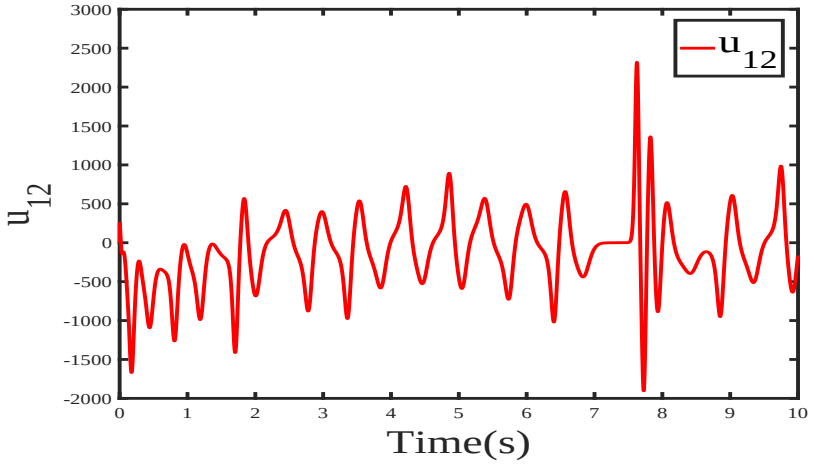

(b)

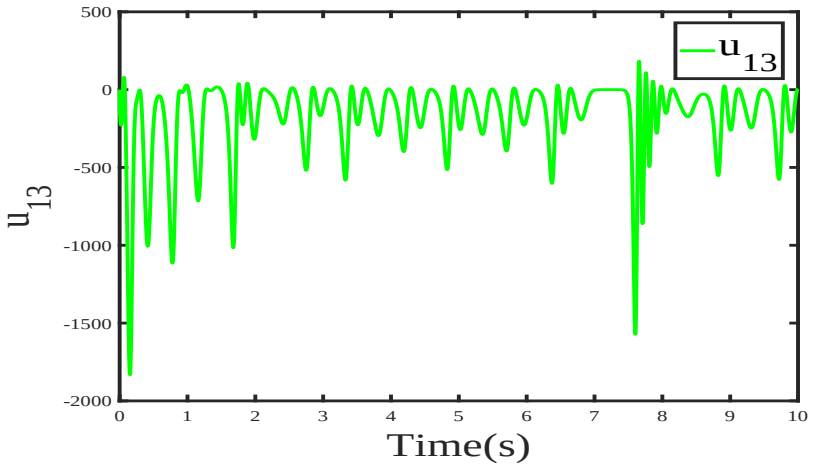

(c)

FIGURE 4.4: Control effort (a) u_{11} (b) u_{12} (c) u_{13}

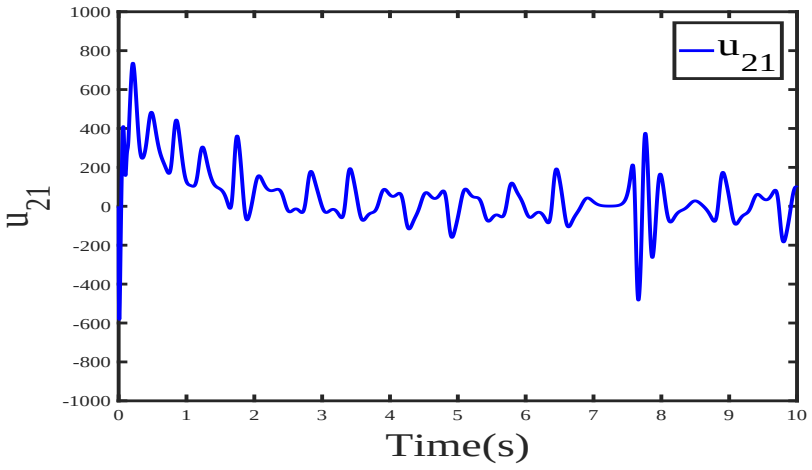

(a)

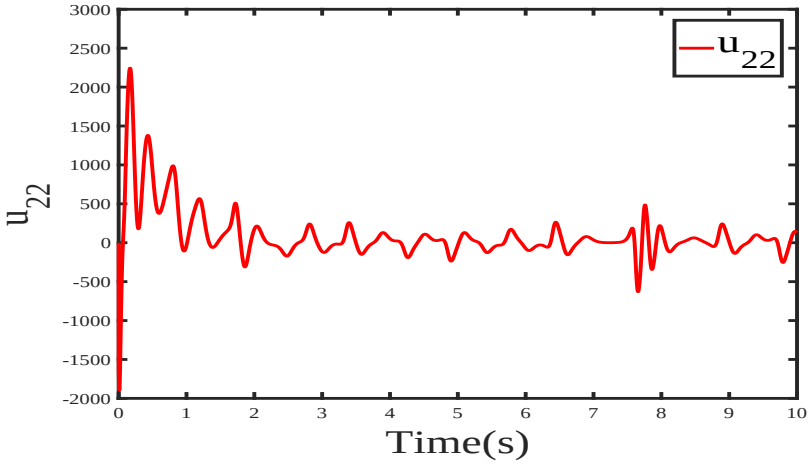

(b)

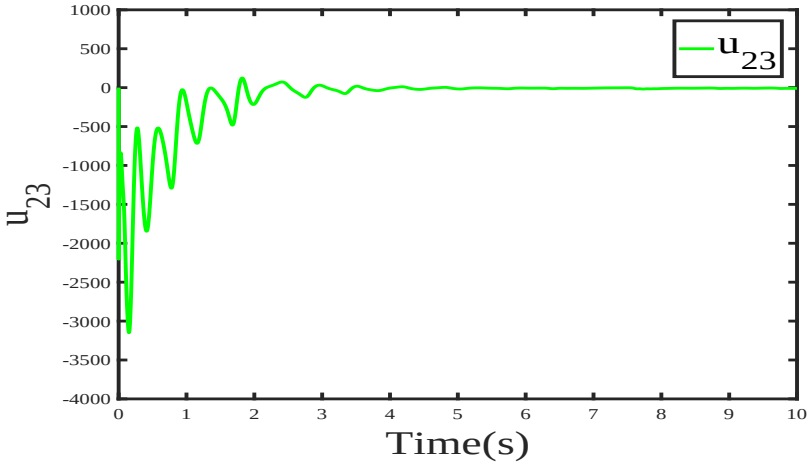

(c)

FIGURE 4.5: Control effort (a) u_{21} (b) u_{22} (c) u_{23}

4.4.2 Dynamical Network (DN) of Identical Systems

In this section HS in a DN of identical chaotic systems connected in ring topology is discussed. To examine HS, Lorenz chaotic systems are considered with uncertain parameters. The structure of the dynamic network comprising four Lorenz systems is defined as:

$$\begin{aligned}\dot{x}_{11} &= -10x_{11} + 10x_{12} + d'_{11}(x_{41} - x_{11}) \\ \dot{x}_{12} &= 28x_{11} - x_{12} - x_{11}x_{13} + d'_{12}(x_{42} - x_{12}) \\ \dot{x}_{11} &= -\frac{8}{3}x_{13} + x_{11}x_{12} + d'_{13}(x_{43} - x_{13})\end{aligned} \tag{4.35}$$

$$\begin{aligned}\dot{x}_{21} &= -10x_{21} + 10x_{22} + d'_{21}(x_{11} - x_{21}) + \mu'_{11} \\ \dot{x}_{22} &= 28x_{21} - x_{22} - x_{21}x_{23} + d'_{22}(x_{12} - x_{22}) + \mu'_{12} \\ \dot{x}_{23} &= -\frac{8}{3}x_{23} + x_{21}x_{22} + d'_{23}(x_{13} - x_{23}) + \mu'_{13}\end{aligned} \tag{4.36}$$

$$\begin{aligned}\dot{x}_{31} &= -10x_{31} + 10x_{32} + d'_{31}(x_{21} - x_{31}) + \mu'_{21} \\ \dot{x}_{32} &= 28x_{31} - x_{32} - x_{31}x_{33} + d'_{32}(x_{22} - x_{32}) + \mu'_{22} \\ \dot{x}_{33} &= -\frac{8}{3}x_{33} + x_{31}x_{32} + d'_{33}(x_{23} - x_{33}) + \mu'_{23}\end{aligned} \tag{4.37}$$

$$\begin{aligned}\dot{x}_{41} &= -10x_{41} + 10x_{42} + d'_{41}(x_{31} - x_{41}) + \mu'_{31} \\ \dot{x}_{42} &= 28x_{41} - x_{42} - x_{41}x_{43} + d'_{42}(x_{32} - x_{42}) + \mu'_{32} \\ \dot{x}_{43} &= -\frac{8}{3}x_{43} + x_{41}x_{42} + d'_{43}(x_{33} - x_{43}) + \mu'_{33}\end{aligned} \tag{4.38}$$

If the constant parameters in the above ring connected network are uncertain then the Eqs. (4.35), (4.36), (4.37), (4.38) can be rewritten as:

$$\begin{aligned}\dot{x}_{11} &= -ax_{11} + bx_{12} + d'_{11}(x_{41} - x_{11}) \\ \dot{x}_{12} &= cx_{11} - x_{12} - x_{11}x_{13} + d'_{12}(x_{42} - x_{12}) \\ \dot{x}_{11} &= -dx_{13} + x_{11}x_{12} + d'_{13}(x_{43} - x_{13})\end{aligned} \tag{4.39}$$

$$\begin{aligned}\dot{x}_{21} &= -ax_{21} + bx_{22} + d'_{21}(x_{11} - x_{21}) + \mu'_{11} \\ \dot{x}_{22} &= cx_{21} - x_{22} - x_{21}x_{23} + d'_{22}(x_{12} - x_{22}) + \mu'_{12} \\ \dot{x}_{23} &= -dx_{23} + x_{21}x_{22} + d'_{23}(x_{13} - x_{23}) + \mu'_{13}\end{aligned} \tag{4.40}$$

$$\begin{aligned}
\dot{x}_{31} &= -ax_{31} + bx_{32} + d_{31}^{'}(x_{21} - x_{31}) + \mu_{21}^{'} \\
\dot{x}_{32} &= cx_{31} - x_{32} - x_{31}x_{33} + d_{32}^{'}(x_{22} - x_{32}) + \mu_{22}^{'} \\
\dot{x}_{33} &= -dx_{33} + x_{31}x_{32} + d_{33}^{'}(x_{23} - x_{33}) + \mu_{23}^{'} \\
\dot{x}_{41} &= -ax_{41} + bx_{42} + d_{41}^{'}(x_{31} - x_{41}) + \mu_{31}^{'} \\
\dot{x}_{42} &= cx_{41} - x_{42} - x_{41}x_{43} + d_{42}^{'}(x_{32} - x_{42}) + \mu_{32}^{'} \\
\dot{x}_{43} &= -dx_{43} + x_{41}x_{42} + d_{43}^{'}(x_{33} - x_{43}) + \mu_{33}^{'}
\end{aligned} \tag{4.41}$$

Let $\hat{a}, \hat{b}, \hat{c}, \hat{d}$ be the estimates of a, b, c, d respectively and let $\tilde{a} = a - \hat{a}, \tilde{b} = b - \hat{b}, \tilde{c} = c - \hat{c}, \tilde{d} = d - \hat{d}$ be the errors in estimation of a, b, c, d respectively. Defining the dynamic states of the network nodes in a vector form as:

$$\begin{aligned}
x_1 &= \begin{bmatrix} x_{11} & x_{12} & x_{13} \end{bmatrix}, x_2 = \begin{bmatrix} x_{21} & x_{22} & x_{23} \end{bmatrix}, x_3 = \begin{bmatrix} x_{31} & x_{32} & x_{33} \end{bmatrix} \\
x_4 &= \begin{bmatrix} x_{41} & x_{42} & x_{43} \end{bmatrix}, \mu_1^{'} = \begin{bmatrix} \mu_{11}^{'} & \mu_{12}^{'} & \mu_{13}^{'} \end{bmatrix}, \mu_2^{'} = \begin{bmatrix} \mu_{21}^{'} & \mu_{22}^{'} & \mu_{23}^{'} \end{bmatrix} \\
\mu_3^{'} &= \begin{bmatrix} \mu_{31}^{'} & \mu_{32}^{'} & \mu_{33}^{'} \end{bmatrix}, \hat{\theta} = \begin{bmatrix} \hat{a} & \hat{b} & \hat{c} & \hat{d} \end{bmatrix}, \tilde{\theta} = \begin{bmatrix} \tilde{a} & \tilde{b} & \tilde{c} & \tilde{d} \end{bmatrix}
\end{aligned} \tag{4.42}$$

the dynamic systems of Eqs. (4.39)-(4.41) are rewritten as:

$$\begin{aligned}
\dot{x}_1 &= f_1(x_1) + F_1(x_1)\hat{\theta} + F_1(x_1)\tilde{\theta} \\
\dot{x}_2 &= f_2(x_2) + F_2(x_2)\hat{\theta} + F_2(x_2)\tilde{\theta} + \mu_1^{'} \\
\dot{x}_3 &= f_3(x_3) + F_3(x_3)\hat{\theta} + F_3(x_3)\tilde{\theta} + \mu_2^{'} \\
\dot{x}_4 &= f_4(x_4) + F_4(x_4)\hat{\theta} + F_4(x_4)\tilde{\theta} + \mu_3^{'}
\end{aligned} \tag{4.43}$$

where

$$f_1(x_1) = \begin{bmatrix} d_{11}^{'}(x_{41} - x_{11}) \\ -x_{12} - x_{11}x_{13} + d_{12}^{'}(x_{42} - x_{12}) \\ x_{11}x_{12} + d_{13}^{'}(x_{43} - x_{13}) \end{bmatrix}, F_1(x_1) = \begin{bmatrix} x_{11} & x_{12} & 0 & 0 \\ 0 & 0 & x_{11} & 0 \\ 0 & 0 & 0 & x_{13} \end{bmatrix}$$

$$f_2(x_2) = \begin{bmatrix} d_{21}^{'}(x_{11} - x_{21}) \\ -x_{22} - x_{21}x_{23} + d_{22}^{'}(x_{12} - x_{22}) \\ x_{21}x_{22} + d_{23}^{'}(x_{13} - x_{23}) \end{bmatrix}, F_2(x_2) = \begin{bmatrix} x_{21} & x_{22} & 0 & 0 \\ 0 & 0 & x_{21} & 0 \\ 0 & 0 & 0 & x_{23} \end{bmatrix}$$

$$f_3(x_3) = \begin{bmatrix} d_{31}^{'}(x_{21} - x_{31}) \\ -x_{32} - x_{31}x_{33} + d_{32}^{'}(x_{22} - x_{32}) \\ x_{31}x_{32} + d_{33}^{'}(x_{23} - x_{33}) \end{bmatrix}, F_3(x_3) = \begin{bmatrix} x_{31} & x_{32} & 0 & 0 \\ 0 & 0 & x_{31} & 0 \\ 0 & 0 & 0 & x_{33} \end{bmatrix}$$
$$f_4(x_4) = \begin{bmatrix} d_{41}^{'}(x_{31} - x_{41}) \\ -x_{42} - x_{41}x_{43} + d_{42}^{'}(x_{32} - x_{42}) \\ x_{41}x_{42} + d_{43}^{'}(x_{33} - x_{43}) \end{bmatrix}, F_4(x_4) = \begin{bmatrix} x_{41} & x_{42} & 0 & 0 \\ 0 & 0 & x_{41} & 0 \\ 0 & 0 & 0 & x_{43} \end{bmatrix} \tag{4.44}$$

For the anti-synchronization, the error vectors $e_{r1} = \begin{bmatrix} e_{r11} & e_{r12} & e_{r13} \end{bmatrix}$, $e_{r2} = \begin{bmatrix} e_{r21} & e_{r22} & e_{r23} \end{bmatrix}$ and $e_{r3} = \begin{bmatrix} e_{r31} & e_{r32} & e_{r33} \end{bmatrix}$ are defined as:

$$\begin{aligned} e_{r1} &= x_2 + x_1 \\ e_{r2} &= x_3 + x_2 \\ e_{r3} &= x_4 + x_3 \end{aligned} \tag{4.45}$$

Therefore,

$$\begin{bmatrix} \dot{e_{r1}} \\ \dot{e_{r2}} \\ \dot{e_{r3}} \end{bmatrix} = \begin{bmatrix} f_1(x_1) + F_1(x_1)\hat{\theta} + f_2(x_2) + F_2(x_2)\hat{\theta} \\ f_2(x_2) + F_2(x_2)\hat{\theta} + f_3(x_3) + F_3(x_3)\hat{\theta} \\ f_3(x_3) + F_3(x_3)\hat{\theta} + f_4(x_4) + F_4(x_4)\hat{\theta} \end{bmatrix} + \begin{bmatrix} (F_1(x_1) + F_2(x_2))\tilde{\theta} \\ (F_2(x_2) + F_3(x_3))\tilde{\theta} \\ (F_3(x_3) + F_4(x_4))\tilde{\theta} \end{bmatrix}$$
$$+ \begin{bmatrix} 1 & 0 & 0 \\ 1 & 1 & 0 \\ 0 & 1 & 1 \end{bmatrix} \begin{bmatrix} \mu_1^{'} \\ \mu_2^{'} \\ \mu_3^{'} \end{bmatrix} \tag{4.46}$$

By designing the control terms present in Eq. (4.46) in the following way,

$$\begin{bmatrix} \mu_1^{'} \\ \mu_2^{'} \\ \mu_3^{'} \end{bmatrix} = \begin{bmatrix} 1 & 0 & 0 \\ 1 & 1 & 0 \\ 0 & 1 & 1 \end{bmatrix}^{-1} \left\{ - \begin{bmatrix} f_1(x_1) + F_1(x_1)\hat{\theta} + f_2(x_2) + F_2(x_2)\hat{\theta} \\ f_2(x_2) + F_2(x_2)\hat{\theta} + f_3(x_3) + F_3(x_3)\hat{\theta} \\ f_3(x_3) + F_3(x_3)\hat{\theta} + f_4(x_4) + F_4(x_4)\hat{\theta} \end{bmatrix} + \begin{bmatrix} e_{r2} \\ e_{r3} \\ v \end{bmatrix} \right\} \tag{4.47}$$

Where, v is the new input vector. By replacing Eq. (4.47) in Eq. (4.46) yields,

$$\begin{bmatrix} \dot{e_{r1}} \\ \dot{e_{r2}} \\ \dot{e_{r3}} \end{bmatrix} = \begin{bmatrix} e_{r2} \\ e_{r3} \\ v \end{bmatrix} + \begin{bmatrix} (F_1(x_1) + F_2(x_2))\tilde{\theta} \\ (F_2(x_2) + F_3(x_3))\tilde{\theta} \\ (F_3(x_3) + F_4(x_4))\tilde{\theta} \end{bmatrix} \tag{4.48}$$

Equation (4.48) can be written as:

$$\begin{aligned} \dot{e_{r1}} &= e_{r2} + (F_1(x_1) + F_2(x_2))\tilde{\theta} \\ \dot{e_{r2}} &= e_{r3} + (F_2(x_2) + F_3(x_3))\tilde{\theta} \\ \dot{e_{r3}} &= v + (F_3(x_3) + F_4(x_4))\tilde{\theta} \end{aligned} \tag{4.49}$$

The nominal system for Eq. (4.49) is defined as:

$$\begin{aligned} \dot{e_{r1}} &= e_{r2} \\ \dot{e_{r2}} &= e_{r3} \\ \dot{e_{r3}} &= v_0 \end{aligned} \tag{4.50}$$

The Hurwitz SS vector for nominal system Eq. (4.50) can be defined as:

$$\begin{aligned} \sigma_0 &= e_{r1} + 2e_{r2} + e_{r3} \\ \sigma_0 &= \begin{bmatrix} \sigma_{01} \\ \sigma_{02} \\ \sigma_{03} \end{bmatrix} = \begin{bmatrix} e_{r11} + 2e_{r21} + e_{r31} \\ e_{r12} + 2e_{r22} + e_{r32} \\ e_{r13} + 2e_{r23} + e_{r33} \end{bmatrix} \end{aligned} \tag{4.51}$$

The time derivative of system (4.51) is $\dot{\sigma}_0 = \dot{e}_{r1} + 2\dot{e}_{r2} + \dot{e}_{r3} = e_{r2} + 2e_{r3} + v_0$. By choosing $v_0 = -e_{r2} - 2e_{r3} - \kappa\sigma_0 - \kappa\,\mathrm{sign}(\sigma_0), \kappa > 0$, it yiekds that $\dot{\sigma_0} = -\kappa\sigma_0 - \kappa\,\mathrm{sign}(\sigma_0)$, this means that the error dynamics in Eq. (4.50) are asymptotically stable.

Now, the sliding surface for Eq. (4.49) including all the terms is designed as:

$$\begin{aligned} \sigma &= \sigma_0 + z \\ &= e_{r1} + 2e_{r2} + e_{r3} + z \end{aligned} \tag{4.52}$$

where $z = \begin{bmatrix} z_1 & z_2 & z_3 \end{bmatrix}^T$ is some integral term designed $z(0)$ in such a way that $\sigma(0) = 0$. In Eq. (4.49) the input term $v = v_0 + v_s$ where $v_0 = \begin{bmatrix} v_{01} & v_{02} & v_{03} \end{bmatrix}^T$ is the nominal input and $v_s = \begin{bmatrix} v_{s1} & v_{s2} & v_{s3} \end{bmatrix}^T$ is compensator term which will be computed later in this section.The error dynamics defined in Eq. (4.49) are rewritten as:

$$\begin{aligned}
\dot{e}_{r11} &= e_{r21} + \tilde{a}x_{21} + \tilde{b}x_{22} + \tilde{a}x_{11} + \tilde{b}x_{12} \\
\dot{e}_{r12} &= e_{r22} + \tilde{c}x_{21} + \tilde{c}x_{11} \\
\dot{e}_{r13} &= e_{r23} + \tilde{d}x_{23} + \tilde{d}x_{13} \\
\dot{e}_{r21} &= e_{r31} + \tilde{a}x_{31} + \tilde{b}x_{32} + \tilde{a}x_{21} + \tilde{b}x_{22} \\
\dot{e}_{r22} &= e_{r32} + \tilde{c}x_{31} + \tilde{c}x_{21} \\
\dot{e}_{r23} &= e_{r33} + \tilde{d}x_{33} + \tilde{d}x_{23} \\
\dot{e}_{r31} &= v_{01} + v_{s1} + \tilde{a}x_{41} + \tilde{b}x_{42} + \tilde{a}x_{31} + \tilde{b}x_{32} \\
\dot{e}_{r32} &= v_{02} + v_{s2} + \tilde{c}x_{41} + \tilde{c}x_{31} \\
\dot{e}_{r33} &= v_{03} + v_{s3} + \tilde{d}x_{43} + \tilde{d}x_{33}
\end{aligned} \tag{4.53}$$

The first derivative of Eq. (4.52) yields: $\dot{\sigma} = \dot{e}_{r1} + 2\dot{e}_{r2} + \dot{e}_{r3} + \dot{z}$ which can be further written as:

$$\begin{aligned}
\dot{\sigma_1} &= e_{r21} + 2e_{r31} + \tilde{a}(3x_{21} + x_{11} + 3x_{31} + x_{41}) + \tilde{b}(3x_{22} + x_{12} + 3x_{32} + x_{42}) \\
&\quad + v_{01} + v_{s1} + \dot{z}_1 \\
\dot{\sigma_2} &= e_{r22} + 2e_{r32} + \tilde{c}(3x_{21} + x_{11} + 3x_{31} + x_{41}) + v_{02} + v_{s2} + \dot{z}_2 \\
\dot{\sigma_3} &= e_{r23} + 2e_{r33} + \tilde{d}(3x_{23} + x_{13} + 3x_{33} + x_{43}) + v_{03} + v_{s3} + \dot{z}_3
\end{aligned} \tag{4.54}$$

To check the stability of sliding surfaces following Lyapunov stability function is defined.

$$V = \frac{1}{2}(\sigma_1^2 + \sigma_2^2 + \sigma_3^2 + \tilde{a}^2 + \tilde{b}^2 + \tilde{c}^2 + \tilde{d}^2) \tag{4.55}$$

The derivative of Eq. (4.55) is taken as:

$$\dot{V} = \sigma_1\dot{\sigma_1} + \sigma_2\dot{\sigma_2} + \sigma_3\dot{\sigma_3} + \tilde{a}\dot{\tilde{a}} + \tilde{b}\dot{\tilde{b}} + \tilde{c}\dot{\tilde{c}} + \tilde{d}\dot{\tilde{d}} \tag{4.56}$$

if the adaptive laws for $\tilde{a}, \tilde{b}, \tilde{c}, \tilde{d}, \hat{a}, \hat{b}, \hat{c}, \hat{d}$ and $v_{so}, o = 1, 2, 3$ are defined as:

$$\begin{aligned}
\dot{z}_1 &= -e_{r21} - 2e_{r31} - v_{01},\ v_{s1} = -\kappa_1 s_1 \\
\dot{z}_2 &= -e_{r22} - 2e_{r32} - v_{02},\ v_{s2} = -\kappa_2 s_2 \\
\dot{z}_3 &= -e_{r23} - 2e_{r33} - v_{03},\ v_{s3} = -\kappa_3 s_3 \\
\dot{\tilde{a}} &= -\sigma_1(3x_{21} + x_{11} + 3x_{31} + x_{41}) - \kappa_4 \tilde{a},\ \dot{\hat{a}} = -\dot{\tilde{a}} \\
\dot{\tilde{b}} &= -\sigma_1(3x_{22} + x_{12} + 3x_{32} + x_{42}) - \kappa_5 \tilde{b},\ \dot{\hat{b}} = -\dot{\tilde{b}} \\
\dot{\tilde{c}} &= -\sigma_2(3x_{21} + x_{11} + 3x_{31} + x_{41}) - \kappa_6 \tilde{c},\ \dot{\hat{c}} = -\dot{\tilde{c}} \\
\dot{\tilde{d}} &= -\sigma_3(3x_{23} + x_{13} + 3x_{33} + x_{43}) - \kappa_7 \tilde{d},\ \dot{\hat{d}} = -\dot{\tilde{d}}, \kappa_o > 0, o = 1, \cdots, 7
\end{aligned} \tag{4.57}$$

By replacing Eq. (4.57) in Eq. (4.56) it yields:

$$\dot{V} = -\kappa_1 \sigma_1^2 - \kappa_2 \sigma_2^2 - \kappa_3 \sigma_3^2 - \kappa_4 \tilde{a}^2 - \kappa_5 \tilde{b}^2 - \kappa_6 \tilde{c}^2 - \kappa_7 \tilde{d}^2 \tag{4.58}$$

From Eq. (4.58) it is clear that $\sigma_1, \sigma_2, \sigma_3, \tilde{a}, \tilde{b}, \tilde{c}, \tilde{d} \to 0$. Since $\sigma_1, \sigma_2, \sigma_3 \to 0$, therefore $e_{r1}, e_{r2}, e_{r3} \to 0$. Thus anti-synchronization achieved.

For CS the errors are defined as:

$$\begin{aligned}
e_{r1}^{'} &= x_3 - x_1 = x_3 + x_2 - x_2 - x_1 = e_{r2} - e_{r1} \\
e_{r2}^{'} &= x_4 - x_2 = x_4 + x_3 - x_3 - x_2 = e_{r3} - e_{r2}
\end{aligned} \tag{4.59}$$

Since $e_{r1}, e_{r2}, e_{r3} \to 0$ therefore $e_{r1}^{'}, e_{r2}^{'} \to 0$ thus complete synchronization is also achieved in a similar way as anti synchronization achieved.

4.4.2.1 Performance Analysis

Figures 4.6 - 4.11 shows simulation results for section 4.4.2 with M=4. The initial (starting point) conditions are chosen as $(x_{11}(0) = 4, x_{12}(0) = 5, x_{13}(0) = -3), (x_{21}(0) = 5, x_{22}(0) = 2, x_{23}(0) = -5), (x_{31}(0) = 11, x_{32}(0) = 15, x_{33}(0) = 10)$ and $(x_{41}(0) = 4, x_{42}(0) = 5, x_{43}(0) = -3)$. The coupling parameters are chosen as $d_{12} = d_{22} = d_{32} = d_{13} = d_{23} = d_{33} = d_{42} = d_{43} = 0, d_{11} = d_{21} = 1$ and $d_{31} = d_{41} = -1$. Figure 4.6(a) shows the errors $e_{r11}, e_{r12}, e_{r13}, e_{r21}, e_{r22}, e_{r23}, e_{r31}, e_{r32}$, and e_{r33}

asymptotically converge to zero. Figure 4.6(b) shows the errors $e`_{r11}, e`_{r12}$, and $e`_{r13}$, asymptotically converge to zero. Figure 4.6(c) depicts the errors $e``_{r21}, e``_{r22}$, and $e``_{r23}$, asymptotically converge to zero. Figure 4.7(a) depicts system states x_{11}, x_{21}, x_{31}, and x_{41}, Figure 4.7(b) depicts system states x_{12}, x_{22}, x_{32}, and x_{42}, and Figure 4.7(c) shows system states x_{13}, x_{23}, x_{33}, and x_{43}. From these figures it can be see that systems $x_1(t)$ and $x_2(t)$, systems $x_2(t)$ and $x_3(t)$, and systems $x_3(t)$ and $x_4(t)$ achieve the anti-synchronization, and systems $x_1(t)$ and $x_3(t)$ and systems $x_2(t)$ and $x_4(t)$ attained the complete synchronization and hence hybrid synchronization attained. Figure 4.8 shows an adaptive estimation of parameters a, b, c, and d for four systems which converge to their true values of $-10, 10, 28$, and $-8/3$ respectively. Figures 4.9 - 4.11 depicts the control effort exerted to achieve the hybrid synchronization.

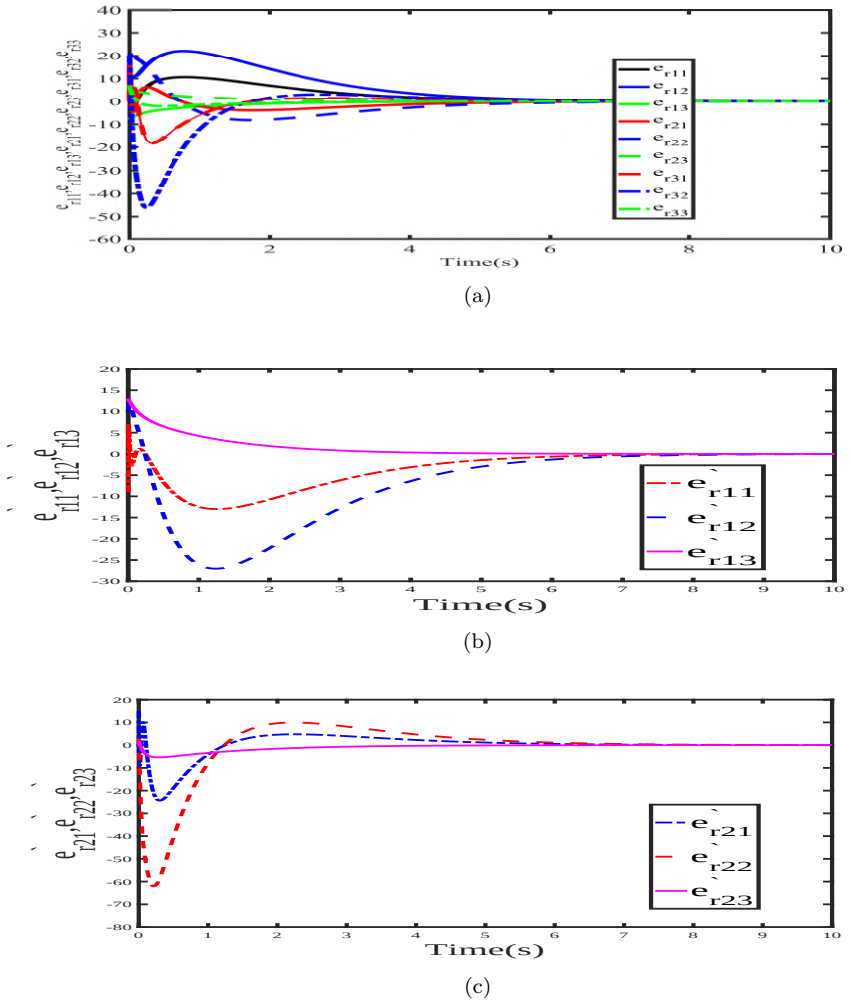

FIGURE 4.6: Convergence of error systems (a) $e_{r11}, e_{r12}, e_{r13}, e_{r21}, e_{r22}, e_{r23}, e_{r31}, e_{r32}, e_{r33}$ (b) $e`_{r11}, e`_{r12}, e`_{r13}$ (c) $e``_{r21}, e``_{r22}, e``_{r23}$

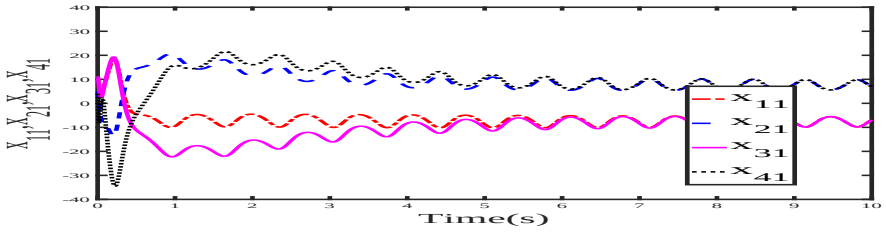

(a)

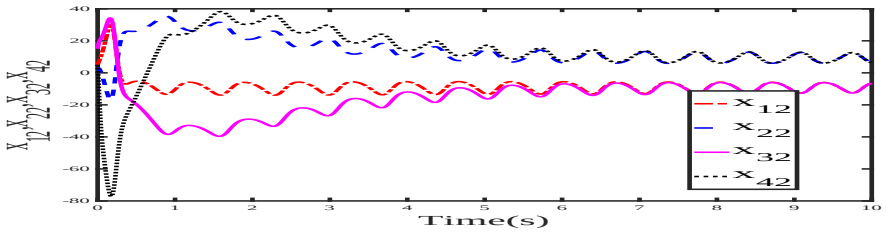

(b)

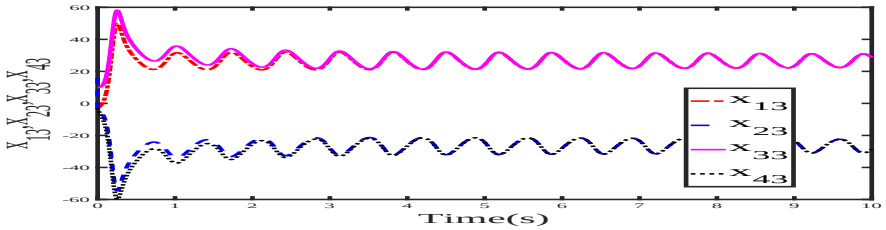

(c)

FIGURE 4.7: Time history of system states (a) $x_{11}, x_{21}, x_{31}, x_{41}$ (b) $x_{12}, x_{22}, x_{32}, x_{42}$ (c) $x_{13}, x_{23}, x_{33}, x_{43}$

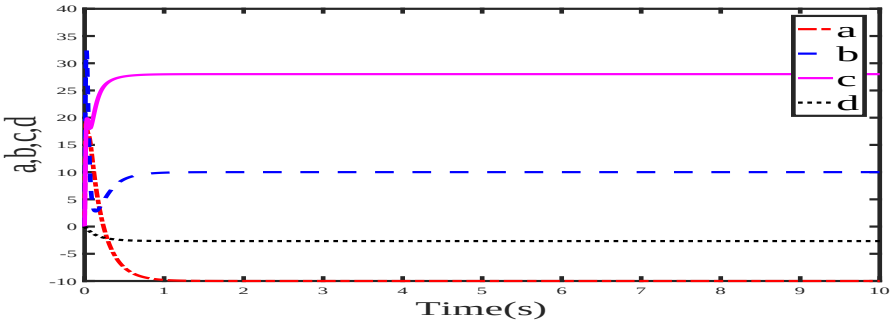

FIGURE 4.8: Convergence of estimated parameters to their actual values a, b, c, and d

4.5 Summary

In this chapter, the control design method is presented for parameter estimation and hybrid synchronization in a DN of non-identical and identical chaotic systems connected in the ring topology. The methodology is created using adaptive ISMC. The error system was transformed into a special structure containing nominal part

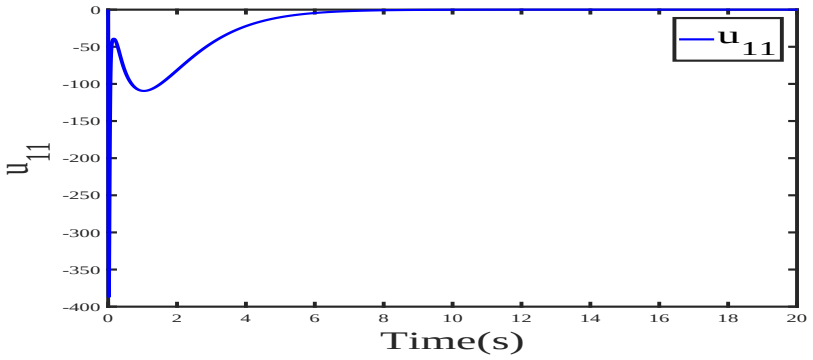

(a)

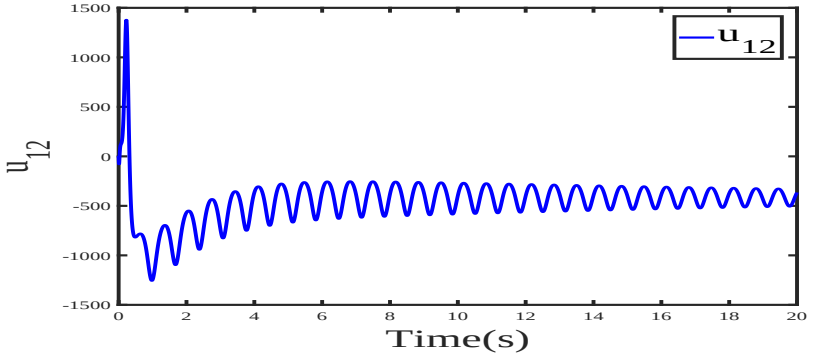

(b)

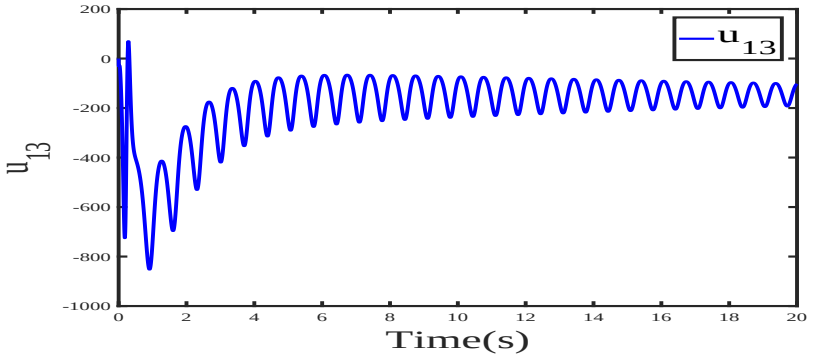

(c)

FIGURE 4.9: Control effort (a) u_{11} (b) u_{12} (c) u_{13}

and some unknown terms. The unknown terms were computed adaptively. Then the error system was stabilized using integral sliding mode control. The stabilizing controller for the error system is created that contains the nominal control and the compensator control. Simulation results show that hybrid synchronization was achieved with the proposed control laws and that the uncertain parameters converge to their actual values.

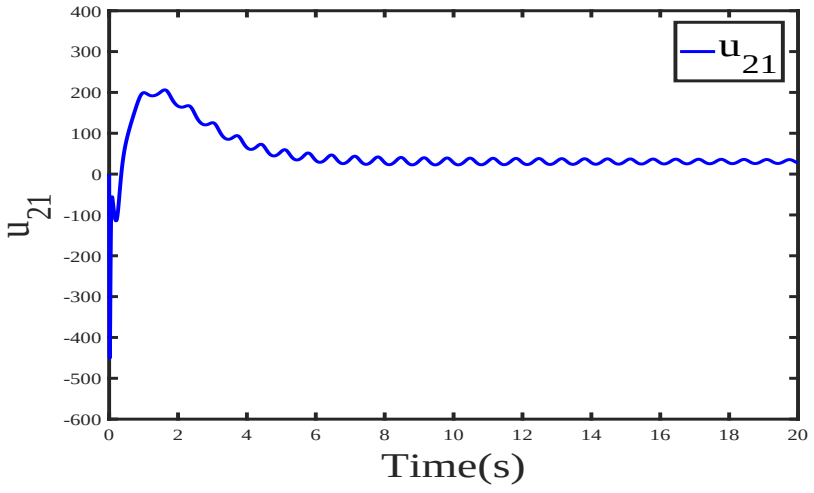

(a)

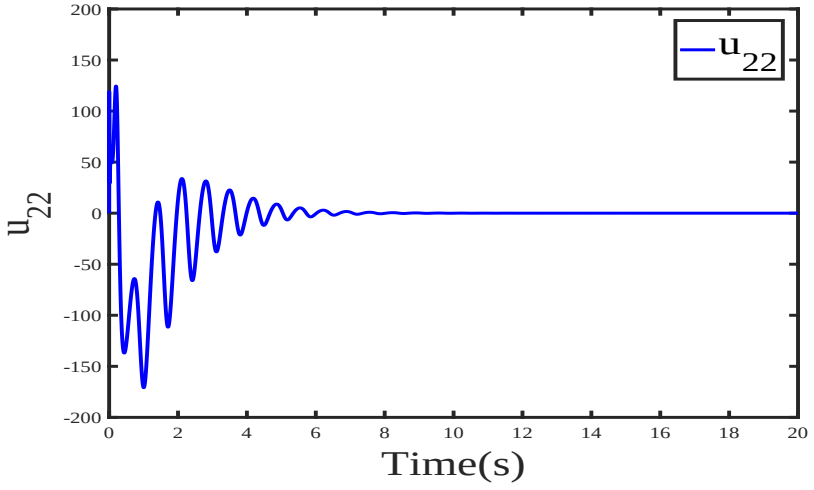

(b)

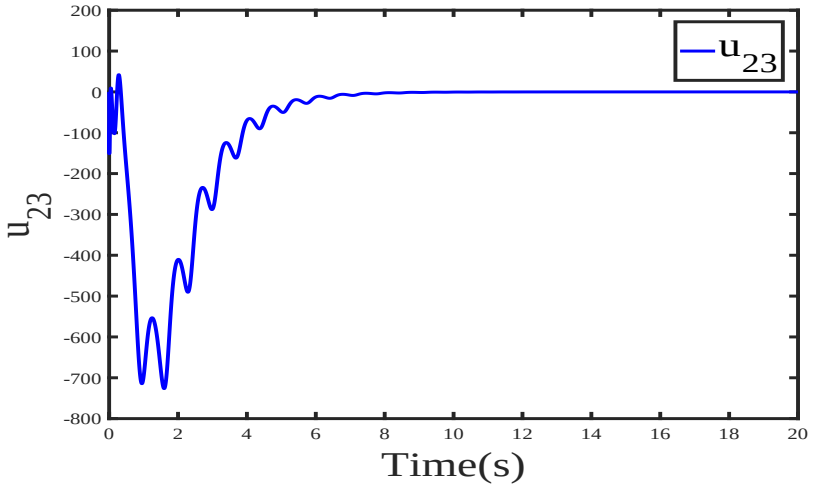

(c)

FIGURE 4.10: Control effort (a) u_{21} (b) u_{22} (c) u_{23}

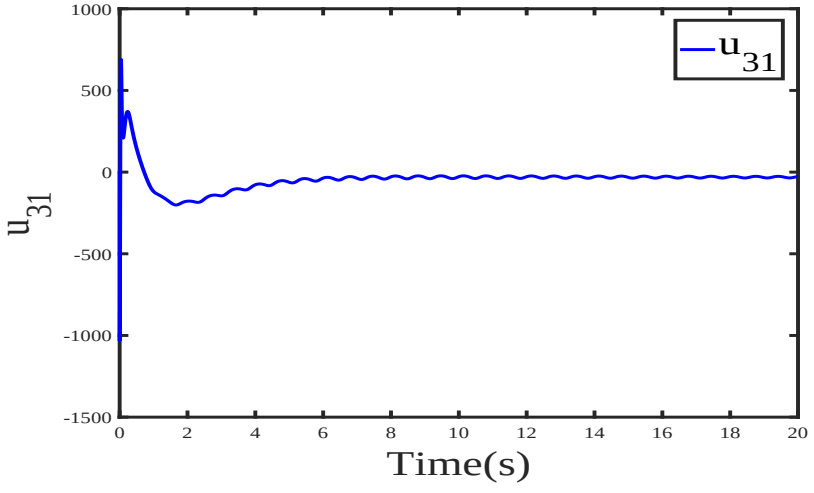

(a)

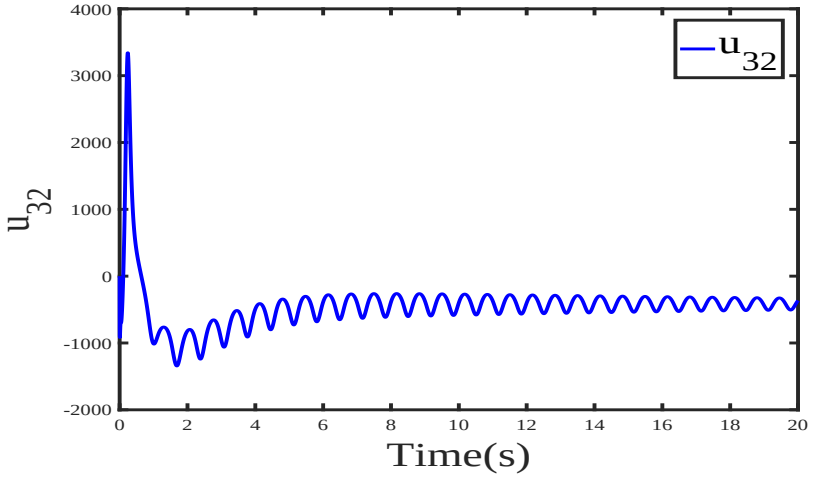

(b)

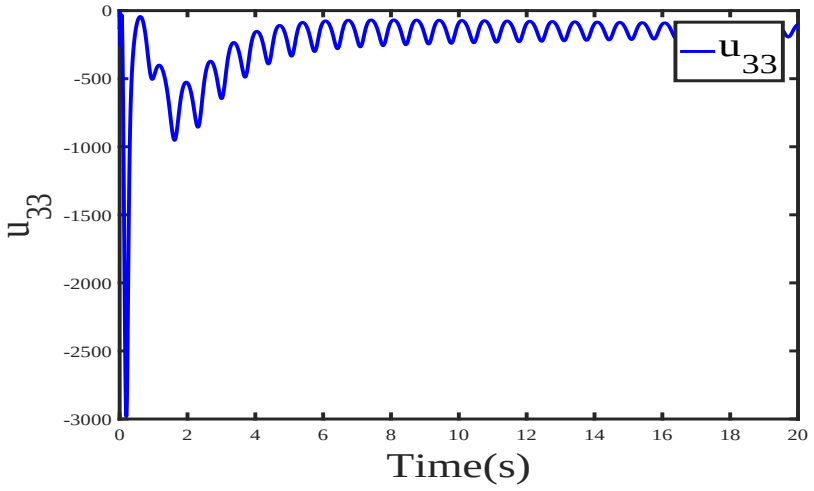

(c)

FIGURE 4.11: Control effort (a) u_{31} (b) u_{32} (c) u_{33}

Chapter 5

Hybrid Synchronization in a Dynamical Network (DN) of Complex Chaotic PMSM Systems

5.1 Introduction

In this chapter, the use of adaptive ISMC is investigated to achieve hybrid synchronization of complex chaotic systems connected in the ring topology as shown in 4.1. In addition, it is considered that due to the uncertainties the parameters of the complex chaotic systems are unknown. As an example, a DN of complex chaotic permanent magnet synchronous motor (PMSM) systems is selected.

Medium power PMSMs are very useful inside industrial areas by reason of their significant features like small size, low cost, high torque, and simple structure as there is no field winding present in the motor. Therefore, a lot of research has been carried out to investigate control and synchronization of real permanent magnet synchronous motors [206–209]. Whereas a very less work is done for complex variable permanent magnet synchronous motors [210, 211]. Practically, in permanent magnet synchronous motors, complex currents and complex voltages are present in the dynamical model and a possibility is there that one or all the parameters

of the systems are disturbed due to noises. So it is practically sound to estimate the unknown parameters for hybrid synchronization of PMSM systems.

5.2 Problem Formulation

5.2.1 System Description and Mathematical Model

In [33, 212] the equivalent circuit diagram Fig. 5.1 and mathematical model of a PMSM field-oriented rotor system are given in Eq. (5.1), where the dynamic state variables i_d, i_q represent currents and w is angular frequency; u_d is the direct axis and u_q is the quadrature-axis component of input stator voltages; T_L is the applied load torque; J is the arctic moment of inertia; β is the adhesive damping constant, R_1 represents resistance of stato wingding; L_d represents direct axis inductance and L_q represents quadrature-axis inductance ;ψ_r represents rotor flux and n_p are the total number of rotor poles.

$$\begin{aligned}
\frac{di_d}{dt} &= \frac{(-R_1 i_d + w i_q L_q + u_d)}{L_d} \\
\frac{di_q}{dt} &= \frac{(-R_1 i_q + w i_d L_d - w\psi_r + u_q)}{L_q} \\
\frac{dw}{dt} &= \frac{(n_p \psi_r i_q + n_p i_d i_q (L_d - L_q) - w\beta - T_L)}{J}
\end{aligned} \tag{5.1}$$

In the presence of even air gap as well as uniform distribution of flux and motor runs with no-load as well as power failure, the equations of PMSM system can be represented in (5.2) this system has two complex variable x_1, x_2 and two constant parameters a, b. In [210] another complex model of permanent magnet synchronous motor is presented in (5.3).

$$\begin{aligned}
\dot{x_1} &= a(x_2 - x_1) \\
\dot{x_2} &= bx_1 - x_2 - x_1 x_3 \\
\dot{x_3} &= x_1 x_2 - x_3
\end{aligned} \tag{5.2}$$

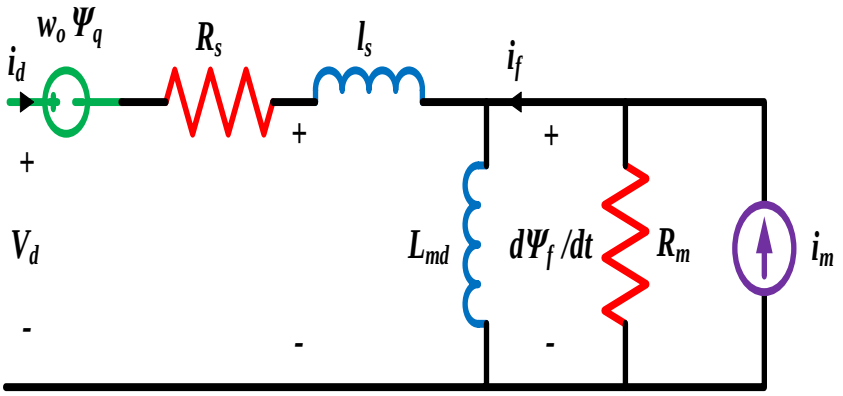

(a)

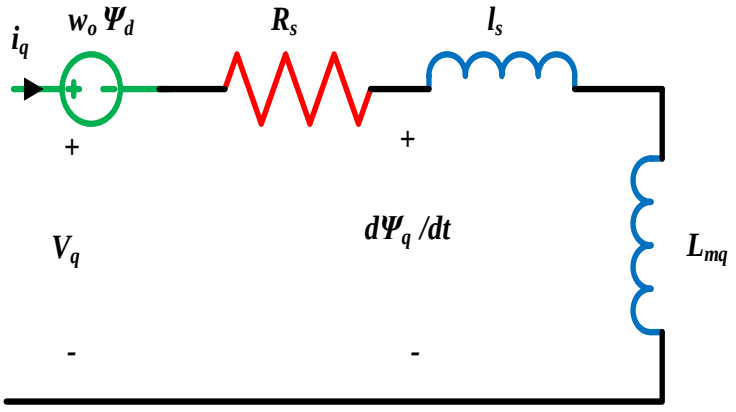

(b)

FIGURE 5.1: Equivalent circuit diagram of PMSM system on (a) $D-Axis$, (b) $Q-Axis$

$$\begin{aligned} \dot{x_1} &= a(x_2 - x_1) \\ \dot{x_2} &= bx_1 - x_1x_3 - x_2 \\ \dot{x_3} &= 0.5(x_2\overline{x}_1 + \overline{x}_2x_1) \end{aligned} \tag{5.3}$$

where $\overline{x}_1, \overline{x}_2$ are in complex conjugate form with $j = \sqrt{-1}$. This system Eq. (5.3) shows chaotic behavior when its constant parameters are selected as $b = 20, a = 11$. Figure 5.3 shows the chaotic behavior of this system. There are many properties of PMSM systems studied in [23,39,40]. In this section, the parameter identification and hybrid synchronization of PMSM systems using adaptive ISMC is investigated

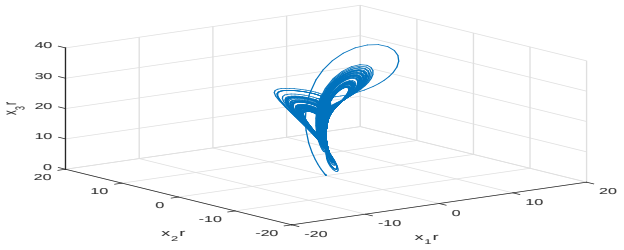

(a)

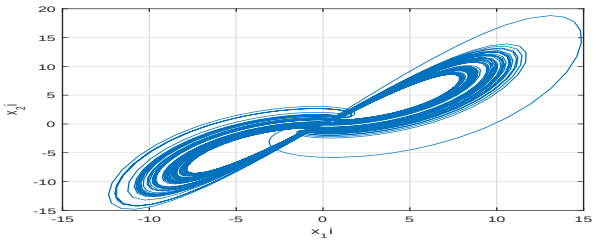

(b)

FIGURE 5.2: Chaotic behaviour of PMSM system on (a) x_{1r}, x_{2r}, x_{3r}, (b) x_{1i}, x_{2i} space Eq. (5.3)

.

5.2.2 Problem statement

In general, N complex chaotic systems connected in a ring topology can be configured as:

$$\begin{aligned}
\dot{x}_1 &= f_1(x_1) + F_1(x_1)\theta_1 + D_1(x_N - x_1) \\
\dot{x}_2 &= f_2(x_2) + F_2(x_2)\theta_2 + D_2(x_1 - x_2) \\
&\vdots \\
\dot{x}_N &= f_N(x_N) + F_N(x_N)\theta_N + D_N(x_{N-1} - x_N)
\end{aligned} \tag{5.4}$$

Where $x_1, x_2, ..., x_N \in C^n$, are defined as the complex state vectors, and $x_i = (x_{i1}, x_{i2}, x_{i3}, ..., x_{in})^T, x_k = x_{kr} + jx_{ki}, k = 1, 2, 3, ..., N$, $j = \sqrt{-1}$, both subscripts r and i represents real and imaginary components from beginning to end of this chapter.$f_i : C^n \to C^n$ are the nonlinear function,$\theta_i \in \Re^p$ are unknown parameters, $F_i(x_i) \in C^(n \times p)$ are matrices, $D_i = diag\{d_{i1}, d_{i2}, ..., d_{iN}\}, i = 1, 2, 3, ..., N$ are diagonal matrices, and $d_{ij} \geq 0$ represents the connected terms of the diagonal matrices. The complex chaotic systems are connected in a ring, where the

dynamic states of the first system are connected with the Nth, the second system is connected with the first, and finally the Nth complex chaotic system is connected with the (Nth-1) system. This kind of coupling scheme to investigate hybrid synchronization can be mathematically represented as:

$$\begin{aligned}
\dot{x}_1 &= f_1(x_1) + F_1(x_1)\theta_1 + D_1(x_N - x_1) \\
\dot{x}_2 &= f_2(x_2) + F_2(x_2)\theta_2 + D_2(x_1 - x_2) + u_1 \\
&\vdots \\
\dot{x}_N &= f(x_N) + F_N(x_N)\theta_N + D_N(x_{N-1} - x_N) + u_{N-1}
\end{aligned} \tag{5.5}$$

Where $u_k = u_{kr} + ju_{ki}, k = 1, 2, ..., N-1$ are the complex inputs. The hybrid synchronization for multiple connected systems is defined as: **Definition.** The chaotic dynamic system Eq. (5.5), it say that there exist HS if the controllers $u_i, i = 1, 2, 3, ..., N-1$ are selected in a manner that all trajectories $x_1(t), x_2(t), ..., x_N(t))$ in Eq. (5.5) with either initial condition $(x_1(0), x_2(0), ..., x_N(0))$ satisfy:For the errors $e_i = (e_{i1}, e_{i2}, ..., e_{iN})^T$, yields:

$$\lim_{t\to\infty} e_i = \lim_{t\to\infty} x_i(t) + qx_{i+1}(t) = 0, i = 1, 2, 3, ..., N-1$$

For the anti-synchronization $q = 1$ and for complete synchronization $q = -1$. The HS control become a problem to design appropriate controller u_i to make $e_i = (e_{i1}, e_{i2}, ..., e_{iN})^T \to 0$ asymptotically.

5.3 Proposed Control Algorithm

For the HS, the error vectors is defined as:

$$\begin{aligned}
e_1 &= x_2 + qx_1 \\
e_2 &= x_3 + qx_2 \\
&\vdots \\
e_{N-1} &= x_N + qx_{N-1}
\end{aligned} \tag{5.6}$$

Let $\hat{\theta}_i$ be the estimate of θ_i and let $\tilde{\theta}_i = \theta_i - \hat{\theta}_i$ be the errors in estimating the parameters $\theta_i, i = 1, 2, ..., N$, respectively.

The derivative of Eq. (5.6) yields:

$$\begin{aligned}
\dot{e}_1 &= \dot{x}_2 + q\dot{x}_1 = f_2(x_2) + F_2(x_2)\hat{\theta}_2 + F_2(x_2)\tilde{\theta}_2 + D_2(x_1 - x_2) + u_1 + qf_1(x_1) \\
&\quad + qF_1(x_1)\hat{\theta}_1 + qF_1(x_1)\tilde{\theta}_1 + qD_1(x_N - x_1) \\
\dot{e}_2 &= \dot{x}_3 + q\dot{x}_2 = f_3(x_3) + F_3(x_3)\hat{\theta}_3 + F_3(x_3)\tilde{\theta}_3 + D_3(x_2 - x_3) + u_2 + qf_2(x_2) \\
&\quad + qF_2(x_2)\hat{\theta}_2 + qF_2(x_2)\tilde{\theta}_2 + qD_2(x_1 - x_2) + qu_1 \\
&\vdots \\
\dot{e}_{N-1} &= \dot{x}_N + q\dot{x}_{N-1} = f_N(x_N) + F_N(x_N)\hat{\theta}_N + F_N(x_N)\tilde{\theta}_N + D_N(x_{N-1} - x_N) \\
&\quad + u_{N-1} + qf_{N-1}(x_{N-1}) + q(F_{N-1}(x_{N-1})\hat{\theta}_{N-1}) + qF_{N-1}(x_{N-1})\tilde{\theta}_{N-1} \\
&\quad + q(D_{N-1}(x_{N-2} - x_{N-1})) + qu_{N-2}
\end{aligned} \tag{5.7}$$

which can be written as:

$$\begin{bmatrix} \dot{e}_1 \\ \vdots \\ \dot{e}_{N-1} \end{bmatrix} = \begin{bmatrix} f_2(x_2) + qf_1(x_1) + F_2(x_2)\hat{\theta}_2 + qF_1(x_1)\hat{\theta}_1 + D_2(x_1 - x_2) \\ +qD_1(x_N - x_1) \\ \vdots \\ f_N(x_N) + qf_{N-1}(x_{N-1}) + F_N(x_N)\hat{\theta}_N + qF_{N-1}(x_{N-1})\hat{\theta}_{N-1} \\ +D_N(x_{N-1} - x_N) + qD_{N-1}(x_{N-2} - x_{N-1}) \end{bmatrix} \tag{5.8}$$

$$+ \begin{bmatrix} F_2(x_2)\tilde{\theta}_2 + qF_1(x_1\tilde{\theta}_1) \\ \vdots \\ F_N(x_N)\tilde{\theta}_N \\ +qF_{N-1}(x_{N-1}\tilde{\theta}_{N-1}) \end{bmatrix} + \begin{bmatrix} 1 & 0 & 0 & \cdots & 0 \\ \vdots & \vdots & \vdots & \vdots & \vdots \\ 0 & 0 & \cdots & q & 1 \end{bmatrix} \begin{bmatrix} u_1 \\ \vdots \\ u_{N-1} \end{bmatrix}$$

By choosing

$$\begin{bmatrix} u_1 \\ \vdots \\ u_{N-1} \end{bmatrix} = \begin{bmatrix} 1 & 0 & 0 & \cdots & 0 \\ \vdots & \vdots & \vdots & \vdots & \vdots \\ 0 & 0 & \cdots & q & 1 \end{bmatrix}^{-1} \left\{ + \begin{bmatrix} e_2 \\ \vdots \\ e_{N-1} \\ v \end{bmatrix} - A \right\} \tag{5.9}$$

where, v is the new input vector and

$$A = \begin{bmatrix} f_2(x_2) + qf_1(x_1) + F_2(x_2)\hat{\theta}_2 + qF_1(x_1)\hat{\theta}_1 + D_2(x_1 - x_2) + qD_1(x_N - x_1) \\ \vdots \\ f_N(x_N) + qf_{N-1}(x_{N-1}) + F_N(x_N)\hat{\theta}_N + qF_{N-1}(x_{N-1})\hat{\theta}_{N-1} + D_N(x_{N-1} - x_N) \\ +qD_{N-1}(x_{N-2} - x_{N-1}) \end{bmatrix} \tag{5.10}$$

Then system Eq. (5.8) becomes:

$$\begin{aligned} \dot{e}_1 &= e_2 + F_2(x_2)\tilde{\theta}_2 + qF_1(x_1)\tilde{\theta}_1 \\ &\vdots \\ \dot{e}_{N-2} &= e_{N-1} + F_{N-1}(x_{N-1})\tilde{\theta}_{N-1} + qF_{N-2}(x_{N-2})\tilde{\theta}_{N-2} \\ \dot{e}_{N-1} &= v + F_N(x_N)\tilde{\theta}_N + qF_{N-1}(x_{N-1})\tilde{\theta}_{N-1} \end{aligned} \tag{5.11}$$

To employ ISMC, first defining the nominal system for Eq. (5.11) as:

$$\begin{aligned} \dot{e}_1 &= e_2 \\ \dot{e}_2 &= e_3 \\ \dot{e}_3 &= e_4 \\ &\vdots \\ \dot{e}_{N-2} &= e_{N-1} \\ \dot{e}_{N-1} &= v_o \end{aligned} \tag{5.12}$$

To stabilize the error system Eq. (5.12), the Hurwitz sliding surface is designed as: $\sigma_o = (1 + \frac{d}{dt})^{N-2} e_1 = e_1 + c_1 e_2 + ... + c_{N-3} e_{N-1}$, where the coefficients c_i are selected in a way that σ_o becomes Hurwitz polynomial.

The first derivative of the above SS will be like this: $\dot{\sigma}_o = e_2 + c_1 e_3 + c_2 e_4 + ... + c_{N-3} e_{N-1} + v_o$. By choosing $v_o = -e_2 - c_1 e_3 - c_2 e_4 - ... - c_{N-3} e_{N-1} - k\sigma_o, k > 0$, it becomes $\dot{\sigma}_o = -k\sigma_o$, consequently $\sigma_o \to 0$,which gives $e_1, e_2, ..., e_{N-1} \to 0$. Therefore system Eq. (5.12) is asymptotically stable. Now designing the SS for system Eq. (5.11) as: $\sigma = \sigma_o + z$ where z is an integral term which shall be

calculated later. To avert the reaching phase set $z(0)$ in such a way that $\sigma(0) = 0$. The time derivative of this sliding manifold will be as following.

$$
\begin{aligned}
\dot{\sigma} &= \dot{\sigma}_o + \dot{z} \\
&= \dot{e}_1 + c_1\dot{e}_2 + \cdots + c_{N-3}\dot{e}_{N-2} + \dot{e}_{N-1} + v + \dot{z} \\
&= e_2 + F_2(x_2)\tilde{\theta}_2 + qF_1(x_1)\tilde{\theta}_1 + c_1e3 + c_1F_3(x_3)\tilde{\theta}_3 + qc_1F_2(x_2)\tilde{\theta}_2 + c_2e_4 \\
&+ c_2F_4(x_4)\tilde{\theta}_4 + qc_2F_3(x_3)\tilde{\theta}_3 + \cdots + c_{N-3}e_{N-1} + c_{N-3}F_{N-1}(x_{N-1})\tilde{\theta}_{N-1} \\
&+ q(c_{N-3}F_{N-2}(x_{N-2})\tilde{\theta}_{N-2}) + F_N(x_N)\tilde{\theta}_N + qF_{N-1}(x_{N-1})\tilde{\theta}_{N-1} + v + \dot{z} \\
&= e_2 + c_1e_3 + c_2e_4 + \cdots + c_{N-3}e_{N-1} + v + \dot{z} + qF_1(x_1)\tilde{\theta}_1 + (1 + qc_1)F_2(x_2)\tilde{\theta}_2 \\
&+ ((c_1 + qc_2)F_3(x_3))\tilde{\theta}_3 + ((c_2 + qc_3)F_4(x_4))\tilde{\theta}_4 + \cdots \\
&+ ((c_{N-4} + qc_{N-3})F_{n-2}(x_{N-2}))\tilde{\theta}_{N-2}) + (c_{N-3} + q)(F_{N-1}(x_{N-1})\tilde{\theta}_{N-1}) \\
&+ F_N(x_N)\tilde{\theta}_N \\
&= e_2 + \sum_{i=3}^{N-1} c_{i-2}e_i + v + \dot{z} + qF_1(x_1)\tilde{\theta}_1 + ((1 + qc_1)F_2(x_2)\tilde{\theta}_2) \\
&+ \sum_{i=1}^{N-4}(c_i + qc_{i+1})F_{i+2}(x_{i+2})\tilde{\theta}_{i+2} + ((c_{N-3} + q)F_{N-1}(x_{N-1})\tilde{\theta}_{N-1}) + F_N(x_N)\tilde{\theta}_N
\end{aligned}
\tag{5.13}
$$

The new input term v in Eq. (5.13) is defined as $v = v_s + v_0$, where v_0 is the nominal input vector as well as the other term v_s is a compensator input vector which will be computed later. By choosing a Lyapunov function for equation Eq. (5.13):

$$
V = \frac{1}{2}\{\sigma^T\sigma + \tilde{\theta}_1^T\tilde{\theta}_1 + \tilde{\theta}_2^T\tilde{\theta}_2 + \sum_{i=1}^{N-4}\tilde{\theta}_{i+2}^T\tilde{\theta}_{i+2} + \tilde{\theta}_{N-1}^T\tilde{\theta}_{N-1} + \tilde{\theta}_N^T\tilde{\theta}_N \tag{5.14}
$$

and designing the adaptive laws for $\tilde{\theta}_i, \hat{\theta}_i, i = 1, 2, 3, ..., N$, computing the compensator input vector v_s such that the derivative of the Lyapunov function becomes $\dot{V} < 0$.

Theorem 5.1. *Consider a Lyapunov function as described in Eq.* (5.14). *Then it is only possible to get* $\dot{V} < 0$ *if the following adaptive laws are derived for* $\tilde{\theta}_i, \hat{\theta}_i, i = 1, 2, 3, ..., N$ *and* v_s *are selected as:*

$$
\begin{aligned}
&\dot{z} = -e_2 - \sum_{i=3}^{N-1} c_{i-2}e_i - v_o, v_s = -k\sigma - k\,\mathrm{sign}(\sigma)\\
&\dot{\tilde{\theta}}_1 = -qF_1^T(x_1)\sigma - k_1\tilde{\theta}_1, \dot{\hat{\theta}}_1 = -\dot{\tilde{\theta}}_1\\
&\dot{\tilde{\theta}}_2 = -(1+qc_1)F_2^T(x_2)\sigma - k_2\tilde{\theta}_2, \dot{\hat{\theta}}_2 = -\dot{\tilde{\theta}}_2\\
&\dot{\tilde{\theta}}_{i+2} = -(c_i + qc_{i+1})F_{i+1}^T(x_{i+2})\sigma - k_{N-1} - k_{i+2}\tilde{\theta}_{i+2}, \dot{\hat{\theta}}_{i+2} = -\dot{\hat{\theta}}_{i+2}, i = 1, ..., N-4\\
&\dot{\tilde{\theta}}_{N-1} = -(c_{N-3}+q)F6T_{N-1}\sigma - k_{N-1}\tilde{\theta}_{N-1}, \dot{\hat{\theta}}_{N-1} = -\dot{\tilde{\theta}}_{N-1}\\
&\dot{\tilde{\theta}}_N = -F_N^T(x_N)\sigma - k_N\tilde{\theta}_N, \dot{\hat{\theta}}_N = -\dot{\tilde{\theta}}_N
\end{aligned}
\tag{5.15}
$$

Proof. Since

$$
\begin{aligned}
&\dot{V} = \sigma^T\dot{\sigma} + \tilde{\theta}_1^T\dot{\tilde{\theta}}_1 + \tilde{\theta}_2^T\dot{\tilde{\theta}}_2 + \sum_{i=1}^{N-4}\tilde{\theta}_{i+2}^T\dot{\tilde{\theta}}_{i+2} + \tilde{\theta}_{N-1}^T\dot{\tilde{\theta}}_{N-1} + \tilde{\theta}_N^T\dot{\tilde{\theta}}_N\\
&= \sigma^T\{e_2 + \sum_{i=3}^{N-1} c_{i-2}e_i + v_o + v_s + \dot{z} + qF_1(x_1)\tilde{\theta}_1 + (1+qc_1)F_2(x_2)\tilde{\theta}_2\\
&+ \sum_{i=1}^{N-4}(c_i + qc_{i+1})F_{i+2}(x_{i+2})\tilde{\theta}_{i+2} + (c_{N-3}+q)F_{N-1}(x_{N-1})\tilde{\theta}_{N-1} + F_N(x_N)\tilde{\theta}_N\}\\
&+ \tilde{\theta}_1^T\dot{\tilde{\theta}}_1 + \tilde{\theta}_2^T\dot{\tilde{\theta}}_2 + \sum_{i=1}^{N-4}\tilde{\theta}_{i+2}^T\dot{\tilde{\theta}}_{i+2} + \tilde{\theta}_{N-1}^T\dot{\tilde{\theta}}_{N-1} + \tilde{\theta}_N^T\dot{\tilde{\theta}}_N\\
&= \sigma^T\{e_2 + \sum_{i=3}^{N-1} c_{i-2}e_i + v_o + v_s + \dot{z}\} + \tilde{\theta}_1^T\{\dot{\tilde{\theta}}_1 + qFF_1^T(x_1)\sigma\} + \tilde{\theta}_2^T\{\dot{\tilde{\theta}}_2 + (1+\\
&qc_1)F_2^T(x_2)\sigma\} + \sum_{i=1}^{N-4}\tilde{\theta}_{i+2}^T\{\dot{\tilde{\theta}}_{i+2} + (c_i + qc_{i+1})F_{i+2}^T(x_{i+2})\sigma\} + \tilde{\theta}_{N-1}^T\{\dot{\tilde{\theta}}_{N-1} + (c_{N-3}+\\
&q)F_{N-1}^T(x_{N-1})\sigma\} + \tilde{\theta}_N^T\{\dot{\tilde{\theta}}_N + F_N^T(x_N)\sigma\}
\end{aligned}
\tag{5.16}
$$

By replacing Eq. (5.15) in Eq. (5.16) it yields:

$$
\dot{V} = -k\sigma^2 - \sum_{i=1}^{N} k_i\tilde{\theta}_i^T\tilde{\theta}_i - k\sigma^T\,\mathrm{sign}(\sigma), k > 0 \tag{5.17}
$$

From Eq. (5.17) it can be concluded that $\sigma, \tilde{\theta}_i \to 0$ and since $\sigma \to 0$, therefore $e_i \to 0, i = 1, 2, 3, .., N-1$.

5.4 Application to Dynamical network (DN) of Complex PMSM Systems

In the following, HS of N - Coupled complex PMSM systems connected in ring topology is investigated. Assuming $N = 4$, the Coupled complex PMSM systems in a ring topology can be represented as:

$$\begin{aligned}
\dot{x}_{11} &= a(x_{12} - x_{11}) + d_{11}(x_{41} - x_{11}) \\
\dot{x}_{12} &= bx_{11} - x_{12} - x_{11}x_{13} + d_{12}(x_{42} - x_{12}) \\
\dot{x}_{13} &= 0.5(\bar{x}_{11}x_{12} + x_{11}\bar{x}_{12}) - x_{13} + d_{13}(x_{43} - x_{13}) \\
\dot{x}_{21} &= a(x_{22} - x_{21}) + d_{21}(x_{11} - x_{21}) + \mu_{11} \\
\dot{x}_{22} &= bx_{21} - x_{22} - x_{21}x_{23} + d_{22}(x_{12} - x_{22}) + \mu_{12} \\
\dot{x}_{23} &= 0.5(\bar{x}_{21}x_{22} + x_{21}\bar{x}_{22}) - x_{23} + d_{23}(x_{13} - x_{23}) + \mu_{13} \\
\dot{x}_{31} &= a(x_{32} - x_{31}) + d_{31}(x_{21} - x_{31}) + \mu_{21} \\
\dot{x}_{32} &= bx_{31} - x_{32} - x_{31}x_{33} + d_{32}(x_{22} - x_{32}) + \mu_{22} \\
\dot{x}_{33} &= 0.5(\bar{x}_{31}x_{32} + x_{31}\bar{x}_{32}) - x_{33} + d_{33}(x_{23} - x_{33}) + \mu_{23} \\
\dot{x}_{41} &= a(x_{42} - x_{41}) + d_{41}(x_{31} - x_{41}) + \mu_{31} \\
\dot{x}_{42} &= bx_{41} - x_{42} - x_{41}x_{43} + d_{42}(x_{32} - x_{42}) + \mu_{32} \\
\dot{x}_{43} &= 0.5(\bar{x}_{41}x_{42} + x_{41}\bar{x}_{42}) - x_{43} + d_{33}(x_{33} - x_{43}) + \mu_{33}
\end{aligned} \tag{5.18}$$

Where, $x_{k1} = x_{k1r} + jx_{k1i}, x_{k2} = x_{k2r} + jx_{k2i}$ are complex and $x_{k3} = x_{k3r}$ are real. $\bar{x}_{k1}$, $\bar{x}_{k2}$ denote the complex conjugate variables of x_{k1}, x_{k2}, k=1,2,3,4 and a,b are unknown real terms.

let $\hat{a}$, $\hat{b}$ be the estimates of the parameters a, b and let $\tilde{a} = a - \hat{a}, \tilde{b} = b - \hat{b}$ be the errors in estimating the parameters a, b respectively. Then Eq. (5.18) after some modification is written in the following:

$$\begin{aligned}
\dot{x}_{1r} &= f_{1r} + F_{1r}\hat{\theta} + F_{1r}\tilde{\theta} + D_1 G_{1r} \\
\dot{x}_{1i} &= f_{1i} + F_{1i}\hat{\theta} + F_{1i}\tilde{\theta} + D_1 G_{1i}
\end{aligned}$$

$$\begin{aligned}
\dot{x}_{2r} &= f_{2r} + F_{2r}\hat{\theta} + F_{2r}\tilde{\theta} + D_2 G_{2r} + \mu_{1r} \\
\dot{x}_{2i} &= f_{2i} + F_{2i}\hat{\theta} + F_{2i}\tilde{\theta} + D_2 G_{2i} + \mu_{1i} \\
\dot{x}_{3r} &= f_{3r} + F_{3r}\hat{\theta} + F_{3r}\tilde{\theta} + D_3 G_{3r} + \mu_{2r} \\
\dot{x}_{3i} &= f_{3i} + F_{3i}\hat{\theta} + F_{3i}\tilde{\theta} + D_3 G_{3i} + \mu_{2i} \\
\dot{x}_{4r} &= f_{4r} + F_{4r}\hat{\theta} + F_{4r}\tilde{\theta} + D_4 G_{4r} + \mu_{3r} \\
\dot{x}_{4i} &= f_{4i} + F_{4i}\hat{\theta} + F_{4i}\tilde{\theta} + D_3 G_{4i} + \mu_{3i}
\end{aligned} \tag{5.19}$$

where

$$f_{kr} = \begin{bmatrix} 0 \\ -x_{k2r} - x_{k1r}x_{k3} \\ 0.5(x_{k1r}x_{k2r} + x_{k1i}x_{k2i}) - x_{k3} \end{bmatrix}, F_{kr} = \begin{bmatrix} x_{k2r} - x_{k1r} & 0 \\ 0 & x_{k1r} \\ 0 & 0 \end{bmatrix}$$

$$f_{ki} = \begin{bmatrix} 0 \\ -x_{k2r} - x_{k1r}x_{k3} \\ 0 \end{bmatrix}, F_{ki} = \begin{bmatrix} x_{k2i} - x_{k1i} & 0 \\ 0 & x_{k1i} \\ 0 & 0 \end{bmatrix}, k = 1, 2, 3, 4$$

$$G_{1r} = \begin{bmatrix} x_{41r} - x_{11r} \\ x_{42r} - x_{12r} \\ x_{4r} - x_{13} \end{bmatrix}, G_{1i} = \begin{bmatrix} x_{41i} - x_{11i} \\ x_{42i} - x_{12i} \\ 0 \end{bmatrix} G_{2r} = \begin{bmatrix} x_{11r} - x_{21r} \\ x_{12r} - x_{22r} \\ x_{13} - x_{43} \end{bmatrix}, G_{2i} = \begin{bmatrix} x_{11i} - x_{21i} \\ x_{12i} - x_{22i} \\ 0 \end{bmatrix}$$

$$G_{3r} = \begin{bmatrix} x_{21r} - x_{31r} \\ x_{22r} - x_{32r} \\ x_{23} - x_{33} \end{bmatrix}, G_{3i} = \begin{bmatrix} x_{21i} - x_{31i} \\ x_{22i} - x_{32i} \\ 0 \end{bmatrix}, G_{4r} = \begin{bmatrix} x_{31r} - x_{41r} \\ x_{32r} - x_{42r} \\ x_{33} - x_{43} \end{bmatrix}, G_{4i} = \begin{bmatrix} x_{31i} - x_{41i} \\ x_{32i} - x_{42i} \\ x_{33} - x_{43} \end{bmatrix}$$

$$u_{lr} = \begin{bmatrix} u_{l1r} \\ u_{l2r} \\ u_{lr} \end{bmatrix}, u_{li} = \begin{bmatrix} u_{l1i} \\ u_{l2i} \\ 0 \end{bmatrix}, l = 1, 2, 3, \hat{\theta} = \begin{bmatrix} \hat{a} \\ \hat{b} \end{bmatrix}, \tilde{\theta} = \begin{bmatrix} \tilde{a} \\ \tilde{b} \end{bmatrix} \tag{5.20}$$

Defining the error as: $e_k = e_{kr} + je_{ki} = x_{k+1} + qx_k = x_{(k+1)r} + qx_{kr} + jx_{(k+1)i} + qx_{ki}, k = 1, 2, 3,$ this gives $e_{kr} = x_{(k+1)r} + qx_{kr}$ and, $e_{ki} = x_{(k+1)i} + qx_{ki},\ k = 1, 2, 3.$ The error dynamics of this system becomes as:

$$\begin{bmatrix}\dot{e}_{1r}\\ \dot{e}_{2r}\\ \dot{e}_{3r}\end{bmatrix} = \begin{bmatrix}(f_{2r}+qf_{1r})+(F_{2r}+qF_{1r}\hat{\theta})+D_2G_{2r}+qD_1G_{1r})\\ (f_{3r}+qf_{2r})+(F_{3r}+qF_{2r}\hat{\theta})+D_3G_{3r}+qD_2G_{2r})\\ (f_{4r}+qf_{3r})+(F_{4r}+qF_{3r}\hat{\theta})+D_4G_{4r}+qD_3G_{3r})\end{bmatrix} + \begin{bmatrix}F_{2r}+qF_{1r}\\ F_{3r}+qF_{2r}\\ F_{4r}+qF_{3r}\end{bmatrix}$$
$$+ \begin{bmatrix}I & 0 & 0\\ -qI & I & 0\\ 0 & -qI & I\end{bmatrix}\begin{bmatrix}\mu_{1r}\\ \mu_{2r}\\ \mu_{3r}\end{bmatrix}$$

$$\begin{bmatrix}\dot{e}_{1i}\\ \dot{e}_{2i}\\ \dot{e}_{3i}\end{bmatrix} = \begin{bmatrix}(f_{2i}+qf_{1i})+(F_{2i}+qF_{1i}\hat{\theta})+D_2G_{2i}+qD_1G_{1i})\\ (f_{3i}+qf_{2i})+(F_{3i}+qF_{2i}\hat{\theta})+D_3G_{3i}+qD_2G_{2i})\\ (f_{4i}+qf_{3i})+(F_{4i}+qF_{3i}\hat{\theta})+D_4G_{4i}+qD_3G_{3i})\end{bmatrix} + \begin{bmatrix}F_{2i}+qF_{1i}\\ F_{3i}+qF_{2i}\\ F_{4i}+qF_{3i}\end{bmatrix}$$
$$+ \begin{bmatrix}I & 0 & 0\\ -qI & I & 0\\ 0 & -qI & I\end{bmatrix}\begin{bmatrix}\mu_{1i}\\ \mu_{2i}\\ \mu_{3i}\end{bmatrix} \tag{5.21}$$

by choosing,

$$\begin{bmatrix}\mu_{1r}\\ \mu_{2r}\\ \mu_{3r}\end{bmatrix} = \begin{bmatrix}I & 0 & 0\\ -qI & I & 0\\ 0 & -qI & I\end{bmatrix}^{-1}\begin{bmatrix}(F_qr1)\\ (F_qr2)\\ (F_qr3)\end{bmatrix} + \begin{bmatrix}e_{2r}\\ e_{3r}\\ v_r\end{bmatrix}$$
$$\begin{bmatrix}\mu_{1i}\\ \mu_{2i}\\ \mu_{3i}\end{bmatrix} = \begin{bmatrix}I & 0 & 0\\ -qI & I & 0\\ 0 & -qI & I\end{bmatrix}^{-1}\begin{bmatrix}(F_qi1)\\ (F_qi2)\\ (F_qi3)\end{bmatrix} + \begin{bmatrix}e_{2i}\\ e_{3i}\\ v_i\end{bmatrix} \tag{5.22}$$

where

$F_qr1 = (f_{2r}+qf_{1r})+(F_{2r}+qF_{1r}\hat{\theta})+D_2G_{2r}+qD_1G_{1r}$ $F_qr2 = (f_{3r}+qf_{2r})+(F_{3r}+qF_{2r}\hat{\theta})+D_3G_{3r}+qD_2G_{2r}$ $F_qr3 = (f_{4r}+qf_{3r})+(F_{4r}+qF_{3r}\hat{\theta})+D_4G_{4r}+qD_3G_{3r}$

$F_qi1 = (f_{2i}+qf_{1i})+(F_{2i}+qF_{1i}\hat{\theta})+D_2G_{2i}+qD_1G_{1i}$ $F_qi2 = (f_{3i}+qf_{2i})+(F_{3i}+qF_{2i}\hat{\theta})+D_3G_{3i}+qD_2G_{2i}$ $F_qi3 = (f_{4i}+qf_{3i})+(F_{4i}-+F_{3i}\hat{\theta})+D_4G_{4i}+qD_3G_{3i}$

The system Eq. (5.21) becomes:

$$\begin{bmatrix} \dot{e}_{1r} \\ \dot{e}_{2r} \\ \dot{e}_{3r} \end{bmatrix} = \begin{bmatrix} e_{2r} \\ e_{3r} \\ v_r \end{bmatrix} + \begin{bmatrix} F_{2r} + qF_{1r} \\ F_{3r} + qF_{2r} \\ F_{4r} + qF_{3r} \end{bmatrix} \tilde{\theta}$$

$$\begin{bmatrix} \dot{e}_{1i} \\ \dot{e}_{2i} \\ \dot{e}_{3i} \end{bmatrix} = \begin{bmatrix} e_{2i} \\ e_{3i} \\ v_i \end{bmatrix} + \begin{bmatrix} F_{2i} + qF_{1i} \\ F_{3i} + qF_{2i} \\ F_{4i} + qF_{3i} \end{bmatrix} \tilde{\theta} \tag{5.23}$$

taking the nominal system for Eq. (5.23) as:

$$\begin{bmatrix} \dot{e}_{1r} \\ \dot{e}_{2r} \\ \dot{e}_{3r} \end{bmatrix} = \begin{bmatrix} e_{2r} \\ e_{3r} \\ v_{0r} \end{bmatrix}, \begin{bmatrix} \dot{e}_{1i} \\ \dot{e}_{2i} \\ \dot{e}_{3i} \end{bmatrix} = \begin{bmatrix} e_{2i} \\ e_{3i} \\ v_{0i} \end{bmatrix} \tag{5.24}$$

and defining the SS for nominal system Eq. (5.24) as:

$$\begin{aligned} \sigma_{0r} &= e_{1r} + 2e_{2r} + e_{3r} \\ \sigma_{0i} &= e_{1i} + 2e_{2i} + e_{3i} \end{aligned} \tag{5.25}$$

then,

$$\begin{aligned} \dot{\sigma}_{0r} &= \dot{e}_{1r} + 2\dot{e}_{2r} + \dot{e}_{3r} = e_{2r} + 2e_{3r} + v_{0r} \\ \dot{\sigma}_{0i} &= \dot{e}_{1i} + 2\dot{e}_{2i} + \dot{e}_{3i} = e_{2i} + 2e_{3i} + v_{0i} \end{aligned} \tag{5.26}$$

by choosing,

$$\begin{aligned} v_{0r} &= -e_{2r} - 2e_{3r} - k_1 \operatorname{sign}(\sigma_{0r}), k_1 > 0 \\ v_{0i} &= -e_{2i} - 2e_{3i} - k_2 \operatorname{sign}(\sigma_{0i}), k_2 > 0 \end{aligned} \tag{5.27}$$

Eq. (5.26) becomes:

$$\begin{aligned} \dot{\sigma}_{0r} &= -k_1\sigma_{0r} - k_1 \operatorname{sign}(\sigma_{0r}) \\ \dot{\sigma}_{0i} &= -k_2\sigma_{0i} - k_2 \operatorname{sign}(\sigma_{0i}) \end{aligned} \tag{5.28}$$

Therefore, from Eq. (5.28) it can be concluded that Eq. (5.25) is asymptotically stable. Now defining the SS for the error dynamic system Eq. (5.24) as:

$$\begin{aligned}\sigma_r &= \sigma_{0r} + z_r = e_{1r} + 2e_{2r} + e_{3r} + z_r \\ \sigma_i &= \sigma_{0i} + z_i = e_{1i} + 2e_{2i} + e_{3i} + z_i\end{aligned} \tag{5.29}$$

where z_r, z_i are some integral terms which will be calculated later. To avert the reaching phase, take up $z_r(0), z_i(0)$ such that $\sigma_r(0) = 0, \sigma_i(0) = 0$. By choosing the following values for v_r and v_i as:

$$\begin{aligned}v_r &= v_{0r} + v_{sr} \\ v_i &= v_{oi} + v_i\end{aligned}$$

where, v_{0r}, v_{0i} are the nominal inputs and v_{sr}, v_{si} are compensator terms computed later. Then the first derivative of Eq. 5.29 becomes:

$$\begin{aligned}\dot{\sigma}_r &= \dot{\sigma}_{0r} + \dot{z}_r = \dot{e}_{1r} + 2\dot{e}_{2r} + \dot{e}_{3r} + \dot{z}_r \\ &= e_{2r} + (F_{2r} + qF_{1r})\tilde{\theta} + 2e_{3r} + 2(F_{3r} + qF_{2r})\tilde{\theta} + (F_{4r} + qF_{3r})\tilde{\theta} + v_{0r} + v_{sr} + \dot{z}_r \\ \dot{\sigma}_i &= \dot{\sigma}_{0i} + \dot{z}_i = \dot{e}_{1i} + 2\dot{e}_{2i} + \dot{e}_{3i} + \dot{z}_i \\ &= e_{2i} + (F_{2i} + qF_{1i})\tilde{\theta} + 2e_{3i} + 2(F_{3i} + qF_{2i})\tilde{\theta} + (F_{4i} + qF_{3i})\tilde{\theta} + v_{0i} + v_{si} + \dot{z}_i\end{aligned} \tag{5.30}$$

by taking a Lyapunov function: $V = \frac{1}{2}\sigma_r^T\sigma_r + \frac{1}{2}\sigma_i^T\sigma_i + \frac{1}{2}\tilde{\theta}^T\tilde{\theta}$, and designing the adaptive laws for $\tilde{\theta}, \hat{\theta}$ and computing v_{sr}, v_{si} in such a manner that $\dot{V} < 0$.

Theorem 5.2. *Consider a Lyapunov function of this kind:* $V = \frac{1}{2}\sigma_r^T\sigma_r + \frac{1}{2}\sigma_i^T\sigma_i + \frac{1}{2}\tilde{\theta}^T\tilde{\theta}$ *then it is possible to get* $\dot{V} < 0$ *if the following adaptive laws are derived for* $\dot{\tilde{\theta}}, \dot{\hat{\theta}}$ *and the values of* v_{sr}, v_i *are chosen as:*

$$\begin{aligned}\dot{z}_r &= -\dot{e}_{2r} - 2e_{3r} - v_{0r}, v_{sr} = -k - 3\sigma_r - k_3\,\mathrm{sign}(\sigma_r) \\ \dot{z}_i &= -\dot{e}_{2i} - 2e_{3i} - v_{0r}\end{aligned}$$

$$
\begin{aligned}
v_{si} &= -k - 4\sigma_i - k_4\,\mathrm{sign}(\sigma_i) \\
\dot{\tilde{\theta}} &= -\sigma_r^T\{(F_{2r}+qF_{1r})^T + 2(F_{3r}+qF_{2r})^T + (F_{4r}+qF_{3r})^T\} - \sigma_i^T\{(F_{2i}+qF_{1i})^T \\
&\quad + 2(F_{3i}+qF_{2i})^T + (F_{4i}+qF_{3i})^T\} - K_5\tilde{\theta} \\
\dot{\hat{\theta}} &= -\dot{\tilde{\theta}}, k_i > 0, i = 1, ..., 5
\end{aligned}
\tag{5.31}
$$

Proof. Since

$$
\begin{aligned}
\dot{V} &= \sigma_r^T\dot{\sigma}_r + \sigma_i^T\dot{\sigma}_i + \tilde{\theta}^T\dot{\tilde{\theta}} \\
\dot{V} &= \sigma_r^T\{e_{2r} + 2e_{3r} + v_{0r} + v_{sr} + \dot{z}_r\} + \sigma_i^T\{e_{2i} + 2e_{3i} + v_{0i} + v_{si} + \dot{z}_i\} \\
&\quad + \tilde{\theta}^T[\dot{\tilde{\theta}} + \sigma_r^T\{(F_{2r}+qF_{1r})^T + 2(F_{3r}+qF_{2r})^T + (F_{4r}+qF_{3r})^T\} \\
&\quad + \sigma_i^T\{(F_{2i}+qF_{1i})^T + 2(F_{3i}+qF_{2i})^T + (F_{4i}+qF_{3i}^T)\}]
\end{aligned}
\tag{5.32}
$$

By replacing the values of adaptive laws $\dot{\tilde{\theta}}$, $\dot{\hat{\theta}}$ and the values of v_{sr}, v_i proposed in Eq. (5.32) the above system Eq. (5.33) becomes:

$$
\begin{aligned}
\dot{V} &= -k_1\sigma_r^T\sigma_r - k_2\sigma_i^T\sigma_i - k_2\tilde{\theta}^T\tilde{\theta} - k_3\sigma_r^T\,\mathrm{sign}(\sigma_r) - k_4\sigma_i^T\,\mathrm{sign}(\sigma_i) < 0 \\
&= -k_1\sigma_r^T\sigma_r - k_2\sigma_i^T\sigma_i - k_2\tilde{\theta}^T\tilde{\theta} - k_3|\sigma_r| - k_4|\sigma_i| < 0, \forall\ k_1, k_2, k_3, k_4 > 0
\end{aligned}
\tag{5.33}
$$

This shows that the designed sliding surfaces σ_r, σ_i and adaptive laws $\tilde{\theta} \to 0$ therefore $e_{kr}, e_{ki} \to 0, k = 1, 2, 3, 4$. Convergence of error system to zero ensures hybrid synchronization of coupled complex chaotic PMSMs connected in ring topology.

5.5 Performance Analysis

The work presented in this chapter can be compared with the work presented in [33]. The network model defined in Eq.(5.1) is different than the network model presented in [33] because it consists of constant parameters which are considered

to be uncertain. The error dynamics defined in Eqs.(5.7,5.8) are entirely different as defined in Eq.(6) of Ref[46]. The proposed control methodology employed in [33] is direct design whereas integral sliding mode control technique is used in this thesis which is advantageous as described in the thesis. Synchronization and anti-synchronization achieved in [33] by considering known parameters whereas Hybrid synchronization is achieved in this thesis by considering unknown parameters. Moreover, estimating the unknown parameters is another valuable difference between [33] and in this thesis.

Simulation results are presented by taking the following initial conditions, $x_1(0) = (1+2j, 3+6j, 5)^T, x_2(0) = (4-2j, 1+2j, 8)^T, x_3(0) = (-3+4j, -2+5j, -1)^T, x_4(0) = (5-5j, 4-2j, 3)^T$. Figure 5.3 displays the convergence of real and imaginary parts of anti-synchronization error dynamics to zero. Figure 5.4 depict that dynamic states of all the systems are anti-synchronized. From this it is very clear that the dynamic states of the second systems are Anti-synchronized with the dynamic states of the first system. Whereas states of the third system are Anti-synchronized with the second system but due to the connection arrangement these are synchronized with the first system. Similarly, states of the fourth system are Anti-synchronized with the third system but are synchronized with the second system. Figure 5.5 shows the convergence of synchronization error dynamics to zero. Synchronization phenomena of the all the systems connected in the ring connection is depicted in Fig. 5.6. Figure 5.7 shows that the estimated parameters $\hat{a}, \hat{b}$ converge to their true values a,b respectively. Figures 5.8 - 5.18 depicts the control effort exerted to achieve the hybrid synchronization.

5.6 Summary

In this chapter, parameter identification and HS of complex chaotic permanent magnet synchronous motors system connected in a ring topology are established. The methodology is based on adaptive ISMC, where synchronization error system

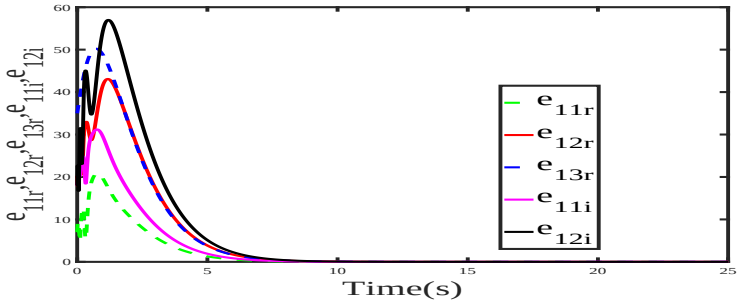

(a)

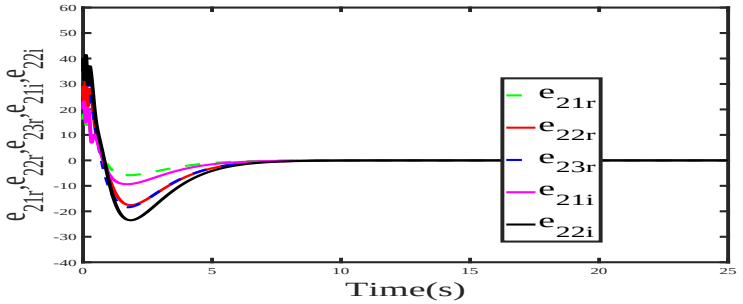

(b)

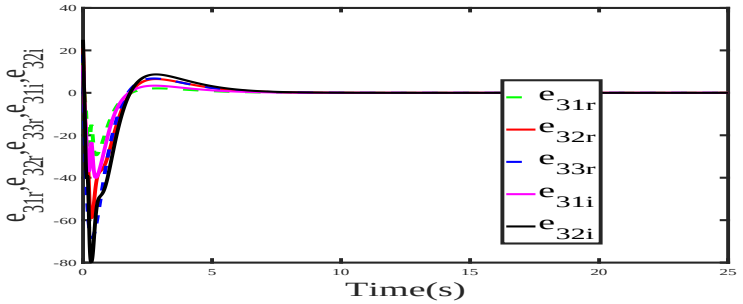

(c)

FIGURE 5.3: Convergence of real and imaginary parts of anti-synchronization error dynamics to zero

is transformed into a typical form which contains nominal part and a few unknown terms. The unknown terms are computed adaptively. Moreover, the error system has been stabilized using ISMC. The stability of the designed sliding surface has been proved by the lyapunov stability theorem. The designed stabilizing controller for error system comprised of nominal control and compensator control. The effectiveness of the proposed technique has been presented through extensive mathematical expressions and MATLAB simulations. The simulation results show that hybrid synchronization is achieved through proposed control laws, another key fact to remember that the uncertain parameters converge to their actual values.

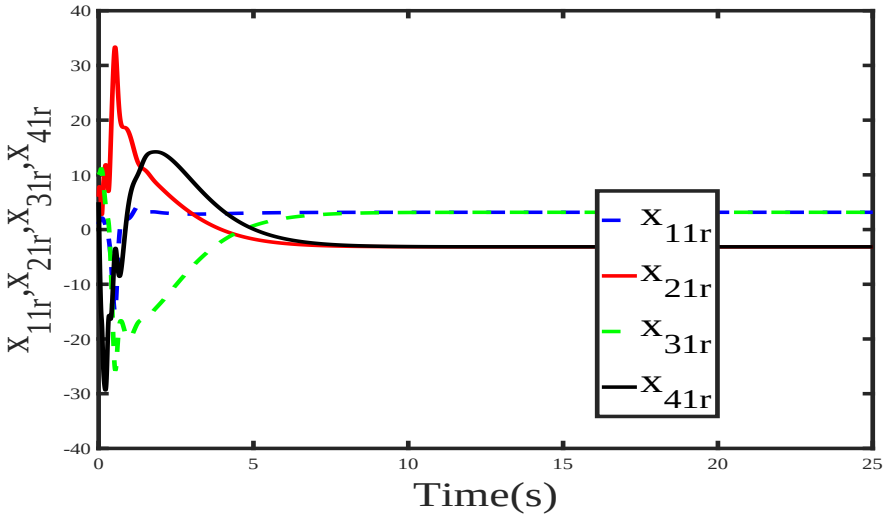
x11r,x21r,x31r,x41r
Time(s)
x11r
x21r
x31r
x41r

(a)

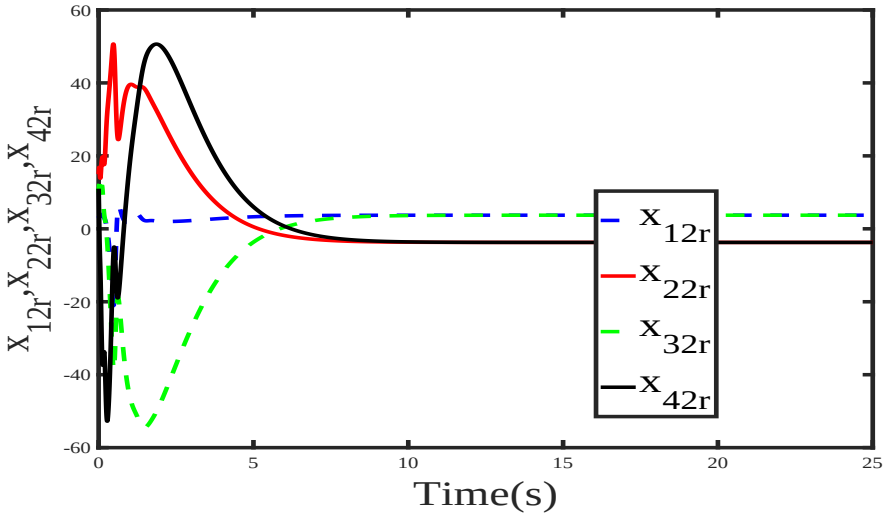
x12r,x22r,x32r,x42r
Time(s)
x12r
x22r
x32r
x42r

(b)

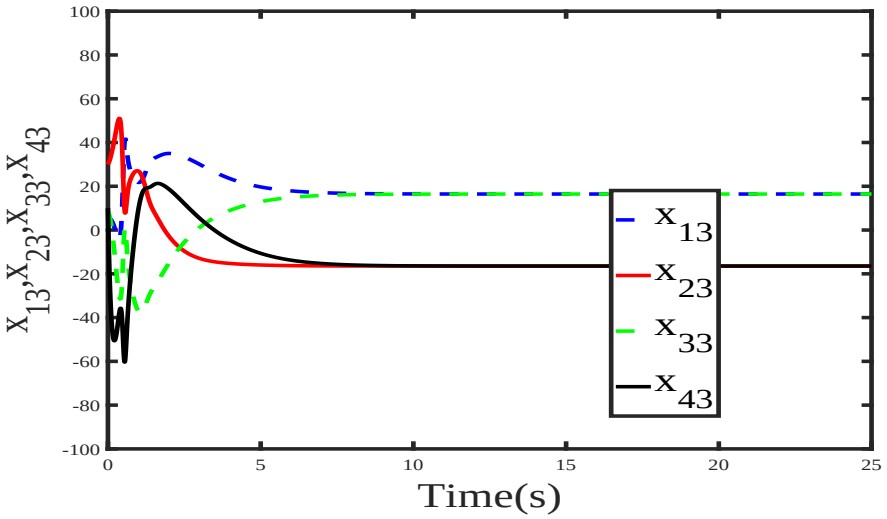
x13,x23,x33,x43
Time(s)
x13
x23
x33
x43

(c)

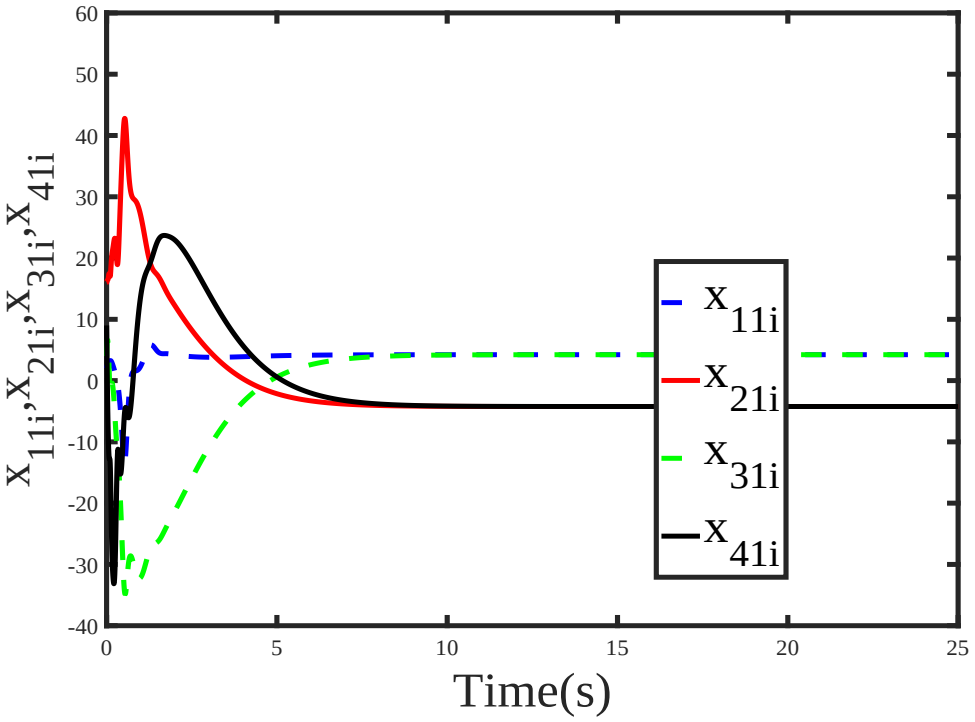

(d)

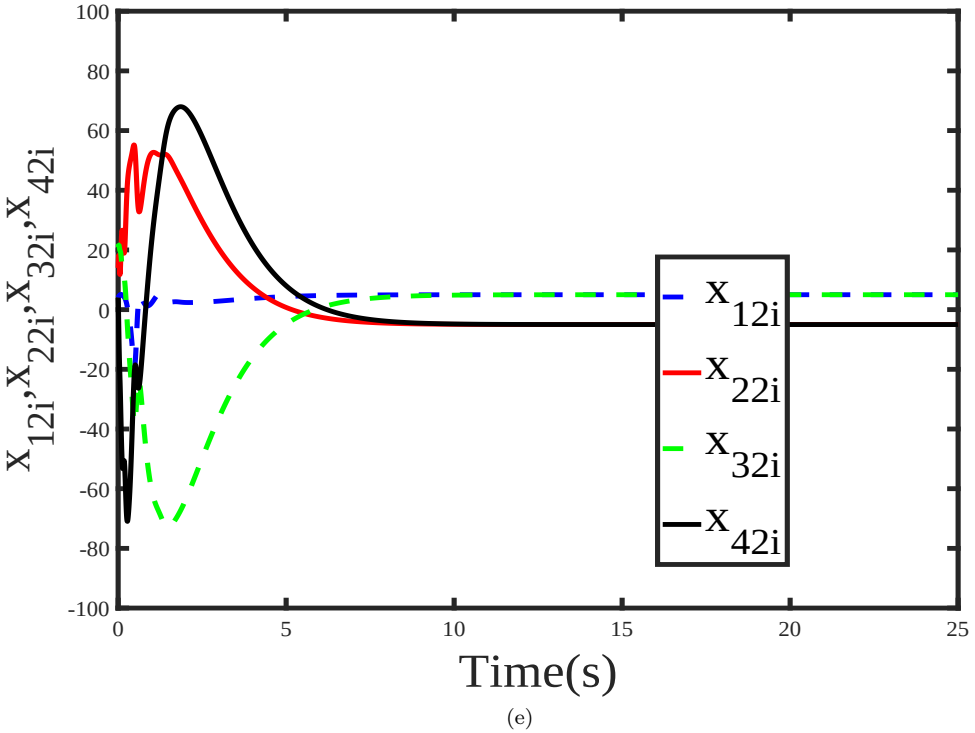

(e)

FIGURE 5.4: Convergence of system states in anti-synchronization scenario (a) AS of real parts of system states $x_{11r}, x_{21r}, x_{31r}, x_{41r}$, (b) AS of imaginary parts of system states $x_{11i}, x_{21i}, x_{31i}, x_{41i}$, (c) AS of real parts of system states $x_{12r}, x_{22r}, x_{32r}, x_{42r}$, (d) AS of imaginary parts of system states $x_{12i}, x_{22i}, x_{32i}, x_{42i}$,(e) AS of system states $x_{13}, x_{23}, x_{33}, x_{43}$.

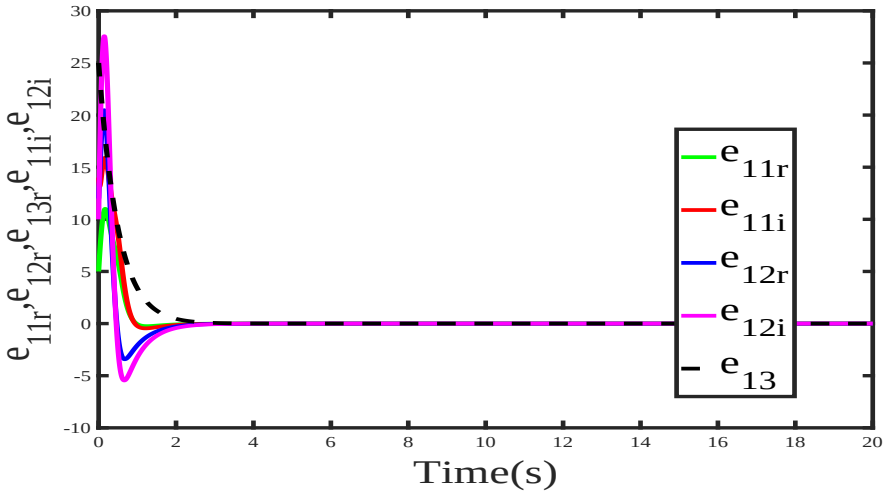

(a)

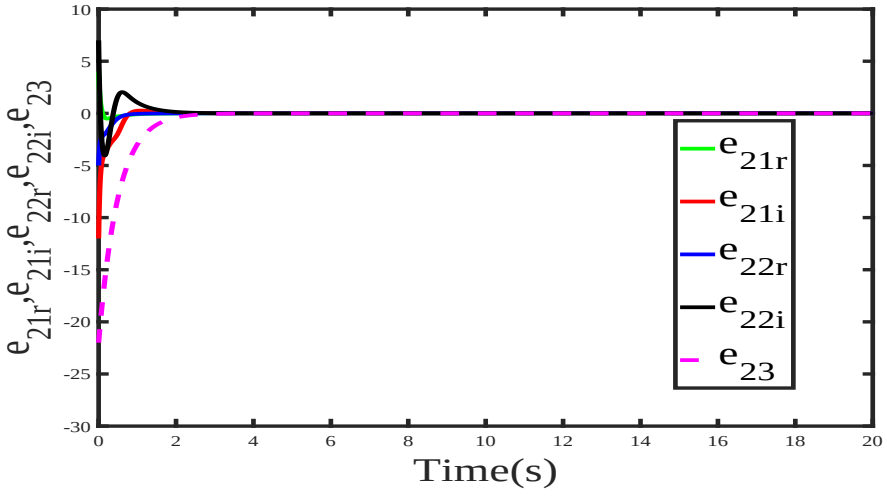

(b)

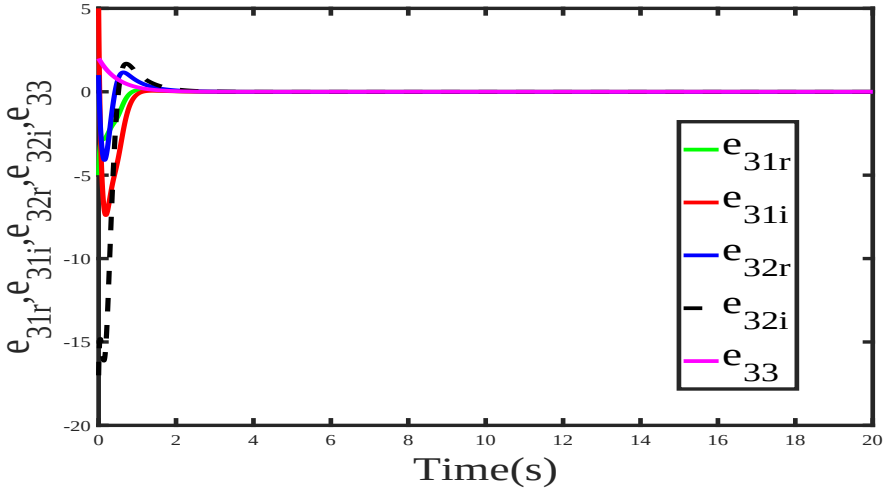

(c)

FIGURE 5.5: Convergence of real and imaginary parts of synchronization errors (a) $e_{11r}, e_{12r}, e_{13r}, e_{11i}, e_{12i}$, (b) $e_{21r}, e_{22r}, e_{23r}, e_{21i}, e_{22i}$, (c) $e_{31r}, e_{32r}, e_{33r}, e_{31i}, e_{32i}$.

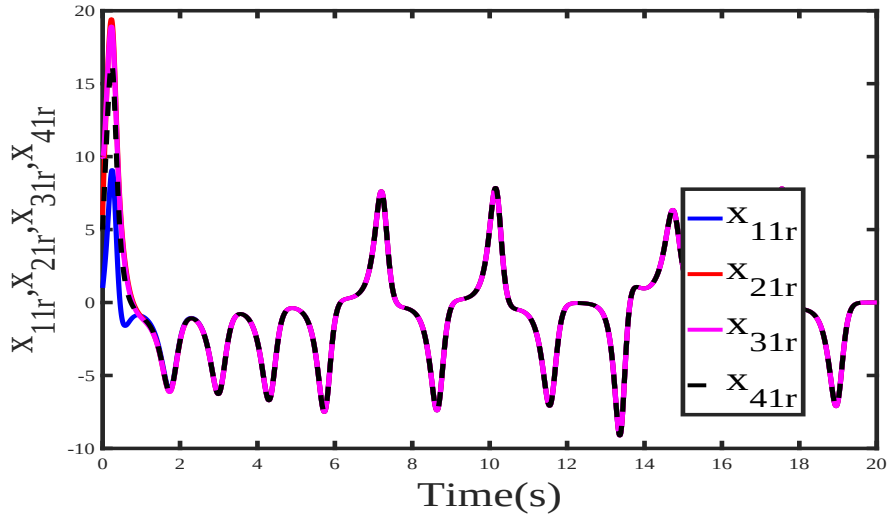
x11r,x21r,x31r,x41r
Time(s)
x11r
x21r
x31r
x41r

(a)

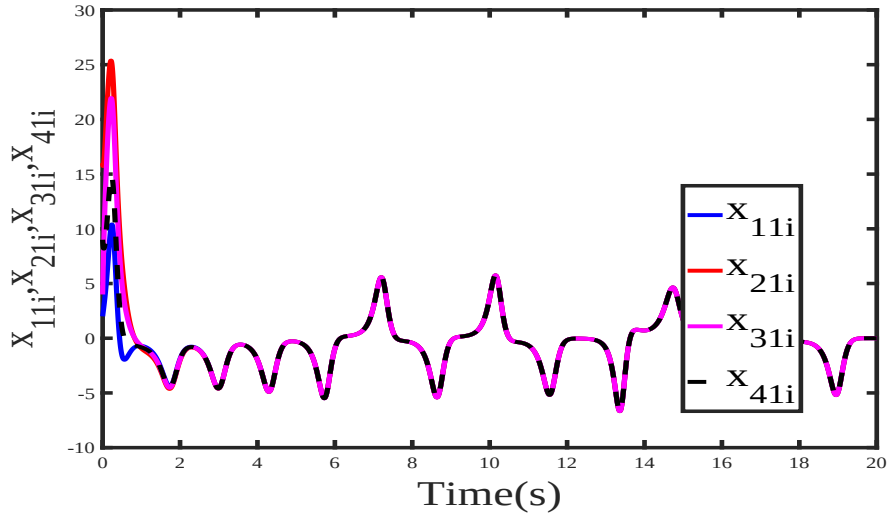
x11i,x21i,x31i,x41i
Time(s)
x11i
x21i
x31i
x41i

(b)

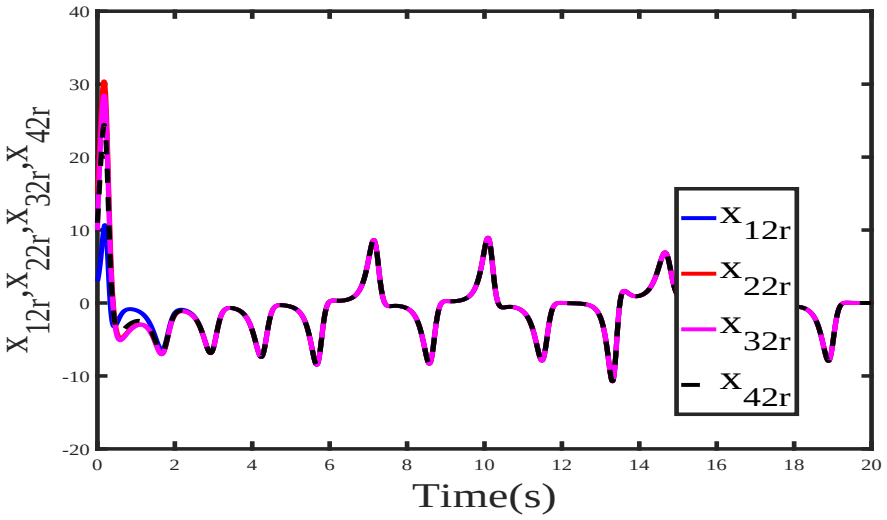
x12r,x22r,x32r,x42r
Time(s)
x12r
x22r
x32r
x42r

(c)

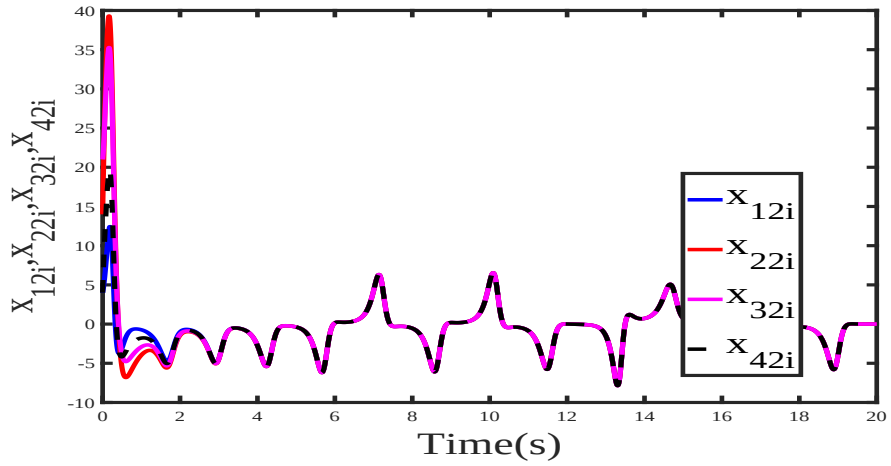

(d)

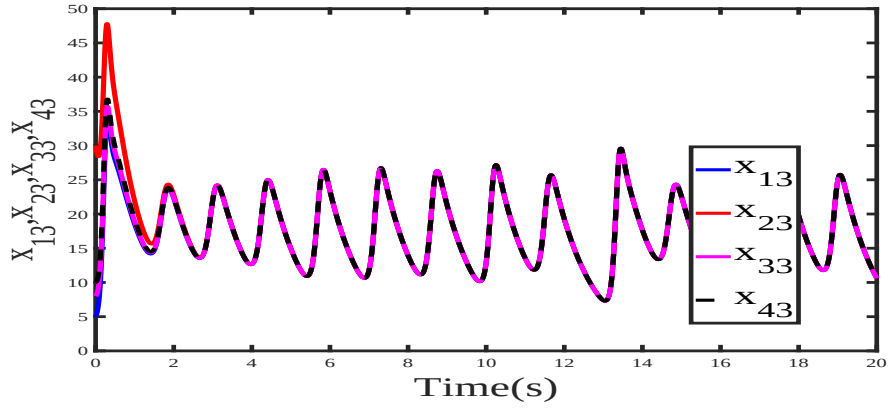

(e)

FIGURE 5.6: Convergence of system states in synchronization scenario (a) synchronization of real parts of system states $x_{11r}, x_{21r}, x_{31r}, x_{41r}$, (b) synchronization of real parts of system states $x_{12r}, x_{22r}, x_{32r}, x_{42r}$, (c) synchronization of real parts of system states $x_{13}, x_{23}, x_{33}, x_{43}$, (d) synchronization of imaginary parts of system states $x_{11i}, x_{21i}, x_{31i}, x_{41i}$, (e) synchronization of imaginary parts of system states $x_{12i}, x_{22i}, x_{32i}, x_{42i}$.

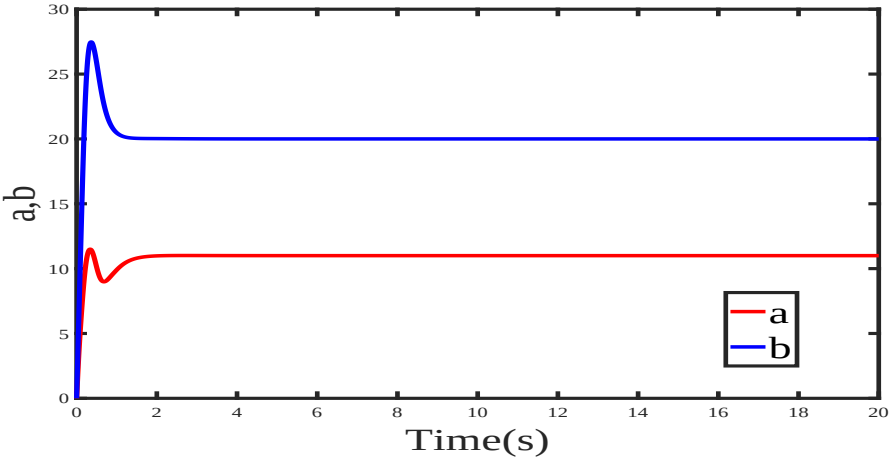

FIGURE 5.7: Convergence of Estimated parameters $\hat{a}, \hat{b}$ to their true values a, b

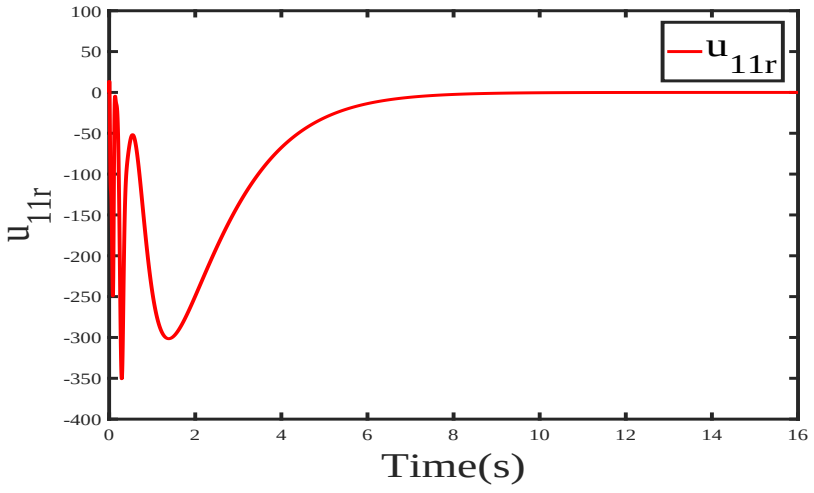

(a)

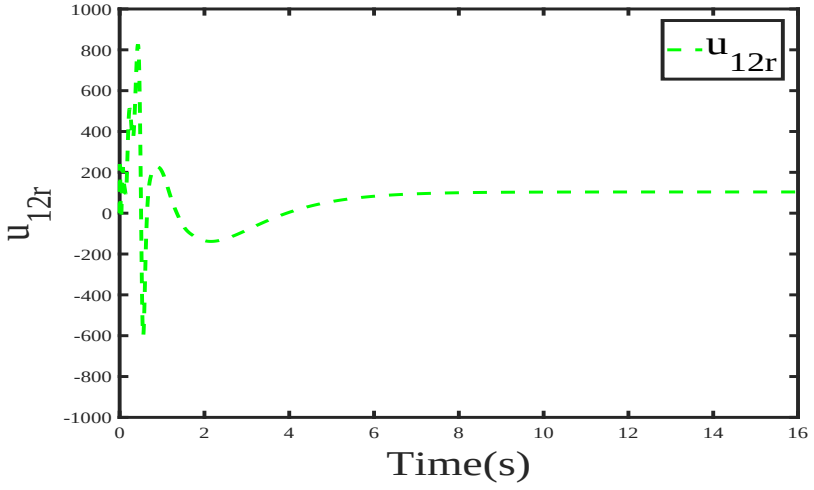

(b)

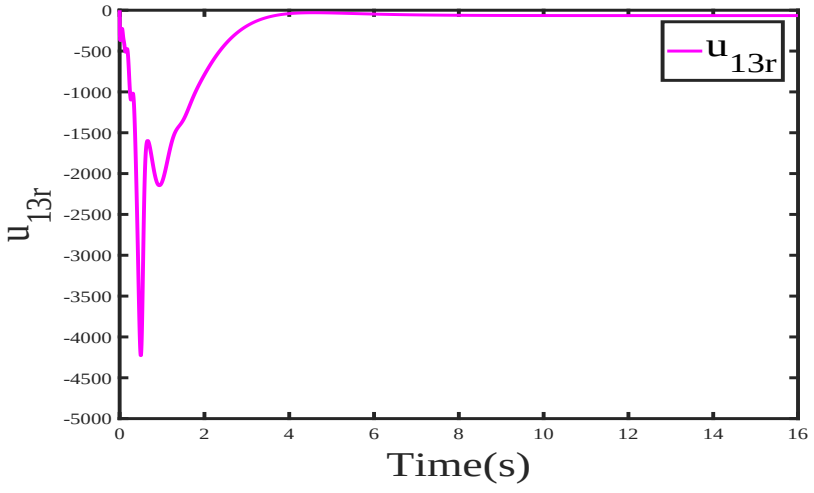

(c)

FIGURE 5.8: Control effort for anti-synchronization (a) u_{11r} (b) u_{12r} (c) u_{13r}

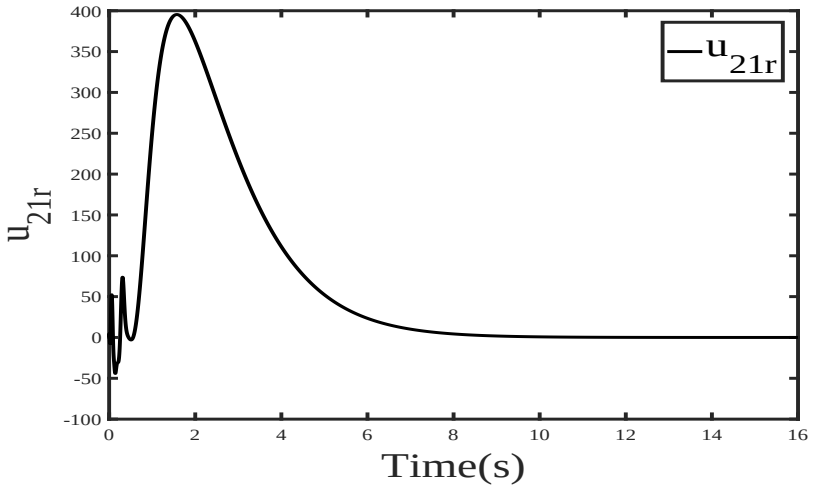

(a)

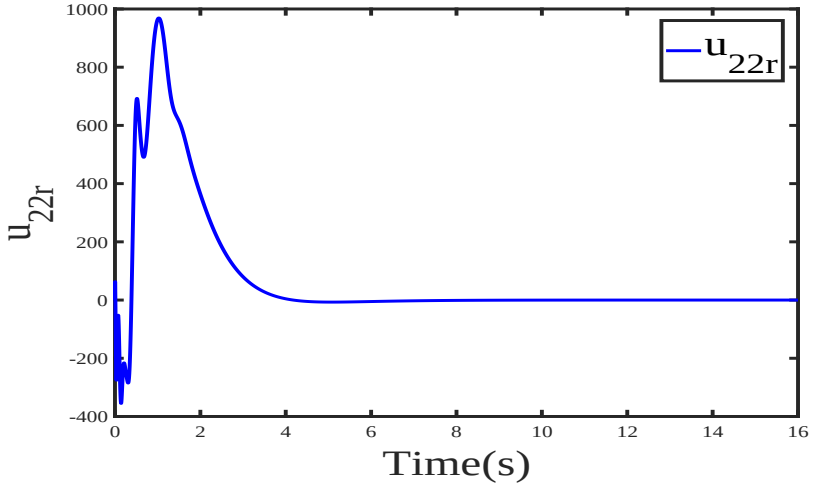

(b)

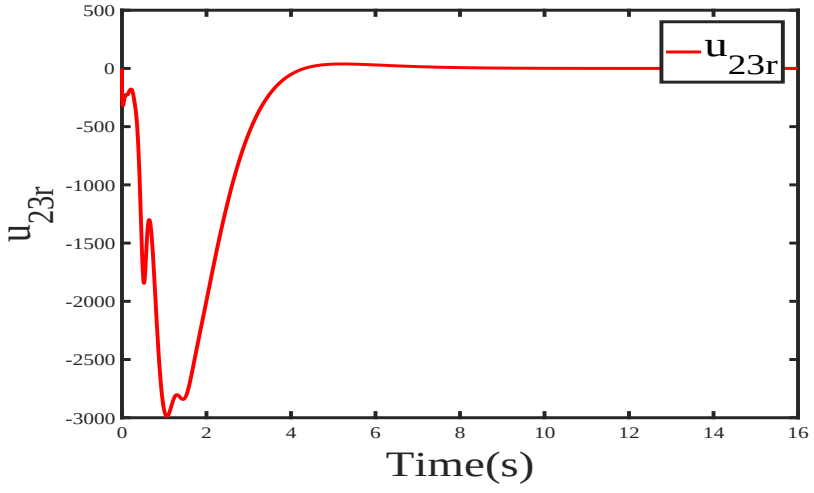

(c)

FIGURE 5.9: Control effort for anti-synchronization (a) u_{21r} (b) u_{22r} (c) u_{23r}

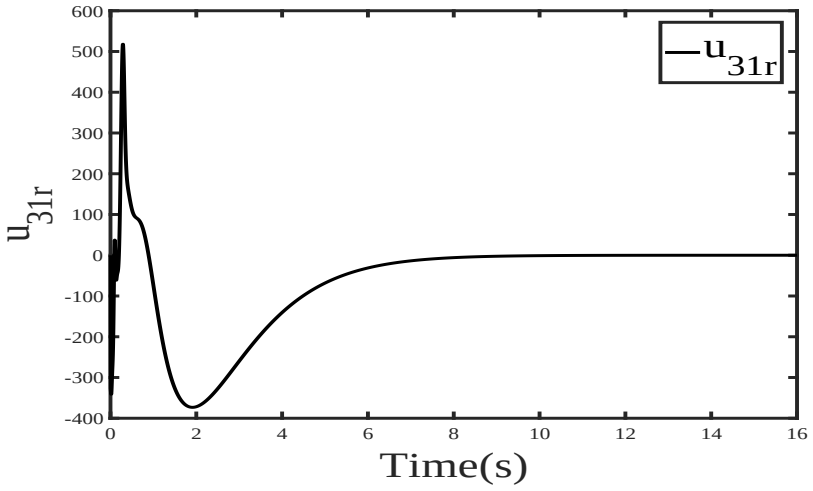

(a)

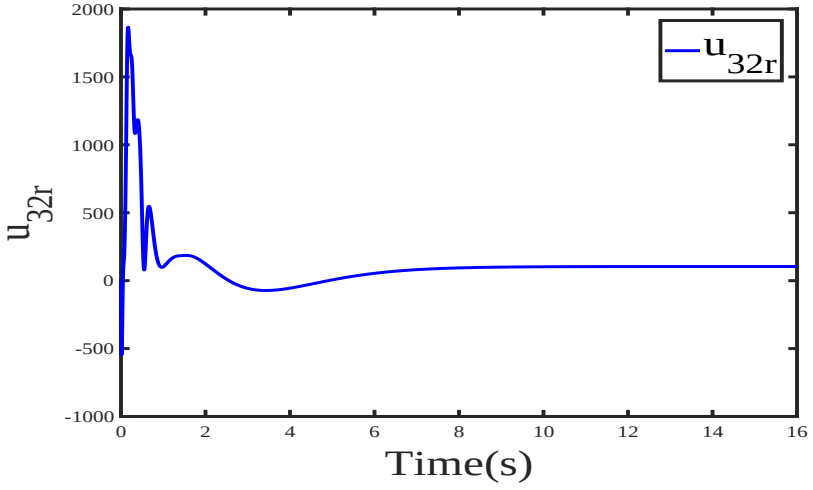

(b)

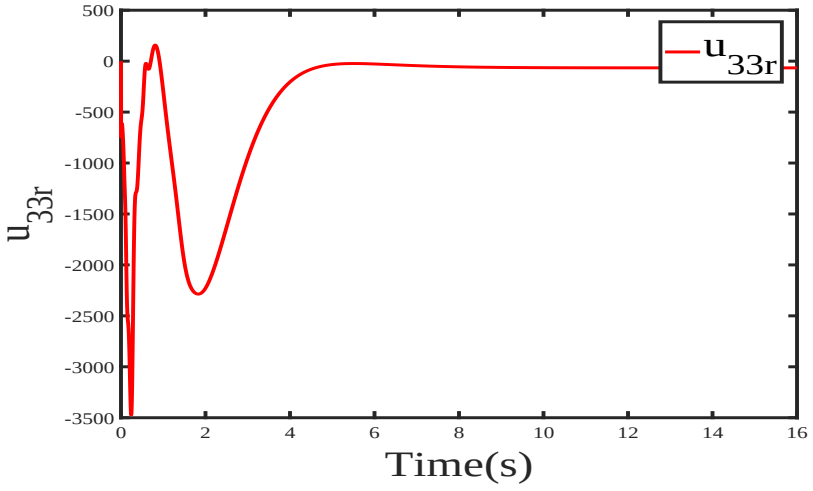

(c)

FIGURE 5.10: Control effort for anti-synchronization (a) u_{31r} (b) u_{32r} (c) u_{33r}

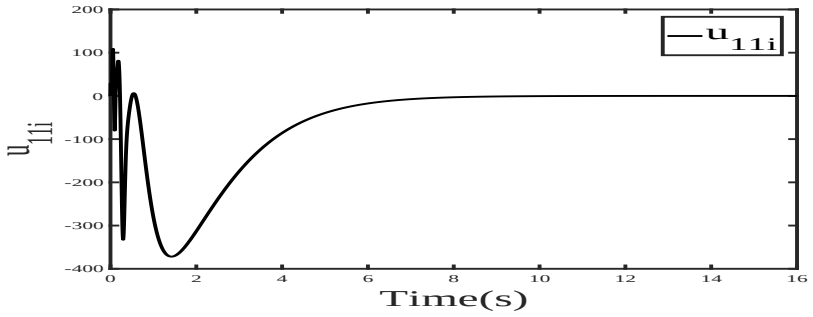

(a)

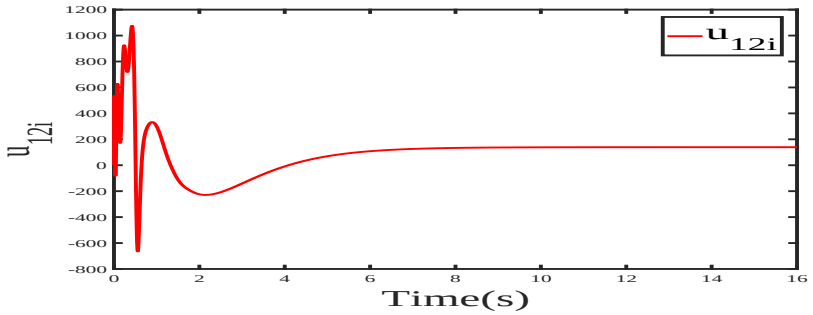

(b)

FIGURE 5.11: Control effort for anti-synchronization (a) u_{11i} (b) u_{12i}

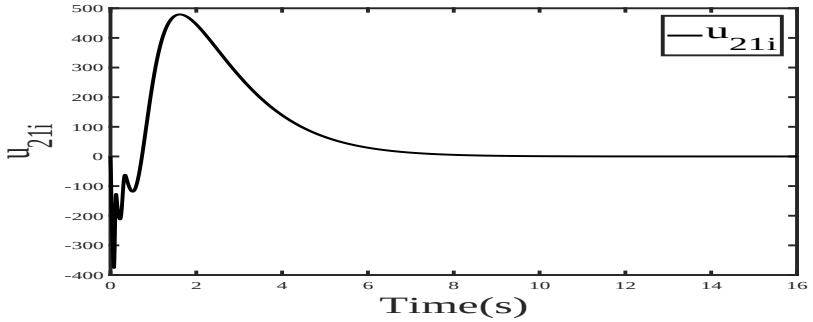

(a)

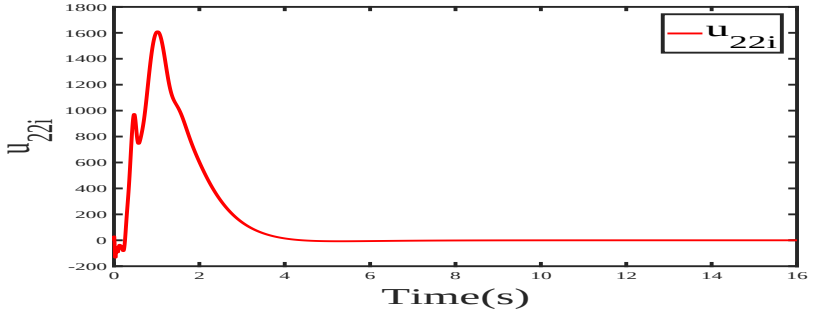

(b)

FIGURE 5.12: Control effort for anti-synchronization (a) u_{21i} (b) u_{22i}

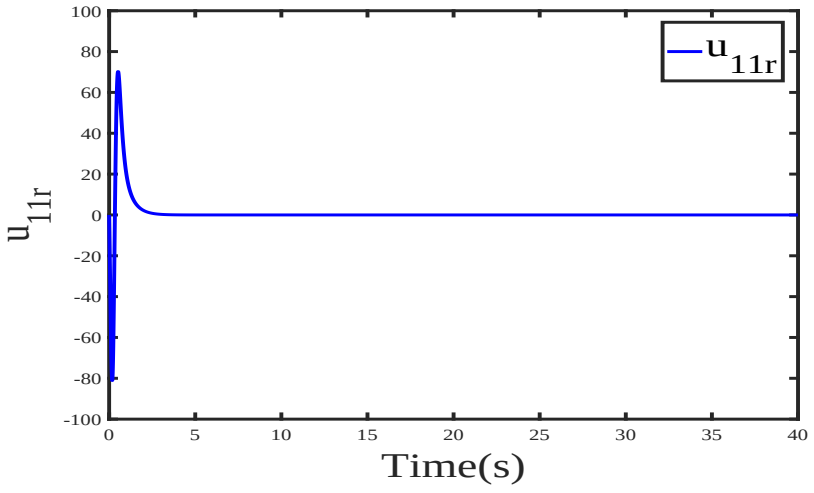

(a)

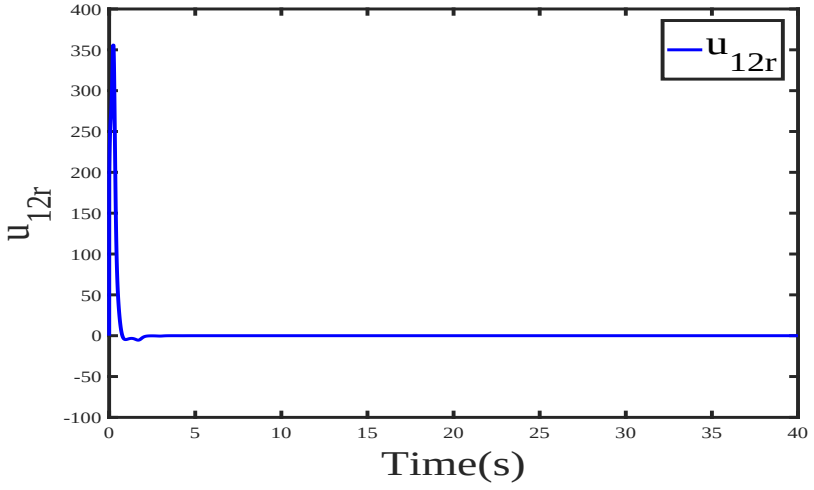

(b)

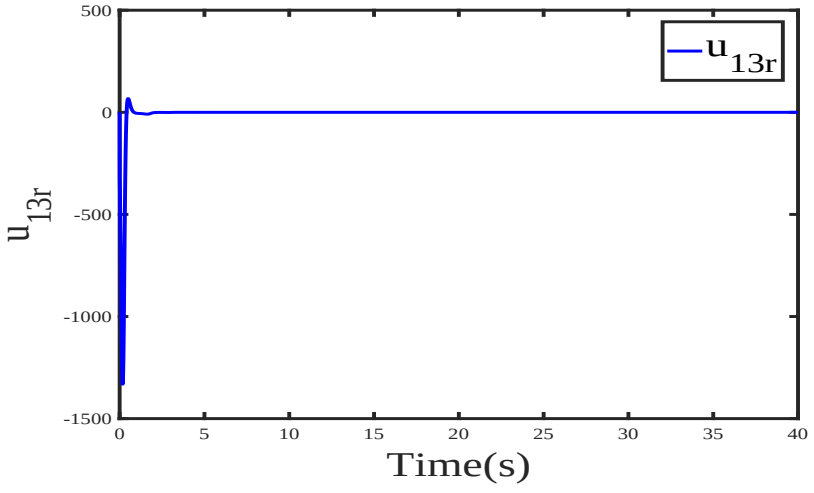

(c)

FIGURE 5.13: Control effort for synchronization (a) u_{11r} (b) u_{12r} (c) u_{13r}

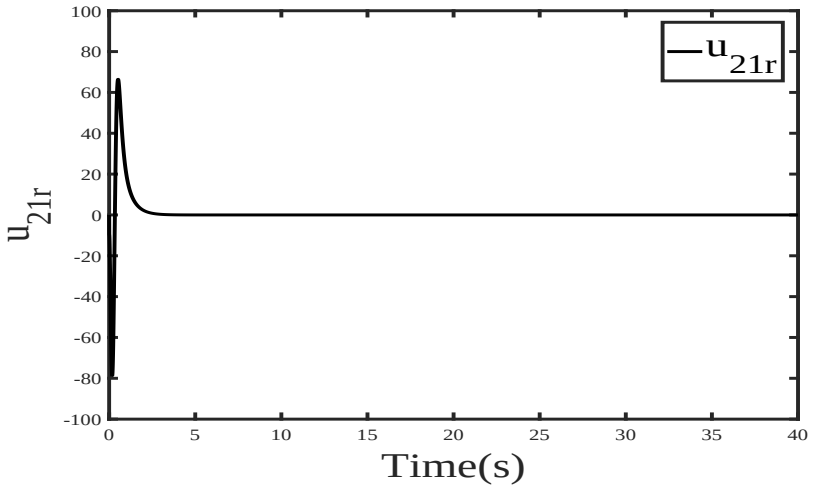

(a)

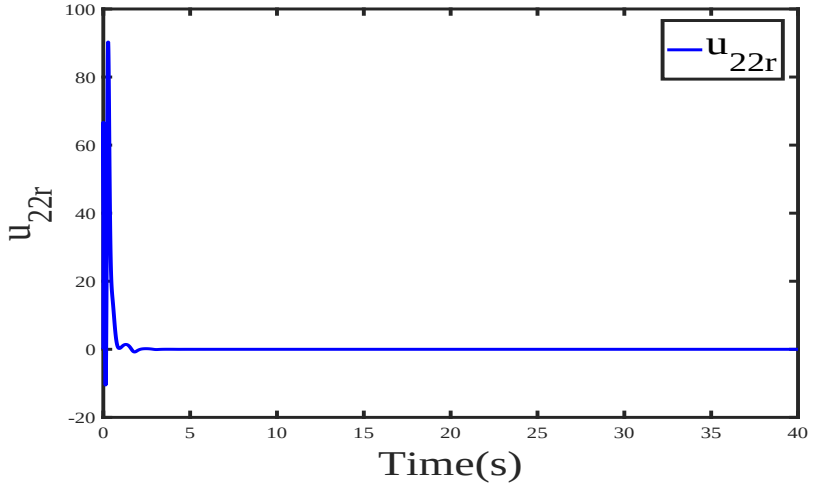

(b)

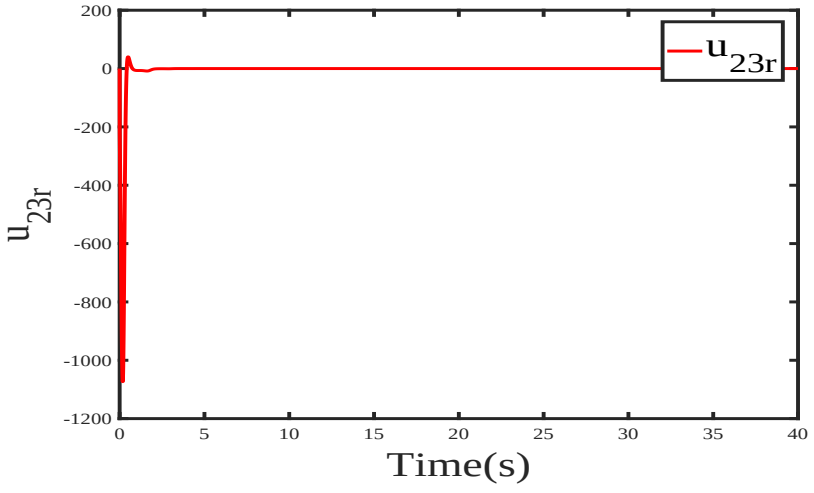

(c)

FIGURE 5.14: Control effort for synchronization (a) u_{21r} (b) u_{22r} (c) u_{23r}

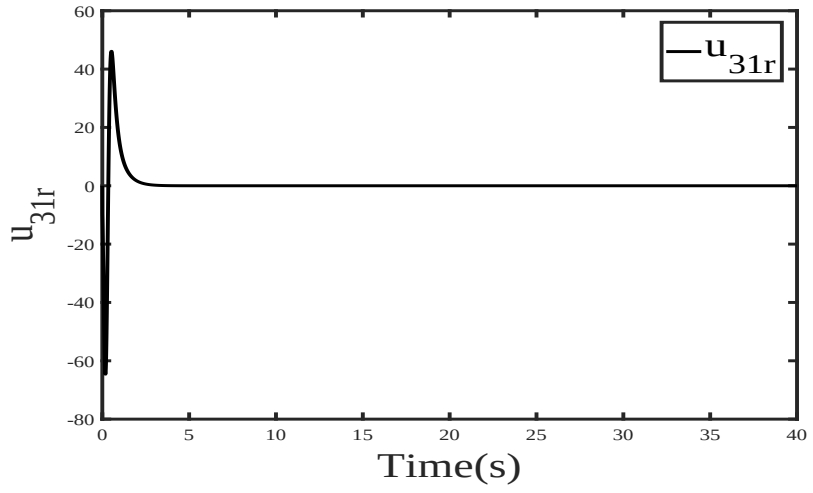

(a)

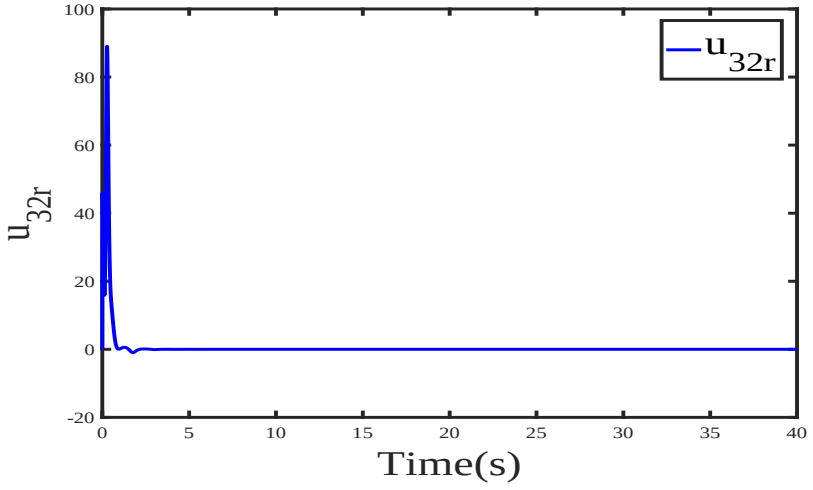

(b)

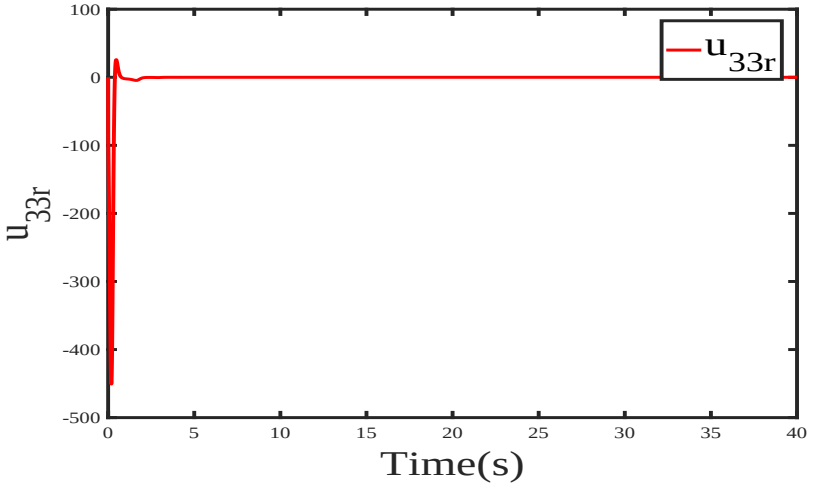

(c)

FIGURE 5.15: Control effort for synchronization (a) u_{31r} (b) u_{32r} (c) u_{33r}

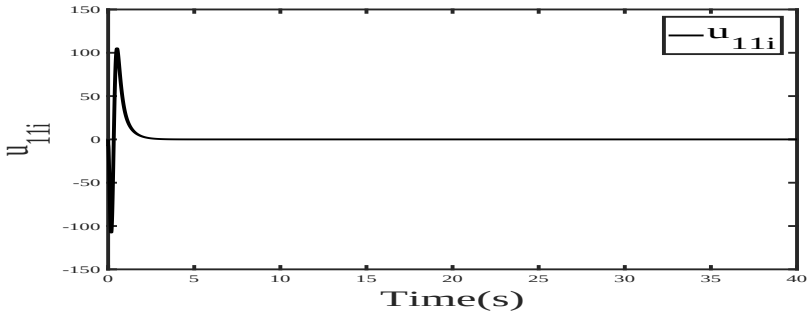

(a)

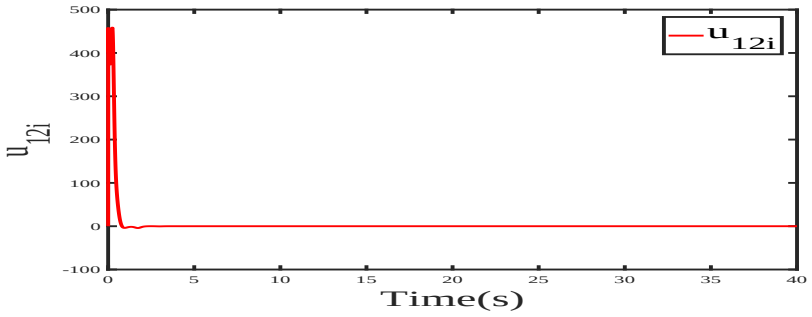

(b)

FIGURE 5.16: Control effort (a) u_{11i} (b) u_{12i}

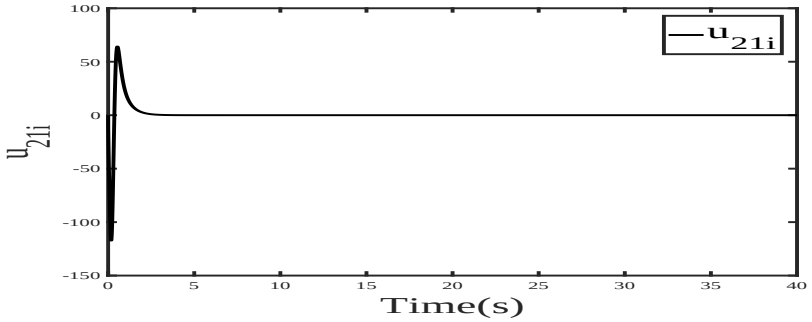

(a)

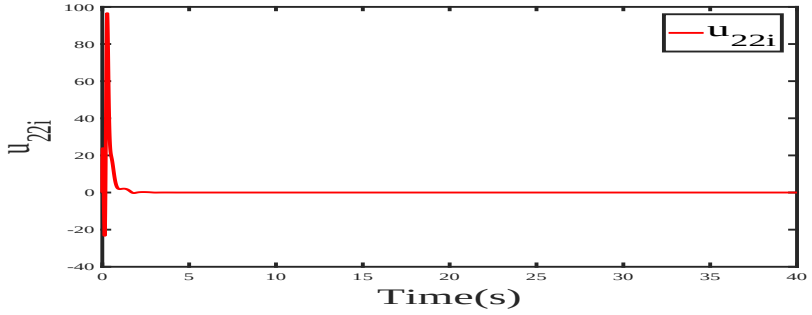

(b)

FIGURE 5.17: Control effort (a) u_{21i} (b) u_{22i}

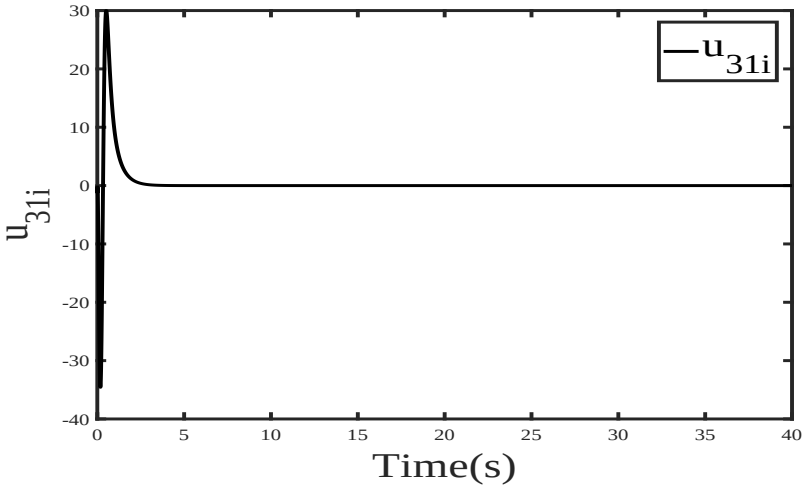

(a)

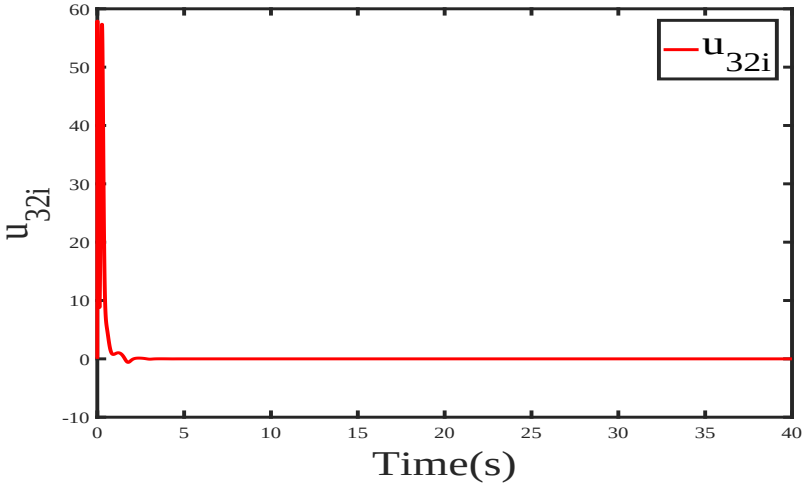

(b)

FIGURE 5.18: Control effort (a) u_{21i} (b) u_{22i}

Chapter 6

Hybrid Synchronization of 3-cell Cellular Nonlinear Network

6.1 Introdution

In this chapter, HOSMC based on SSTA is investigated to achieve hybrid synchronization of cellular Cellular Nonlinear Network network. In addition, it is considered that due to uncertainties the parameters of the CNN are unknown. As an example, 3-cell cellular neural network is considered to check the validation of proposed control algorithm.

Chua and Yang [213] presented for the first time the terminology CNN as cellular neural network. It is considered to be a signal processing system comprised of a lot of processing units called cells. These cells are locally connected to each other to perform complex tasks in a parallel processing regime. Since the cells are locally connected in CNN, this feature makes it different from other neural networks [214] which is advantageous in a sense that its implementation becomes easier in the current planar technologies [215–217]. Several applications of CNN are reported in the literature [218–230] after its invention, specially in image processing. CNNs are non-linear complex DNs and the occurrence of chaos is very obvious. From an electrical Engineering perspective, CNNs are considered to be DNs comprising of

nodes which are coupled locally to perform some information processes to generate specific behaviors. Since, CCNs exhibit chaotic behavior, so in this chapter HS of CNNs is investigated by employing SSTA. Smooth super twisting algorithm is a special flavor of HOSMC. There are two reasons of proposing SSTA. First, to achieve smooth control needed for hybrid synchronization of CNN by eliminating chattering, which is unwanted, and second, to achieve robustness contrary to the uncertainties by ensuring the correctness of sliding modes.

6.2 Problem Formulation

6.2.1 System Description and Mathematical Model

A 3-cells CNN attractor was firstly introduced by Arena et al. [231], which is described as:

$$\begin{aligned} \dot{x_1} &= -x_1 + \alpha\Psi(x_1) - \delta\Psi(x_2) - \delta\Psi(x_3) \\ \dot{x_2} &= -x_2 - \delta\Psi(x_1) + \beta\Psi(x_2) - \gamma\Psi(x_3) \\ \dot{x_3} &= -x_3 - \delta\Psi(x_1) + \gamma\Psi(x_2) + \Psi(x_3) \end{aligned} \tag{6.1}$$

where x_j and $\Psi(x_j)$ are the state variables and output function of j^{th} cell, respectively; γ, δ, α and β are the real parameters. Output $\Psi(x_j)$ is the piecewise linear function defined as: $\Psi(x_j) = 0.5|x_j + 1| - 0.5|x_j - 1|, j = 1, 2, 3$. In [231, 232], the chaotic behavior of Eq. (6.1) is analyzed by considering these parametric values: $\alpha = 1.24$, $\beta = 1.1, \gamma = 4.4, \delta = 3.21$ and the starting points for the dynamic states are considered as: $x_1(0) = 0.1$, $x_2(0) = 0.1$, $x_3(0) = 0.1$. The 3-D and 2-D phase portraits of Eq. (6.1) are shown in Fig. 6.1a-d.

6.2.2 Problem Statement

The chaotic nature of the 3-cells CNN attractor [231] is a renowned case of a chaotic CNN system. To achieve hybrid synchronization Eq. (6.1) is considered

as master and the slave systems is defined as following:

$$\begin{aligned}
\dot{y_1} &= -y_1 + \alpha\Psi(y_1) - \delta\Psi(y_2) - \delta\Psi(y_3) + \hbar_1 + \mu_1 \\
\dot{y_2} &= -y_2 - \delta\Psi(y_1) + \beta\Psi(y_2) - \gamma\Psi(y_3) + \hbar_2 + \mu_2 \\
\dot{y_3} &= -y_3 - \delta\Psi(y_1) + \gamma\Psi(y_2) + \Psi(y_3) + \hbar_3 + \mu_3
\end{aligned} \tag{6.2}$$

where y_1, y_2, y_3 are the states of the slave system, $\hbar_1, \hbar_2, \hbar_3$ are bounded disturbances, μ_1, μ_2, μ_3 are the control inputs to be determined, and $\Psi(y_j) = 0.5|y_j + 1| - 0.5|y_j - 1|, j = 1, 2, 3$.

Definition. The 3-cell CNN Eq. (6.1), it say that there exist HS if the controllers $\mu_i, i = 1, 2, 3$ are selected in such a manner that all trajectories $y_1(t), y_2(t), y_3(t)$ in Eq. (6.2) with either starting points $(y_1(0), y_2(0), y_3(0))$ satisfy: for the errors $e(t) = (e_1, e_2, e_3)$, yields:

$$\lim_{t\to\infty} e(t) = \lim_{t\to\infty} y_i(t) + qx_i(t) = 0, i = 1, 2, 3$$

For the AS $q = 1$ and for complete synchronization $q = -1$. The HS control become a problem to design appropriate controller μ_i to make $e_i = (e_1, e_2, e_3) \to 0$ asymptotically.

6.3 Proposed Control Algorithm and Numerical Example

To investigate smooth twisting algorithm for hybrid synchronization of 3-cell CNN, following two cases are considered.

Case (i) Assuming system parameters $\gamma, \delta, \alpha, \beta$ are known and defining the error as:

$$\begin{aligned}
e_1 &= y_1 - qx_1 \\
e_2 &= y_2 - qx_2 \\
e_3 &= y_3 - qx_3
\end{aligned} \tag{6.3}$$

When $q = 1$, it obtain synchronization and when $q = -1$, anti-synchronization is achieved. The error dynamical system is obtained as:

$$\begin{aligned}
\dot{e_1} &= \dot{y_1} - q\dot{x_1} \\
&= -y_1 + \alpha\Psi(y_1) - \delta\Psi(y_2) - \delta\Psi(y_3) + \hbar_1 + \mu_1 - q\{-x_1 + \alpha\Psi(x_1) - \delta\Psi(x_2) - \delta\Psi(x_3)\} \\
\dot{e_2} &= \dot{y_2} - q\dot{x_2} \\
&= -y_2 - \delta\Psi(y_1) + \beta\Psi(y_2) - \gamma\Psi(y_3) + \hbar_2 + \mu_2 - q\{-x_2 - \delta\Psi(x_1) + \beta\Psi(x_2) - \gamma\Psi(x_3)\} \\
\dot{e_3} &= \dot{y_3} - q\dot{x_3} \\
&= -y_3 - \delta\Psi(y_1) + \gamma\Psi(y_2) + \Psi(y_3) + \hbar_3 + \mu_3 - q\{-x_3 - \delta\Psi(x_1) + \gamma\Psi(x_2) + \Psi(x_3)\}
\end{aligned} \tag{6.4}$$

by choosing

$$\mu_1 = y_1 - \alpha\Psi(y_1) + \delta\Psi(y_2) + \delta\Psi(y_3) + q\{-x_1 + \alpha\Psi(x_1) - \delta\Psi(x_2) - \delta\Psi(x_3)\} + e_2$$

$$\mu_2 = y_2 + \delta\Psi(y_1) - \beta\Psi(y_2) + \gamma\Psi(y_3) + q\{-x_2 - \delta\Psi(x_1) + \beta\Psi(x_2) - \gamma\Psi(x_3)\} + e_3$$

$$\mu_3 = y_3 + \delta\Psi(y_1) - \gamma\Psi(y_2) - \Psi(y_3) + q\{-x_3 - \delta\Psi(x_1) + \gamma\Psi(x_2) + \Psi(x_3)\} + \nu \tag{6.5}$$

where ν is the new input. then the error dynamic becomes

$$\begin{aligned}
\dot{e_1} &= e_2 + \hbar_1 \\
\dot{e_2} &= e_3 + \hbar_2 \\
\dot{e_3} &= \nu + \hbar_3
\end{aligned} \tag{6.6}$$

By choosing the Hurwitz SS for Eq. (6.6) as: $\sigma = e_1 + 2e_2 + e_3$ and its derivative is taken as:

$$\dot{\sigma} = \dot{e_1} + 2\dot{e_2} + \dot{e_3} = e_2 + 2e_3 + \nu + \hbar_1 + \hbar_2 + \hbar_3 \tag{6.7}$$

By selecting,

$$\nu = \nu_{eq} + \nu_s \tag{6.8}$$

where

$$\begin{aligned}\nu_{eq} &= -e_2 - 2e_3,\\ \nu_s &= -\kappa_1|\sigma|^{\frac{\rho-1}{\rho}}\,\mathrm{sign}(\sigma) + w,\\ \dot{w} &= -\kappa_2|\sigma|^{\frac{\rho-2}{\rho}}\,\mathrm{sign}(\sigma), \kappa_1, \kappa_2 > |\hbar_1 + \hbar_2 + \hbar_3|, \rho \geq 2\end{aligned} \tag{6.9}$$

then Eq. (6.7) becomes:

$$\begin{aligned}\dot{\sigma} &= -\kappa_1|\sigma|^{y}\,\mathrm{sign}(\sigma) + w,\\ \dot{w} &= -\kappa_2|\sigma|^{y-\frac{1}{\rho}}\,\mathrm{sign}(\sigma), y = \frac{\rho-1}{\rho}\end{aligned} \tag{6.10}$$

Defining a new parameter as: $\zeta = \begin{bmatrix} |\sigma|^{y}\,\mathrm{sign}(\sigma) \\ w \end{bmatrix}$ and taking its derivative yields:

$$\begin{aligned}\dot{\zeta} &= \begin{bmatrix} y|\sigma|^{y-1}\dot{\sigma} \\ \dot{w} \end{bmatrix}\\ &= \begin{bmatrix} y|\sigma|^{\frac{-1}{\rho}} - \kappa_1|s|^{y}\,\mathrm{sign}(\sigma) + w \\ -\kappa_2|\sigma|^{y-\frac{1}{\rho}}\,\mathrm{sign}(\sigma) \end{bmatrix}\\ &= |\sigma|^{-\frac{1}{\rho}} \begin{bmatrix} y - \kappa_1|\sigma|^{y}\,\mathrm{sign}(\sigma) + w \\ -\kappa_2|\sigma|^{y}\,\mathrm{sign}(\sigma) \end{bmatrix}\\ &= |\sigma|^{-\frac{1}{\rho}} \begin{bmatrix} -y\kappa_1 & y \\ -\kappa_2 & 0 \end{bmatrix} \begin{bmatrix} |\sigma|^{y}\,\mathrm{sign}(\sigma) \\ w \end{bmatrix}\\ &= |\sigma|^{-\frac{1}{\rho}} A\zeta\end{aligned} \tag{6.11}$$

where, $A = \begin{bmatrix} -y\kappa_1 & y \\ -\kappa_2 & 0 \end{bmatrix}$ i.e. $\dot{\zeta} = |\sigma|^{-\frac{1}{\rho}} A\zeta$. The eigenvalues of $A = \begin{bmatrix} -y\kappa_1 & y \\ -\kappa_2 & 0 \end{bmatrix}$ are the roots of the Hurwitz polynomial: $|\lambda I - A| = \begin{vmatrix} \lambda + y\kappa_1 & -y \\ \kappa_2 & \lambda \end{vmatrix} = \lambda^2 + \lambda(y\kappa_1) + (yk_2) = 0$, therefore $A = \begin{bmatrix} -y\kappa_1 & y \\ -\kappa_2 & 0 \end{bmatrix}$ is strictly stable. Therefore, there is a symmetric and positive definite matrix $P \in R^{2X2}$ satisfying the Lyapunov equation [197]: $A^T P + PA = -Q$, where $Q \in R^{2X2}$ is the positive definite and

symmetric matrix.

Theorem 6.1. *Examine a Lyapunov function of the kind:* $V = \zeta^T P \zeta$, *where*

$$P = \begin{bmatrix} p_1 & p_2 \\ p_2 & p_3 \end{bmatrix} \tag{6.12}$$

if the Eq. (6.12) *satisfies the basic Lyapunov equation:* $A^T P + PA = -Q$, *where* $Q \in R^{2X2}$ *is a symmetric and positive definite matrix. Then* $\dot{V} = -|\sigma|^{-\frac{1}{\rho}} \zeta^T Q \zeta < 0$. *Consequently Eq.* (6.3) *is asymptotically stable. For simulation purpose the parametric values are as:* $\alpha = 1.24, \beta = 1.1, \gamma = 4.4, \delta = 3.21, \hbar_1 = \hbar_2 = \hbar_3 = 0.02, \kappa_1 = \kappa_2 = 5$.

Case (ii) *Assume systems parameters are unknown and let* $\hat{\gamma}, \hat{\delta}, \hat{\alpha}, \hat{\beta}$ *be estimate of* $\gamma, \delta, \alpha, \beta$ *respectively and let* $\tilde{\gamma} = \gamma - \hat{\gamma}$, $\tilde{\delta} = \delta - \hat{\delta}$, $\tilde{\alpha} = \alpha - \hat{\alpha}$, $\tilde{\beta} = \beta - \hat{\beta}$ *be the errors in estimating the unknown parameters. Then systems* (6.1) *and* (6.2) *are rewritten as:*

$$\begin{aligned}
\dot{x_1} &= -x_1 + \hat{\alpha}\Psi(x_1) + \tilde{\alpha}\Psi(x_1) - \hat{\delta}\Psi(x_2) - \tilde{\delta}\Psi(x_2) - \hat{\delta}\Psi(x_3) - \tilde{\delta}\Psi(x_3) \\
\dot{x_2} &= -x_2 - \hat{\delta}\Psi(x_1) - \tilde{\delta}\Psi(x_1) + \hat{\beta}\Psi(x_2) + \tilde{\beta}\Psi(x_2) - \hat{\gamma}\Psi(x_3) - \tilde{\gamma}\Psi(x_3) \\
\dot{x_3} &= -x_3 - \hat{\delta}\Psi(x_1) - \tilde{\delta}\Psi(x_1) + \hat{\gamma}\Psi(x_2) + \tilde{\gamma}\Psi(x_2) + \Psi(x_3)
\end{aligned} \tag{6.13}$$

$$\begin{aligned}
\dot{y_1} &= -y_1 + \hat{\alpha}\Psi(y_1) + \tilde{\alpha}\Psi(y_1) - \hat{\delta}\Psi(y_2) - \tilde{\delta}\Psi(y_2) - \hat{\delta}\Psi(y_3) - \tilde{\delta}\Psi(y_3) + \hbar_1 + \mu_1 \\
\dot{y_2} &= -y_2 - \hat{\delta}\Psi(y_1) - \tilde{\delta}\Psi(y_1) + \hat{\beta}\Psi(y_2) + \tilde{\beta}\Psi(y_2) - \hat{\gamma}\Psi(y_3) - \tilde{\gamma}\Psi(y_3) + \hbar_2 + \mu_2 \\
\dot{y_3} &= -y_3 - \hat{\delta}\Psi(y_1) - \tilde{\delta}\Psi(y_1) + \hat{\gamma}\Psi(y_2) + \tilde{\gamma}\Psi(y_2) + \Psi(y_3) + \hbar_3 + \mu_3
\end{aligned} \tag{6.14}$$

Defining the error between Eq. (6.13) *and Eq.* (6.14) *as:* $e_1 = y_1 - qx_1, e_2 = y_2 - qx_2, e_3 = y_3 - qx_3$. *When* $q = 1$, *it obtain synchronization and when* $q = -1$, *anti-synchronization is achieved. The error dynamics are obtained as:*

$$\begin{aligned}
\dot{e_1} &= \dot{y_1} - q\dot{x_1} \\
&= -y_1 + \hat{\alpha}\Psi(y_1) + \tilde{\alpha}\Psi(y_1) - \hat{\delta}\Psi(y_2) - \tilde{\delta}\Psi(y_2) - \hat{\delta}\Psi(y_3) - \tilde{\delta}\Psi(y_3) + \hbar_1 + \mu_1 \\
&\quad - q\{-x_1 + \hat{\alpha}\Psi(x_1) + \tilde{\alpha}\Psi(x_1) - \hat{\delta}\Psi(x_2) - \tilde{\delta}\Psi(x_2) - \hat{\delta}\Psi(x_3) - \tilde{\delta}\Psi(x_3)\}
\end{aligned}$$

$$
\begin{aligned}
\dot{e_2} &= \dot{y_2} - q\dot{x_2} \\
&= -y_2 - \hat{\delta}\Psi(y_1) - \tilde{\delta}\Psi(y_1) + \hat{\beta}\Psi(y_2) + \tilde{\beta}\Psi(y_2) - \hat{\gamma}\Psi(y_3) - \tilde{\gamma}\Psi(y_3) + \hbar_2 + \mu_2 \\
&\quad - q\{-x_2 - \hat{\delta}\Psi(x_1) - \tilde{\delta}\Psi(x_1) + \hat{\beta}\Psi(x_2) + \tilde{\beta}\Psi(x_2) - \hat{\gamma}\Psi(x_3) - \tilde{\gamma}\Psi(x_3)\} \\
\dot{e_3} &= \dot{y_3} - q\dot{x_3} \\
&= -y_3 - \hat{\delta}\Psi(y_1) - \tilde{\delta}\Psi(y_1) + \hat{\gamma}\Psi(y_2) + \tilde{\gamma}\Psi(y_2) + \Psi(y_3) + \hbar_3 + \mu_3 \\
&\quad - q\{-x_3 - \hat{\delta}\Psi(x_1) - \tilde{\delta}\Psi(x_1) + \hat{\gamma}\Psi(x_2) + \tilde{\gamma}\Psi(x_2) + \Psi(x_3)\}
\end{aligned}
\tag{6.15}
$$

By choosing

$$
\begin{aligned}
\mu_1 &= y_1 - \hat{\alpha}\Psi(y_1) + \hat{\delta}\Psi(y_2) + \hat{\delta}\Psi(y_3) + q\{-x_1 + \hat{\alpha}\Psi(x_1) - \hat{\delta}\Psi(x_2) - \hat{\delta}\Psi(x_3)\} + e_2 \\
\mu_2 &= y_2 + \hat{\delta}\Psi(y_1) - \hat{\beta}\Psi(y_2) + \hat{\gamma}\Psi(y_3) + q\{-x_2 - \hat{\delta}\Psi(x_1) + \hat{\beta}\Psi(x_2) - \hat{\gamma}\Psi(x_3)\} + e_3 \\
\mu_3 &= y_3 + \hat{\delta}\Psi(y_1) - \hat{\gamma}\Psi(y_2) - \Psi(y_3) + q\{-x_3 - \hat{\delta}\Psi(x_1) + \hat{\gamma}\Psi(x_2) + \Psi(x_3)\} + \nu
\end{aligned}
\tag{6.16}
$$

where ν is the new input. Then the error dynamics becomes

$$
\begin{aligned}
\dot{e_1} &= e_2 + \tilde{\alpha}\Psi(y_1) - \tilde{\delta}\Psi(y_2) - \tilde{\delta}\Psi(y_3) - q\{\tilde{\alpha}\Psi(x_1) - \tilde{\delta}\Psi(x_2) - \tilde{\delta}\Psi(x_3)\} \\
&= e_2 + \tilde{\alpha}\{\Psi(y_1) - q\Psi(x_1)\} - \tilde{\delta}\{\Psi(y_2) - q\Psi(x_2)\} - \tilde{\delta}\{\Psi(y_3) - q\Psi(x_3)\} + \hbar_1 \\
\\
\dot{e_2} &= e_3 - \tilde{\delta}\Psi(y_1) + \tilde{\beta}\Psi(y_2) - \tilde{\gamma}\Psi(y_3) - q\{-\tilde{\delta}\Psi(x_1) + \tilde{\beta}\Psi(x_2) - \tilde{\gamma}\Psi(x_3)\} \\
&= e_3 - \tilde{\delta}\{\Psi(y_1) - q\Psi(x_1)\} + \tilde{\beta}\{\Psi(y_2) - q\Psi(x_2)\} - \tilde{\gamma}\{\Psi(y_3) - q\Psi(x_3)\} + \hbar_2 \\
\dot{e_3} &= \nu - \tilde{\delta}\Psi(y_1) + \tilde{\gamma}\Psi(y_2) - q\{-\tilde{\delta}\Psi(x_1) + \tilde{\gamma}\Psi(x_2)\} \\
&= \nu - \tilde{\delta}\{\Psi(y_1) - q\Psi(x_1)\} + \tilde{\gamma}\{\Psi(y_2) - q\Psi(x_2)\} + \hbar_3
\end{aligned}
\tag{6.17}
$$

or

$$
\begin{aligned}
\dot{e_1} &= e_2 + \tilde{\alpha}\{\Psi(y_1) - q\Psi(x_1)\} - \tilde{\delta}\{\Psi(y_2) - q\Psi(x_2)\} - \tilde{\delta}\{\Psi(y_3) - q\Psi(x_3)\} + \hbar_1 \\
\dot{e_2} &= e_3 - \tilde{\delta}\{\Psi(y_1) - q\Psi(x_1)\} + \tilde{\beta}\{\Psi(y_2) - q\Psi(x_2)\} - \tilde{\gamma}\{\Psi(y_3) - q\Psi(x_3)\} + \hbar_2 \\
\dot{e_3} &= \nu - \tilde{\delta}\{\Psi(y_1) - q\Psi(x_1)\} + \tilde{\gamma}\{\Psi(y_2) - q\Psi(x_2)\} + \hbar_3
\end{aligned}
\tag{6.18}
$$

By choosing the Hurwitz SS for system Eq. (6.18) *as:* $\sigma = e_1 + 2e_2 + e_3$. *Then its derivative gives:*

$$\begin{aligned}\dot{\sigma} &= \dot{e_1} + 2\dot{e_2} + \dot{e_3} \\ &= e_2 + \tilde{\alpha}\{\Psi(y_1) - q\Psi(x_1)\} - \tilde{\delta}\{\Psi(y_2) - q\Psi(x_2)\} - \tilde{\delta}\{\Psi(y_3) - q\Psi(x_3)\} + 2e_3 \\ &- 2\tilde{\delta}\{\Psi(y_1) - q\Psi(x_1)\} + 2\tilde{\beta}\{\Psi(y_2) - q\Psi(x_2)\} - 2\tilde{\gamma}\{\Psi(y_3) - q\Psi(x_3)\} \\ &- \tilde{\delta}\{\Psi(y_1) - q\Psi(x_1)\} + \tilde{\gamma}\{\Psi(y_2) - q\Psi(x_2)\} + \nu + \hbar_1 + \hbar_2 + \hbar_3\end{aligned} \tag{6.19}$$

By choosing $\nu = \nu_{eq} + \nu_s + z$, *where*

$$\begin{aligned}\nu_{eq} &= -e_2 - 2e_3 \\ \nu_s &= -\kappa_1 |\sigma|^{\frac{\rho-1}{\rho}} \operatorname{sign}(\sigma) + w \\ \dot{w} &= -\kappa_2 |\sigma|^{\frac{\rho-2}{\rho}} \operatorname{sign}(\sigma), \kappa_1, \kappa_2 > |\hbar_1 + \hbar_2 + \hbar_3|, \rho \geq 2\end{aligned} \tag{6.20}$$

then Eq. (6.19) *becomes*

$$\begin{aligned}&\dot{\sigma} = -\kappa_1 |\sigma|^y \operatorname{sign}(\sigma) + w + z, \\ &\dot{w} = -\kappa_2 |\sigma|^{y-\frac{1}{\rho}} \operatorname{sign}(\sigma), y = \frac{\rho - 1}{\rho} \\ &z = \tilde{\alpha}\{\Psi(y_1) - q\Psi(x_1)\} - \tilde{\delta}\{\Psi(y_2) - q\Psi(x_2)\} - \tilde{\delta}\{\Psi(y_3) - q\Psi(x_3)\} - 2\tilde{\delta}\{\Psi(y_1) - q\Psi(x_1)\} \\ &\quad + 2\tilde{\beta}\{\Psi(y_2) - q\Psi(x_2)\} - 2\tilde{\gamma}\{\Psi(y_3) - q\Psi(x_3)\} - \tilde{\delta}\{\Psi(y_1) - q\Psi(x_1)\} + \tilde{\gamma}\{\Psi(y_2) - q\Psi(x_2)\}\end{aligned} \tag{6.21}$$

Defining a new parameter $\zeta = \begin{bmatrix} |\sigma|^y \operatorname{sign}(\sigma) & w \end{bmatrix}^T$ *and taking its derivative yields:*

$$\begin{aligned}\dot{\zeta} &= \begin{bmatrix} y|\sigma|^{y-1}\dot{\sigma} \\ \dot{w} \end{bmatrix} = \begin{bmatrix} y|\sigma|^{\frac{-1}{\rho}} - \kappa_1 |\sigma|^y \operatorname{sign}(\sigma) + w + z \\ -\kappa_2 |\sigma|^{y-\frac{1}{\rho}} \operatorname{sign}(\sigma) \end{bmatrix} \\ &= |\sigma|^{-\frac{1}{\rho}} \begin{bmatrix} y - \kappa_1 |\sigma|^y \operatorname{sign}(\sigma) + w + z \\ -\kappa_2 |\sigma|^y \operatorname{sign}(\sigma) \end{bmatrix} \\ &= |\sigma|^{-\frac{1}{\rho}} \begin{bmatrix} -y\kappa_1 & y \\ -\kappa_2 & 0 \end{bmatrix} \begin{bmatrix} |\sigma|^y \operatorname{sign}(\sigma) \\ w + z \end{bmatrix} = |\sigma|^{-\frac{1}{\rho}} A\zeta + |\sigma|^{-\frac{1}{\rho}} \begin{bmatrix} yz \\ 0 \end{bmatrix}\end{aligned} \tag{6.22}$$

where, $A = \begin{bmatrix} -y\kappa_1 & y \\ -\kappa_2 & 0 \end{bmatrix}$ *i.e.* $\dot{\zeta} = |\sigma|^{-\frac{1}{\rho}}(A\zeta + \begin{bmatrix} yz \\ 0 \end{bmatrix})$. *The eigenvalues of* $A = \begin{bmatrix} -y\kappa_1 & y \\ -\kappa_2 & 0 \end{bmatrix}$ *are the roots of the Hurwitz polynomial:* $|\lambda I - A| = \begin{vmatrix} \lambda + y\kappa_1 & -y \\ \kappa_2 & \lambda \end{vmatrix} = \lambda^2 + \lambda(y\kappa_1) + (y\kappa_2) = 0$, *therefore* $A = \begin{bmatrix} -y\kappa_1 & y \\ -\kappa_2 & 0 \end{bmatrix}$ *is strictly stable.*

Theorem 6.2. *Examine a Lyapunov function of the kind* $V = \zeta^T P\zeta + \frac{1}{2}(\tilde{\gamma}^2 + \tilde{\delta}^2 + \tilde{\alpha}^2 + \tilde{\beta}^2)$, *where* $P = \begin{bmatrix} p_1 & p_2 \\ p_2 & p_3 \end{bmatrix}$ *is a symmetric and positive definite matrix satisfying:* $A^T P + PA = -Q$, *where* $Q \in R^{2X2} > 0$ *is a symmetric and positive definite matrix. In this way* V *is global and strict Lyapunov function [197]. Then the finite time convergence of* $\dot{V} = -|\sigma|^{-\frac{1}{\rho}}\zeta^T Q\zeta \leq 0$ *is possible if the adaptive laws are chosen as:*

$$\begin{aligned}
&\dot{\tilde{\gamma}} = 2l(\Psi(y_3) - q\Psi(x_3))\gamma - l(\Psi(y_2) - q\Psi(x_2)) - \kappa_1\tilde{\gamma},\ \dot{\tilde{\gamma}} = -\dot{\tilde{\gamma}} \\
&\dot{\tilde{\delta}} = l(\Psi(y_2) - q\Psi(x_2)) + l(\Psi(y_3) - q\Psi(x_3)) + l(\Psi(y_1) - q\Psi(x_1)) - \kappa_2\tilde{\delta}, \dot{\tilde{\delta}} = -\dot{\tilde{\delta}} \\
&\dot{\tilde{\alpha}} = -l(\Psi(y_1) - q\Psi(x_1)) - \kappa_3\tilde{\alpha},\ \dot{\tilde{\alpha}} = -\dot{\tilde{\alpha}} \\
&\dot{\tilde{\beta}} = -2l(\Psi(y_2) - q\Psi(x_2)) - \kappa_4\tilde{\beta},\ \dot{\tilde{\beta}} = -\dot{\tilde{\beta}}, \kappa_i > 0, i = 1, ..., 4
\end{aligned} \tag{6.23}$$

Proof. since

$$\begin{aligned}
\dot{V} &= \dot{\zeta}^T P\zeta + P\zeta^T\dot{\zeta} + \tilde{\gamma}\dot{\tilde{\gamma}} + \tilde{\delta}\dot{\tilde{\delta}} + \tilde{\alpha}\dot{\tilde{\alpha}} + \tilde{\beta}\dot{\tilde{\beta}} \\
&= \{|\sigma|^{-\frac{1}{\rho}}\zeta^T A^T + |\sigma|^{-\frac{1}{\rho}}\{\begin{bmatrix} yz & 0 \end{bmatrix}\}P\zeta + \zeta^T P\{|\sigma|^{-\frac{1}{\rho}}A\zeta + |\sigma|^{-\frac{1}{\rho}}\begin{bmatrix} yz \\ 0 \end{bmatrix}\} \\
&+ \tilde{\gamma}\dot{\tilde{\gamma}} + \tilde{\delta}\dot{\tilde{\delta}} + \tilde{\alpha}\dot{\tilde{\alpha}} + \tilde{\beta}\dot{\tilde{\beta}} \\
&= |\sigma|^{-\frac{1}{\rho}}\{\zeta^T\{A^T P + PA\}\zeta\} + |\sigma|^{-\frac{1}{\rho}}\{\begin{bmatrix} yz & 0 \end{bmatrix} P\zeta + \zeta^T P\begin{bmatrix} yz \\ 0 \end{bmatrix}\} \\
&+ \tilde{\gamma}\dot{\tilde{\gamma}} + \tilde{\delta}\dot{\tilde{\delta}} + \tilde{\alpha}\dot{\tilde{\alpha}} + \tilde{\beta}\dot{\tilde{\beta}} \\
&= -|\sigma|^{-\frac{1}{\rho}}\zeta^T Q\zeta + 2y|\sigma|^{-\frac{1}{\rho}}(P_1\zeta_1 + P_2\zeta_2) + \tilde{\gamma}\dot{\tilde{\gamma}} + \tilde{\delta}\dot{\tilde{\delta}} + \tilde{\alpha}\dot{\tilde{\alpha}} + \tilde{\beta}\dot{\tilde{\beta}}
\end{aligned}$$

$$
\begin{aligned}
&= -|\sigma|^{-\frac{1}{\rho}}\zeta^T Q\zeta + l[\tilde{\alpha}\{\Psi(y_1) - q\Psi(x_1)\} - \tilde{\delta}\{\Psi(y_2) - q\Psi(x_2)\} - \tilde{\delta}\{\Psi(y_3) \\
&- q\Psi(x_3)\} - 2\tilde{\delta}\{\Psi(y_1) - q\Psi(x_1)\} + \tilde{\beta}\{\Psi(y_2) - q\Psi(x_2)\} - 2\tilde{\gamma}\{\Psi(y_3) - q\Psi(x_3)\} \\
&- \tilde{\delta}\{\Psi(y_1) - q\Psi(x_1)\} + \tilde{\gamma}\{\Psi(y_2) - q\Psi(x_2)\}] + \tilde{\gamma}\dot{\tilde{\gamma}} + \tilde{\delta}\dot{\tilde{\delta}} + \tilde{\alpha}\dot{\tilde{\alpha}} + \tilde{\beta}\dot{\tilde{\beta}} \\
&= -|\sigma|^{-\frac{1}{\rho}}\zeta^T Q\zeta + \tilde{\gamma}\{\dot{\hat{\gamma}} - 2l(\Psi(y_3) - q\Psi(x_3)) + l(\Psi(y_2) - q\Psi(x_2))\} \\
&+ \delta\{\dot{\hat{\delta}} - l(\Psi(y_2) - q\Psi(x_2)) - l(\Psi(y_3) - q\Psi(x_3)) - l(\Psi(y_1) - q\Psi(x_1))\} \\
&+ \alpha\{\dot{\hat{\alpha}} + l(\Psi(y_1) - q\Psi(x_1))\} + \beta\{\dot{\hat{\beta}} + 2l(\Psi(y_2) - q\Psi(x_2))\}
\end{aligned}
\tag{6.24}
$$

where $l = 2y|\sigma|^{-\frac{1}{\rho}}(P_1\zeta_1 + P_2\zeta_2) = 2y|\sigma|^{-\frac{1}{\rho}}(P_1|\sigma|^y sign(\sigma) + P_2 w)$

by using

$$
\begin{aligned}
&\dot{\tilde{\gamma}} = 2l(\Psi(y_3) - q\Psi(x_3)) - l(\Psi(y_2) - q\Psi(x_2)) - \kappa_1\tilde{\gamma},\ \dot{\hat{\gamma}} = -\dot{\tilde{\gamma}} \\
&\dot{\tilde{\delta}} = l(\Psi(\gamma_2) - q\Psi(x_2)) + l(\Psi(y_3) - q\Psi(x_3)) + l(\Psi(y_1) - q\Psi(x_1)) - \kappa_2\tilde{\delta}, \dot{\hat{\delta}} = -\dot{\tilde{\delta}} \\
&\dot{\tilde{\alpha}} = -l(\Psi(y_1) - q\Psi(x_1)) - \kappa_3\tilde{\alpha},\ \dot{\hat{\alpha}} = -\dot{\tilde{\alpha}} \\
&\dot{\tilde{\beta}} = -2l(\Psi(y_2) - q\Psi(x_2)) - \kappa_4\tilde{\beta},\ \dot{\hat{\beta}} = -\dot{\tilde{\beta}}, \kappa_i > 0, i = 1, ..., 4
\end{aligned}
\tag{6.25}
$$

Eq. (6.24) becomes: $\dot{V} = -|\sigma|^{-\frac{1}{\rho}}\zeta^T Q\zeta - \kappa_1\tilde{\gamma}^2 - \kappa_2\tilde{\delta}^2 - \kappa_3\tilde{\alpha}^2 - \kappa_4\tilde{\beta}^2 < 0$. For simulation purpose parametric values are selected as: $\alpha = 1.24, \beta = 1.1, \gamma = 4.4, \delta = 3.21, \hbar_1 = \hbar_2 = \hbar_3 = 0.02, \kappa_1 = \kappa_2 = 5$.

6.4 Performance Analysis

Simulation results are presented by taking the following initial conditions, $x_1(0) = 12.4, x_2(0) = 21.7, x_3(0) = 10.3$,$y_1(0) = 5.3, y_2(0) = 23.4, y_3(0) = 18.7$,$\hat{\alpha}(0) = \hat{\beta}(0) = \hat{a}(0) = \hat{b}(0) = 0$. For synchronization the initial conditions for errors are $e_1(0) = -7.1, , e_2(0) = 1.7, e_3(0) = 8.4$ and for anti-synchronization the initial conditions for errors are $e_1(0) = 17.7, e_2(0) = 45.1, e_3(0) = 29$. Simulation results

depicted in Figs. 6.2-6.9 are presented for Case I and simulation results depicted in Figs. 6.10-6.14 are presented for Case II. In Fig. 6.2 synchronization error dynamics are converging to zero which means that the states of master CNN are synchronized with the states of slave CNN. Figure 6.3 presents the time evolution of the states of both the master CNN and slave CNN and it can be observed that the states are completely synchronized with each other. Figure 6.4 presents the control effort exerted to achieve the target. Figure 6.5 depicts the establishment of sliding manifold and it can be observed very clearly that the SS is very smooth and there are no chattering in the steady state which validates the claim. Figure 6.6 displays the convergence of AS error dynamics to zero which infers that AS is achieved. Figure 6.7 shows the time evolution of master CNN and slave CNN and it is very clear that the states of both CNNs are now anti synchronized. Similarly Fig. 6.8 represents the control effort exerted to achieve the desire goal and Fig. 6.9 shows the establishment of smooth sliding surface. Figure 6.10 represents the convergence of synchronization error dynamics to zero for Case II where it is assumed that the parameters are uncertain. Figure 6.11 shows the time evolution of states of the master CNN and slave CNN. Figure 6.12 displays the convergence of AS error dynamics to zero and Fig. 6.13 depicts the time evolution of the dynamic states of master CNN and slave CNN and it is very clear that the states of both CNN are fully anti-synchronized with each other. Figure 6.14 shows the convergence of estimated parameters $\hat{\alpha}, \hat{\beta}, \hat{\gamma}, \hat{\delta}$ to their true values $\alpha, \beta, \gamma, \delta$.

6.5 Summary

In this chapter parameter estimation and hybrid synchronization of 3-cell cellular neural network is achieved. The methodology is based on the SSTA which is a special flavor of SOSMC. The chaotic behavior of the CNN is analyzed and the Hybrid synchronization is achieved by using the Master/Slave type configuration of CNNs. A smooth sliding surface is established which ensures smooth control and robustness to uncertainties. The uncertain parameters are figured out adaptively and the stability of the smooth sliding surface is checked by using the Lyapunov

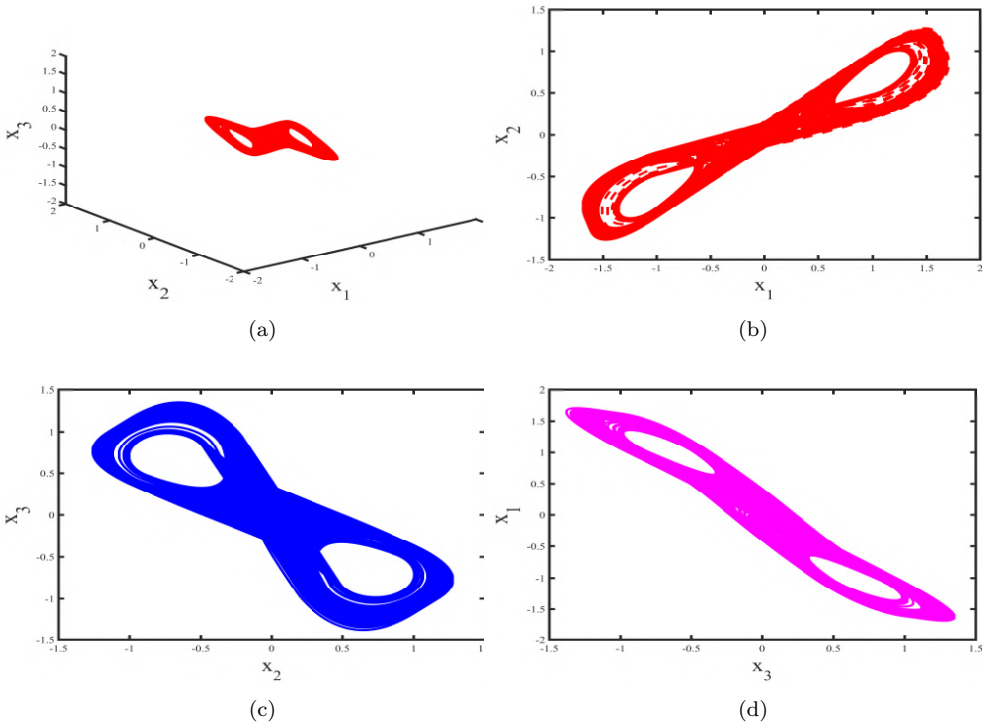

FIGURE 6.1: Chaotic behavior of 3-cell cellular neural network on (a) x_1, x_2, x_3 space (b) x_1, x_2 space (c) x_2, x_3 space and (d) x_3, x_1 space.

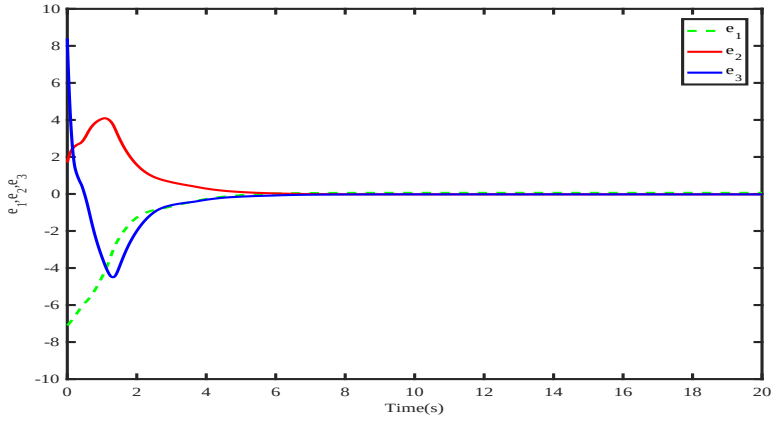

FIGURE 6.2: Convergence of synchronization error dynamics to zero

stability theorem. The effectiveness of the proposed control algorithm has been presented through extensive mathematical expressions and MATLAB simulations. The simulation results are very attractive and provides the proof of trueness of the proposed control technique. The simulation results shows the achievement of hybrid Synchronization of CNNs by the proposed control laws, another key fact to remember that the uncertain parameters converge to their real values.

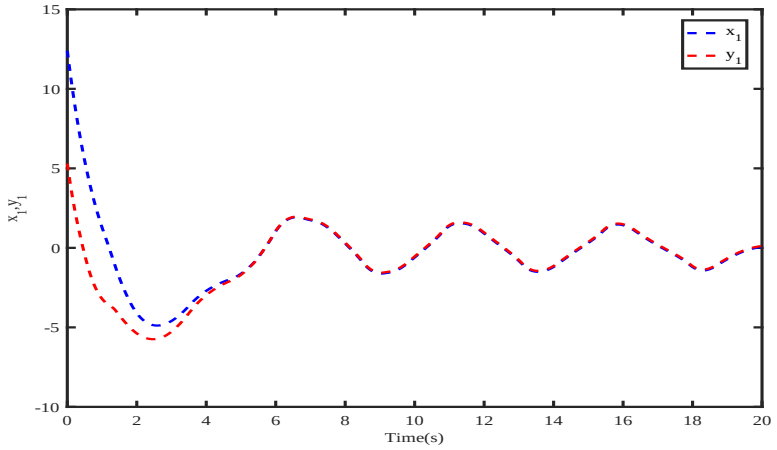

(a)

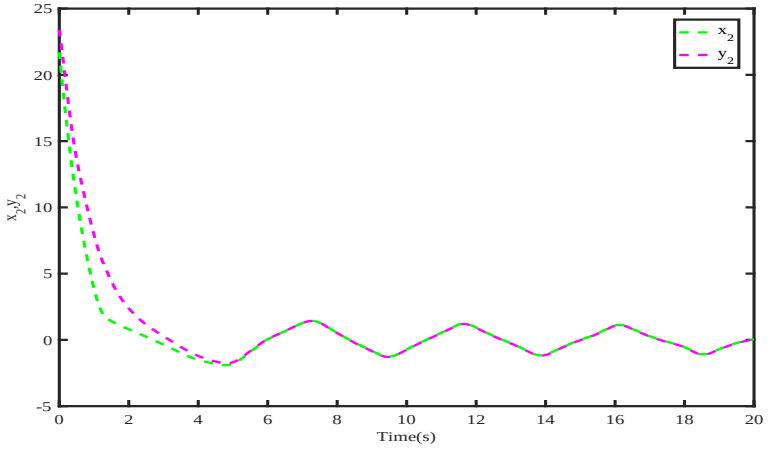

(b)

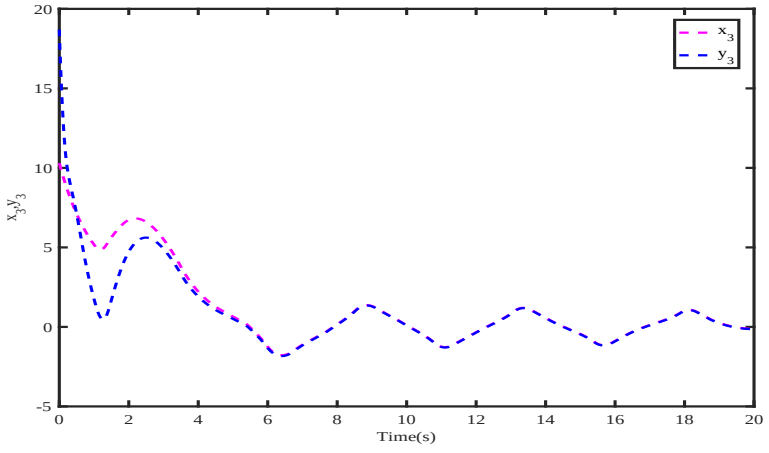

(c)

FIGURE 6.3: States in synchronization of Master CNN and Slave CNN (Case I)

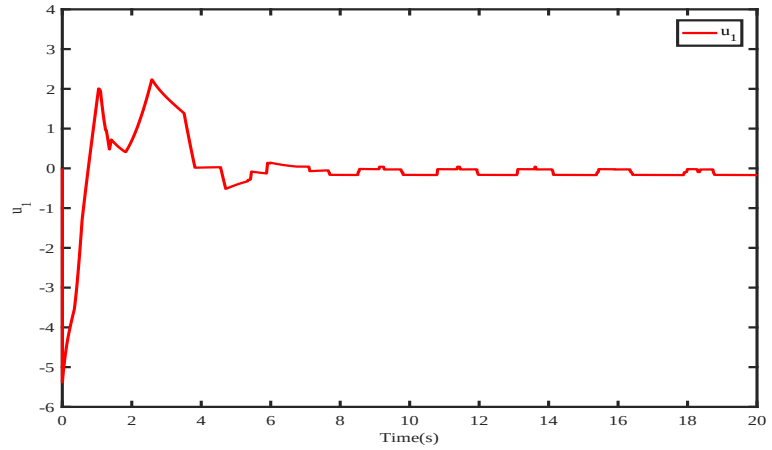

(a)

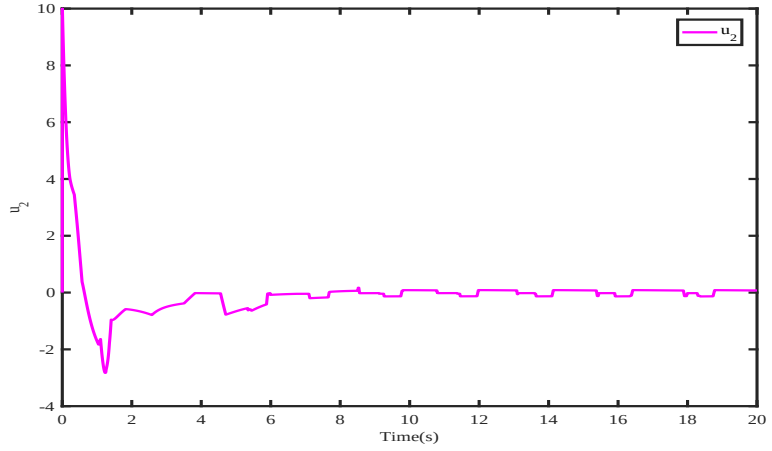

(b)

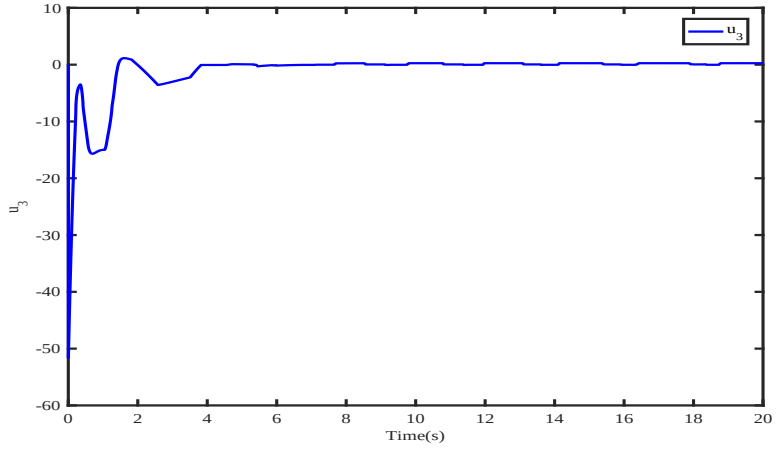

(c)

FIGURE 6.4: Control effort exerted to achieve state synchronization between Master CNN and Slave CNN

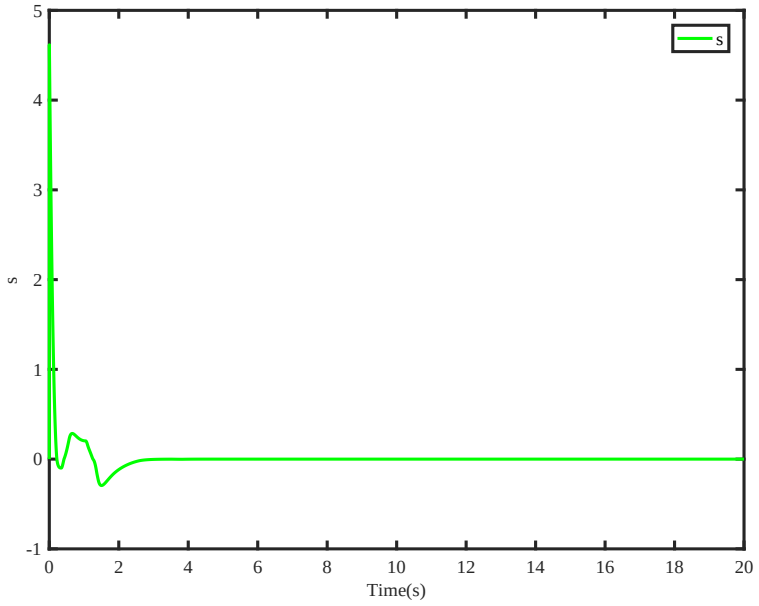

FIGURE 6.5: Sliding Surface for synchronization in (Case I)

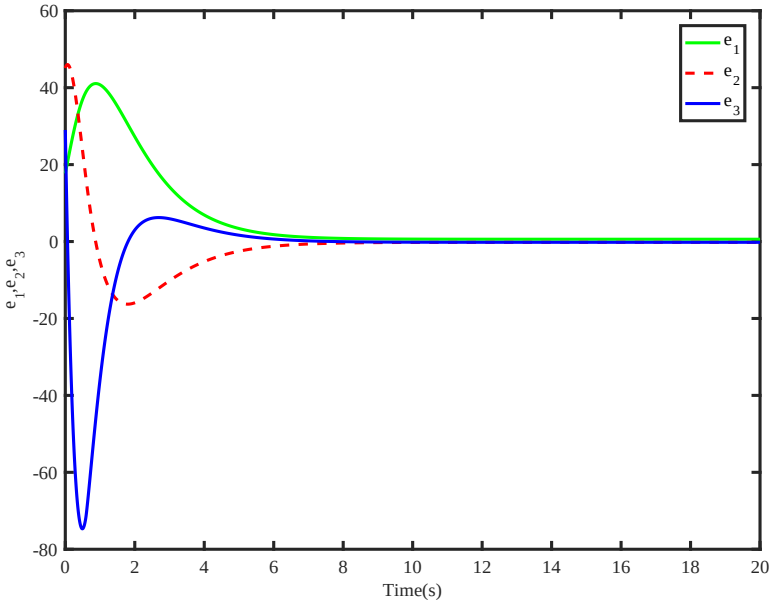

FIGURE 6.6: Convergence of Anti-synchronization error dynamic to zero (Case I)

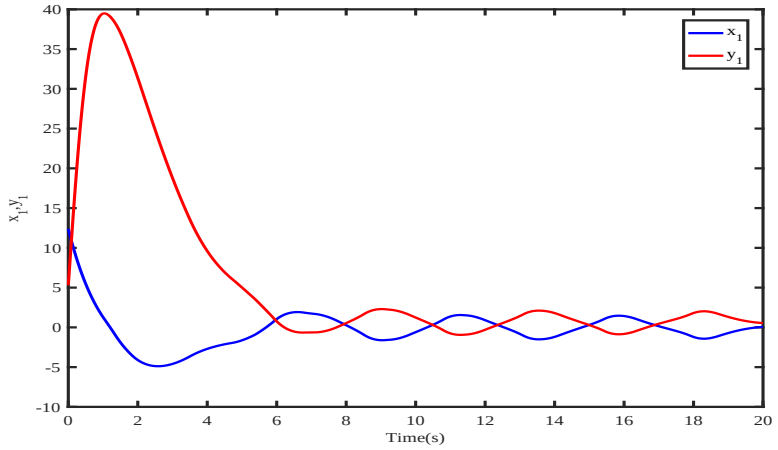

(a)

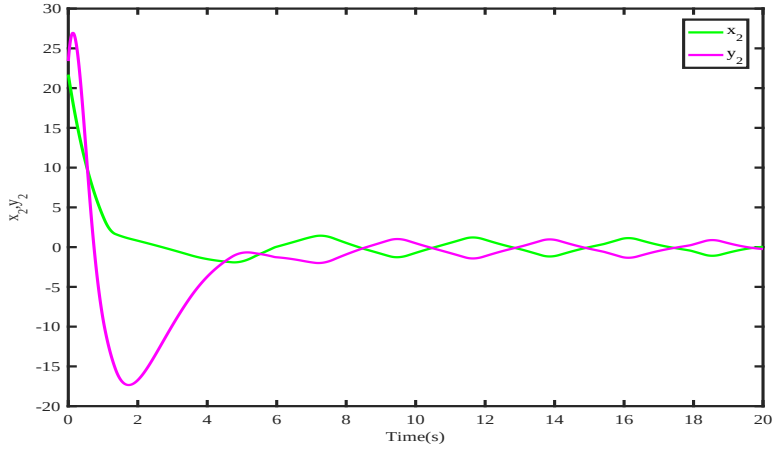

(b)

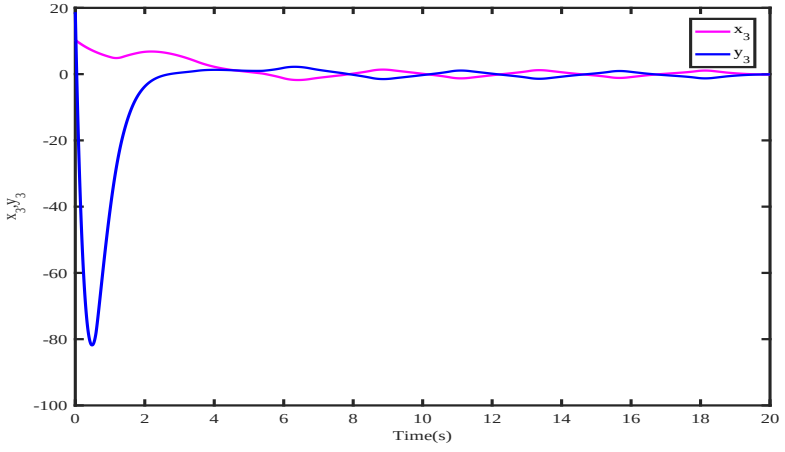

(c)

FIGURE 6.7: States in Anti-synchronization of Master CNN and Slave CNN (Case I)

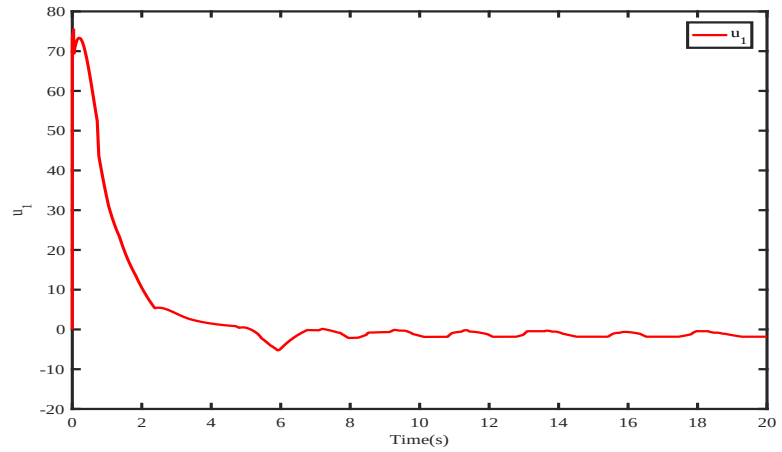

(a)

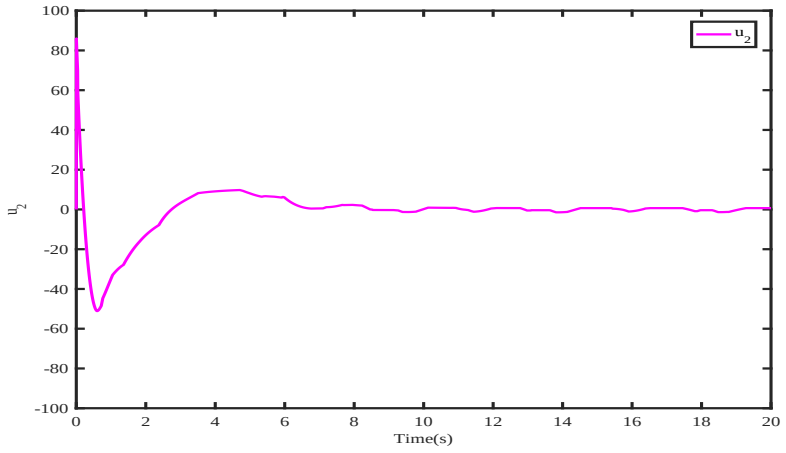

(b)

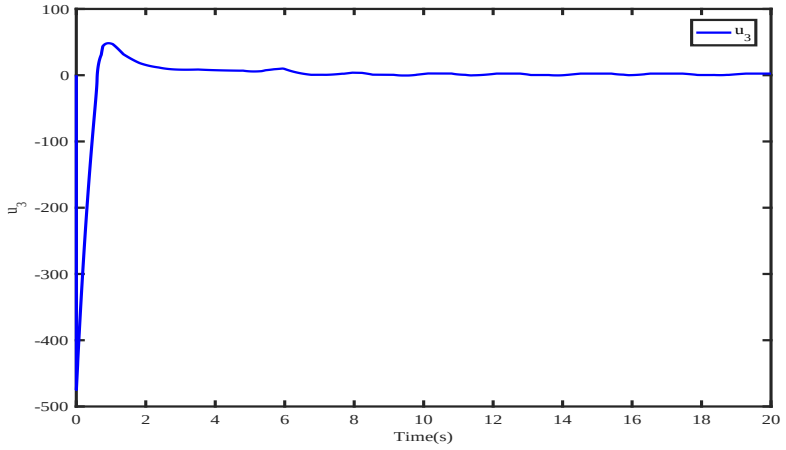

(c)

FIGURE 6.8: Control effort

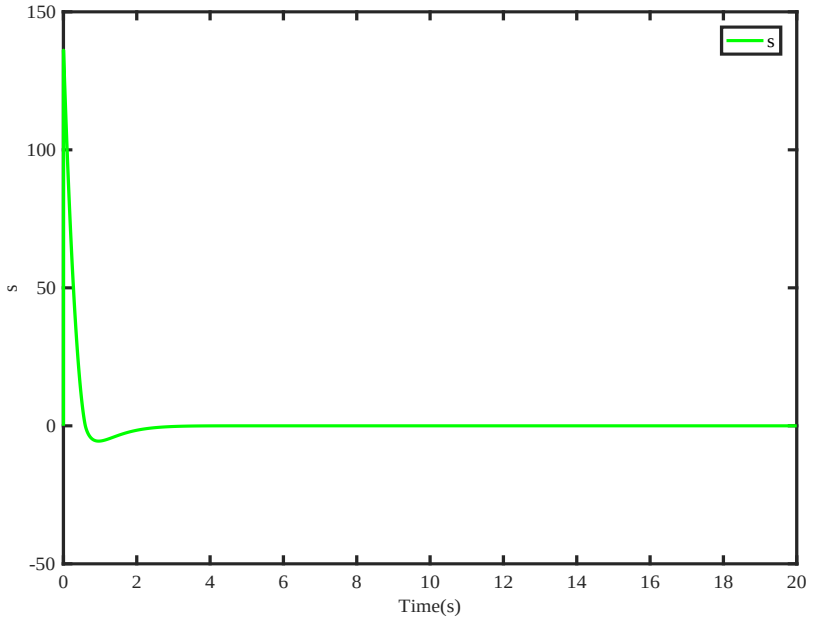

FIGURE 6.9: Sliding Surface for Anti-synchronization in (Case I)

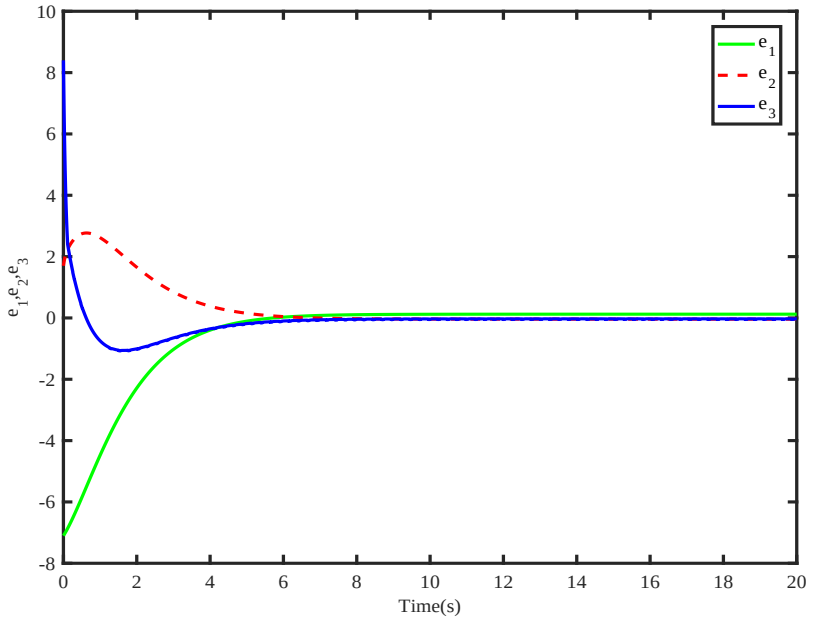

FIGURE 6.10: Convergence of synchronization error dynamics to zero (Case II)

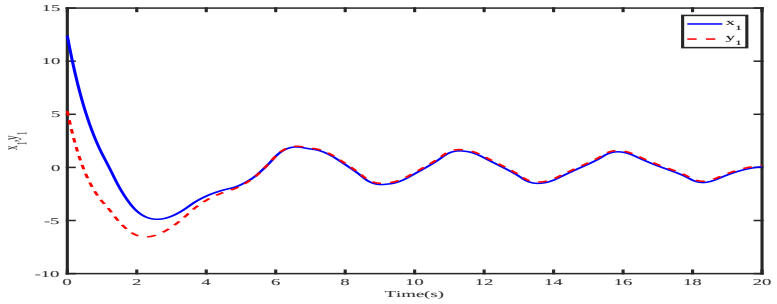

(a)

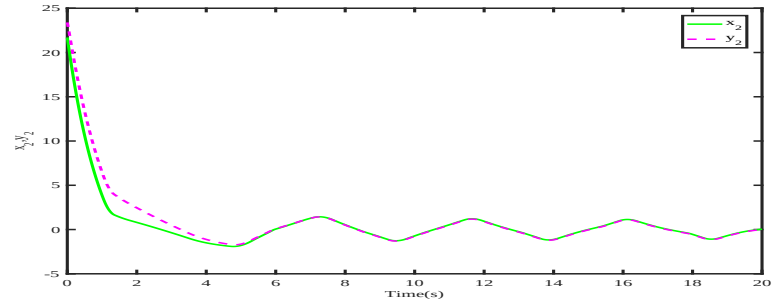

(b)

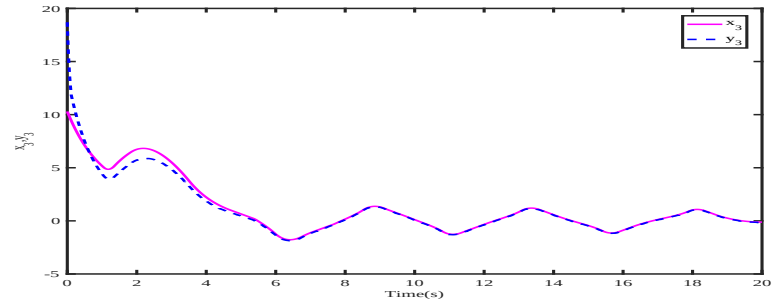

(c)

FIGURE 6.11: States in synchronization of Master CNN and Slave CNN (Case II)

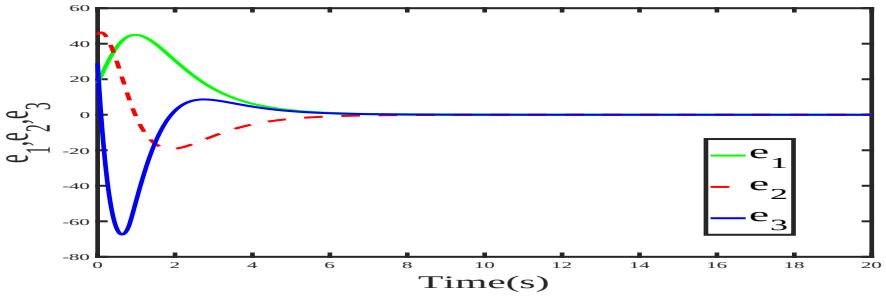

FIGURE 6.12: Convergence of Anti-synchronization error dynamic to zero (Case II)

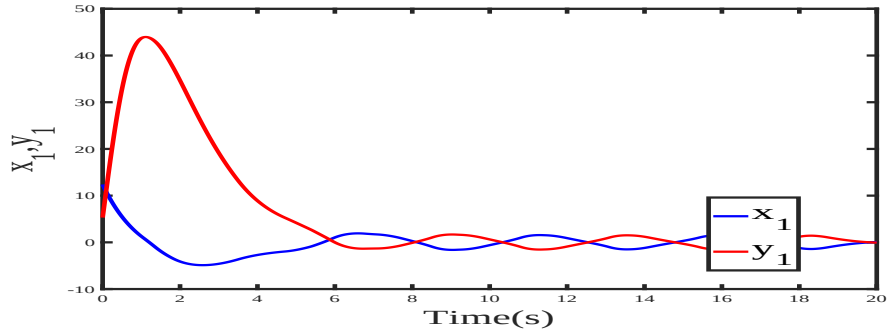

(a)

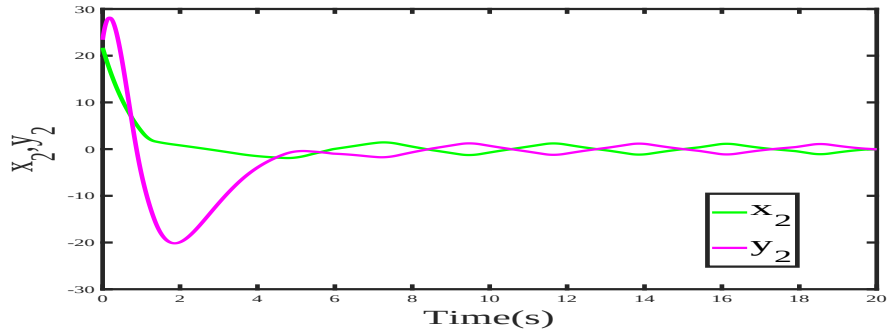

(b)

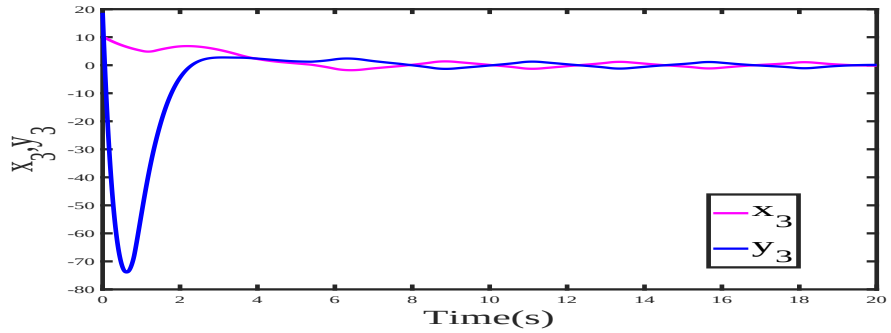

(c)

FIGURE 6.13: States in Anti-synchronization of Master CNN and Slave CNN (Case II)

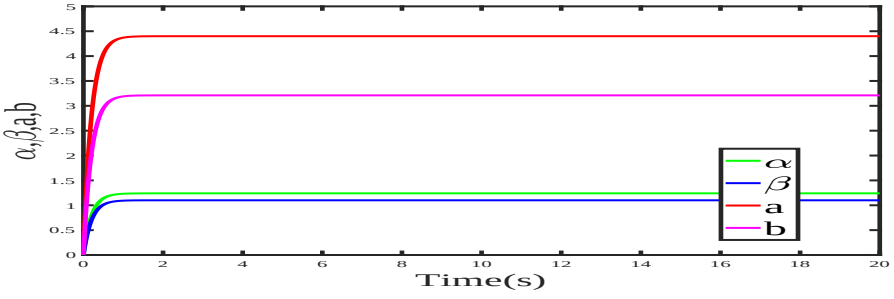

FIGURE 6.14: Estimation of Uncertain parameters $\hat{\alpha}, \hat{\beta}, \hat{a}, \hat{b}$ (Case II)

Chapter 7

Conclusion and Future Work

7.1 Conclusion

The goal of this thesis is to propose new and novel control algorithm for the hybrid synchronization of DN with coupled nodes and uncertain parameters. Control of HS of a DN is quite difficult task due to the chaotic nature of the nodes. Furthermore, in the presence of uncertain parameters this becomes a real challenging task. A generalized algorithm is designed in this thesis for DN of N systems to investigate the co-existence of synchronization and anti-synchronization.

The theoretical problems considered in the most literature as reviewed in this thesis are considering synchronization between two and more chaotic systems. The synchronization problem for multiple chaotic systems coupled in a network like the proposed in this thesis is addressed in a less work. The problem formulation presented in this thesis considers Hybrid synchronization in dynamical network with uncertain parameters. It is more practical because it considers the unknown parameters. Practically the constant parameters of the network are more prone to disturbances. In the presence of uncertain parameters it becomes genuinely difficult to control the hybrid synchronization in a dynamical network.

Based on the comprehensive study on types of synchronization and control techniques in the literature, Two different kinds of DNs are considered. To gain insight and to create interest to deal with the DNs with uncertain parameters, ring type and cellular neural networks are considered. An adaptive ISMC and SSTA techniques are used to investigate hybrid synchronization of DNs and following conclusions are drawn:

- The proposed control algorithm addresses the problem of HS in DNs comprehensively.
- The Adaptive control laws have faithfully estimated the uncertain parameters.
- The theoretical results presented in this thesis are in agreement with the simulation results for the challenging problem of HS of ring type DNs and cellular neural network.
- Since the control methodology is based on the sliding mode control and its variants ISMC and SSTA, the control design procedure is simple and robust to disturbances and parametric variations.

In the presence of uncertain parameters the HS of DN using adaptive ISMC and SSTA, set new paradigm in this field of research. Practically, the constant parameters are more prone to disturbances so achieving the HS with unknown parameters is presented in this thesis. Simulation results provide the proofs of achieving the objectives and the effectiveness of the proposed control framework.

7.2 Future Work

Future research will include in-depth study of star topology and chain formation of chaotic systems. More complex network like the secure communication network and electrical grid are of high interest.
A list of few topics for future research is:

- Investigation of hybrid synchronization in time-delayed coupling network.
- application of adaptive integral sliding mode control to investigate hybrid synchronization considering uncertain states of chaotic systems in a DN
- hybrid synchronization of DN considering the occurrence of faults using adaptive ISMC.
- Investigation of hybrid synchronization in secure communication network.
- Investigation of hybrid synchronization in time delay and non-time delay power grids.

Bibliography

[1] G. Birkhoff, *Lattice theory*, 1st ed. American Mathematical Soc., 1940, vol. 25.

[2] G. D. Birkhoff, *Dynamical systems*, 1st ed. American Mathematical Soc., 1927, vol. 9.

[3] J. Barrow-Green, *Poincaré and the three body problem*. American Mathematical Soc., 1997, no. 11.

[4] J. Eckmann, "J.-p. eckmann and d. ruelle, rev. mod. phys. 57, 617 (1985)," *Rev. Mod. Phys*, vol. 57, p. 617, 1985.

[5] A. Lichtenberg and M. Lieberman, "Regular and stochastic motion springer-verlag new york," *Heidelberg Berlin*, vol. 277, 1983.

[6] P. De Grauwe, H. Dewachter, and M. Embrechts, "Exchange rate theory: chaotic models of foreign exchange markets," 1995.

[7] B. Blasius, A. Huppert, and L. Stone, "Complex dynamics and phase synchronization in spatially extended ecological systems," *Nature*, vol. 399, no. 6734, pp. 354–359, 1999.

[8] B. D. L. Costello and A. Adamatzky, "Experimental implementation of collision-based gates in belousov–zhabotinsky medium," *Chaos, Solitons & Fractals*, vol. 25, no. 3, pp. 535–544, 2005.

[9] T. Alligood, "Sauer, and yorke ja," *Chaos-An Introduction to Dynamical Systems,. Springer-Verlag, New York*, 1997.

[10] H. Fujisaka and T. Yamada, "Stability theory of synchronized motion in coupled-oscillator systems," *Progress of theoretical physics*, vol. 69, no. 1, pp. 32–47, 1983.

[11] L. M. Pecora and T. L. Carrol, "Synchronization in chaotic systems," *Phys. Rev. Lett.*, vol. 64, p. 821, 1990.

[12] V. K. Yadav, R. Kumar, A. Leung, and S. Das, "Dual phase and dual anti-phase synchronization of fractional order chaotic systems in real and complex variables with uncertainties," *Chinese journal of physics*, vol. 57, pp. 282–308, 2019.

[13] H. Fujisaka and T. Yamada, "Stability theory of synchronized motion in coupled-oscillator systems. ." *Prog. Theor. Phys.*, vol. 69, p. 32, 1983.

[14] P. P. Singh and B. K. Roy, "Microscopic chaos control of chemical reactor system using nonlinear active plus proportional integral sliding mode control technique," *The European Physical Journal Special Topics*, vol. 228, no. 1, pp. 169–184, 2019.

[15] Y. Guan, L. K. Li, B. Ahn, and K. T. Kim, "Chaos, synchronization, and desynchronization in a liquid-fueled diffusion-flame combustor with an intrinsic hydrodynamic mode," *Chaos: An Interdisciplinary Journal of Nonlinear Science*, vol. 29, no. 5, p. 053124, 2019.

[16] N. Pillai, S. L. Schwartz, T. Ho, A. Dokoumetzidis, R. Bies, and I. Freedman, "Estimating parameters of nonlinear dynamic systems in pharmacology using chaos synchronization and grid search," *Journal of pharmacokinetics and pharmacodynamics*, vol. 46, no. 2, pp. 193–210, 2019.

[17] G. Tang, I. E. Polykretis, V. A. Ivanov, A. Shah, and K. P. Michmizos, "Introducing astrocytes on a neuromorphic processor: Synchronization, local plasticity and edge of chaos," in *Proceedings of the 7th Annual Neuro-inspired Computational Elements Workshop*, 2019, pp. 1–9.

[18] F. Parastesh, C.-Y. Chen, H. Azarnoush, S. Jafari, and B. Hatef, "Synchronization patterns in a blinking multilayer neuronal network," *The European Physical Journal Special Topics*, vol. 228, no. 11, pp. 2465–2474, 2019.

[19] T. Jüngling, X. Porte, N. Oliver, M. C. Soriano, and I. Fischer, "A unifying analysis of chaos synchronization and consistency in delay-coupled semiconductor lasers," *IEEE Journal of Selected Topics in Quantum Electronics*, vol. 25, no. 6, pp. 1–9, 2019.

[20] O. Spitz, A. Herdt, J. Wu, G. Maisons, M. Carras, C.-W. Wong, W. Elsäßer, and F. Grillot, "Private communication with quantum cascade laser photonic chaos," *Nature communications*, vol. 12, no. 1, pp. 1–8, 2021.

[21] H. Poincaré, "On the three-body problem and the equations of dynamics," in *The Kinetic Theory Of Gases: An Anthology of Classic Papers with Historical Commentary*. World Scientific, 2003, pp. 368–376.

[22] L. O. Chua, M. Itoh, L. Kocarev, and K. Eckert, "Chaos synchronization in chua's circuit," *Journal of Circuits, Systems, and Computers*, vol. 3, no. 01, pp. 93–108, 1993.

[23] L. M. Pecora and T. L. Carroll, "Synchronization in chaotic systems," *Physical review letters*, vol. 64, no. 8, p. 821, 1990.

[24] F. Zou and J. A. Nossek, "A chaotic attractor with cellular neural networks," *IEEE Transactions on circuits and systems*, vol. 38, no. 7, pp. 811–812, 1991.

[25] A. Choudhary, J. F. Lindner, E. G. Holliday, S. T. Miller, S. Sinha, and W. L. Ditto, "Physics-enhanced neural networks learn order and chaos," *Physical Review E*, vol. 101, no. 6, p. 062207, 2020.

[26] Z.-G. Wu, P. Shi, H. Su, and J. Chu, "Exponential synchronization of neural networks with discrete and distributed delays under time-varying sampling," *IEEE Transactions on Neural Networks and Learning Systems*, vol. 23, no. 9, pp. 1368–1376, 2012.

[27] A. Abdurahman, H. Jiang, and Z. Teng, "Finite-time synchronization for fuzzy cellular neural networks with time-varying delays," *Fuzzy Sets and Systems*, vol. 297, pp. 96–111, 2016.

[28] Y. Yu and H.-X. Li, "Adaptive generalized function projective synchronization of uncertain chaotic systems," *Nonlinear Analysis: Real World Applications*, vol. 11, no. 4, pp. 2456–2464, 2010.

[29] G. M. Mahmoud, E. E. Mahmoud, and A. A. Arafa, "On projective synchronization of hyperchaotic complex nonlinear systems based on passive theory for secure communications," *Physica Scripta*, vol. 87, no. 5, p. 055002, 2013.

[30] J. Zhou, J.-a. Lu, and J. Lu, "Adaptive synchronization of an uncertain complex dynamical network," *IEEE Transactions on Automatic Control*, vol. 51, no. 4, pp. 652–656, 2006.

[31] J. Sun, Q. Yin, and Y. Shen, "Compound synchronization for four chaotic systems of integer order and fractional order," *EPL (europhysics letters)*, vol. 106, no. 4, p. 40005, 2014.

[32] J. Sun, Y. Shen, X. Wang, and J. Chen, "Finite-time combination-combination synchronization of four different chaotic systems with unknown parameters via sliding mode control," *Nonlinear Dynamics*, vol. 76, no. 1, pp. 383–397, 2014.

[33] C. Jiang and S. Liu, "Synchronization and antisynchronization of-coupled complex permanent magnet synchronous motor systems with ring connection," *Complexity*, vol. 2017, 2017.

[34] F. Nian and W. Liu, "Hybrid synchronization of heterogeneous chaotic systems on dynamic network," *Chaos, Solitons & Fractals*, vol. 91, pp. 554–561, 2016.

[35] Q. Wei, X.-y. Wang, and X.-p. Hu, "Hybrid function projective synchronization in complex dynamical networks," *AIP Advances*, vol. 4, no. 2, p. 027128, 2014.

[36] C. Li, Q. Chen, and T. Huang, "Coexistence of anti-phase and complete synchronization in coupled chen system via a single variable," *Chaos, Solitons & Fractals*, vol. 38, no. 2, pp. 461–464, 2008.

[37] S. Wang, Y. Yu, and G. Wen, "Hybrid projective synchronization of time-delayed fractional order chaotic systems," *Nonlinear Analysis: Hybrid Systems*, vol. 11, pp. 129–138, 2014.

[38] A. Khan, S. Singh, and A. T. Azar, "Combination-combination anti-synchronization of four fractional order identical hyperchaotic systems," in *International conference on advanced machine learning technologies and applications*. Springer, 2019, pp. 406–414.

[39] L. Chen, C. Huang, H. Liu, and Y. Xia, "Anti-synchronization of a class of chaotic systems with application to lorenz system: a unified analysis of the integer order and fractional order," *Mathematics*, vol. 7, no. 6, p. 559, 2019.

[40] T. Dahms, J. Lehnert, and E. Schöll, "Cluster and group synchronization in delay-coupled networks," *Physical Review E*, vol. 86, no. 1, p. 016202, 2012.

[41] M. Jiménez-Martín, J. Rodríguez-Laguna, O. D'Huys, J. de la Rubia, and E. Korutcheva, "Synchronization of fluctuating delay-coupled chaotic networks," *Physical Review E*, vol. 95, no. 5, p. 052210, 2017.

[42] Y. Sun, W. Li, and J. Ruan, "Generalized outer synchronization between complex dynamical networks with time delay and noise perturbation," *Communications in Nonlinear Science and Numerical Simulation*, vol. 18, no. 4, pp. 989–998, 2013.

[43] L. Min and G. Chen, "Generalized synchronization in an array of nonlinear dynamic systems with applications to chaotic cnn," *International Journal of Bifurcation and chaos*, vol. 23, no. 01, p. 1350016, 2013.

[44] X. Chen, J. Qiu, J. Cao, and H. He, "Hybrid synchronization behavior in an array of coupled chaotic systems with ring connection," *Neurocomputing*, vol. 173, pp. 1299–1309, 2016.

[45] N. Siddique and F. ur Rehman, "Parameter identification and hybrid synchronization in an array of coupled chaotic systems with ring connection: An adaptive integral sliding mode approach," *Mathematical Problems in Engineering*, vol. 2018, pp. 1–15, 2018.

[46] N. Siddique and F. U. Rehman, "Hybrid synchronization and parameter estimation of a complex chaotic network of permanent magnet synchronous motors using adaptive integral sliding mode control," *Bulletin of the Polish Academy of Sciences: Technical Sciences*, vol. 69, no. 3, pp. 1–9, 2021.

[47] C. Huygens, "The hague the netherlands: Martinus nijhoff," *Oeuvres Complètes de Christiaan Huygens*, vol. 17, 1932.

[48] J. W. S. B. Rayleigh, *The theory of sound*. Macmillan, 1896, vol. 2.

[49] J. Buck and E. Buck, "Mechanism of rhythmic synchronous flashing of fireflies: Fireflies of southeast asia may use anticipatory time-measuring in synchronizing their flashing," *Science*, vol. 159, no. 3821, pp. 1319–1327, 1968.

[50] D. Cysarz and A. Büssing, "Cardiorespiratory synchronization during zen meditation," *European journal of applied physiology*, vol. 95, no. 1, pp. 88–95, 2005.

[51] J. Zamora-Munt, C. Masoller, J. Garcia-Ojalvo, and R. Roy, "Crowd synchrony and quorum sensing in delay-coupled lasers," *Physical review letters*, vol. 105, no. 26, p. 264101, 2010.

[52] S. H. Strogatz, D. M. Abrams, A. McRobie, B. Eckhardt, and E. Ott, "Theoretical mechanics: Crowd synchrony on the millennium bridge," *Nature*, vol. 438, no. 7064, p. 43, 2005.

[53] M. B. Miller and B. L. Bassler, "Quorum sensing in bacteria," *Annual Reviews in Microbiology*, vol. 55, no. 1, pp. 165–199, 2001.

[54] S. Boccaletti, J. Kurths, G. Osipov, D. Valladares, and C. Zhou, "The synchronization of chaotic systems," *Physics reports*, vol. 366, no. 1-2, pp. 1–101, 2002.

[55] A. Pikovsky, M. Rosenblum, and J. Kurths, *Synchronization: a universal concept in nonlinear sciences*. Cambridge university press, 2003, vol. 12.

[56] G. Chen and T. Ueta, *Chaos in circuits and systems*. World Scientific, 2002, vol. 11.

[57] K. Otsuka, *Nonlinear dynamics in optical complex systems*. Springer Science & Business Media, 2000, vol. 7.

[58] C. W. Horton Jr *et al.*, *Chaos and structures in nonlinear plasmas*. World Scientific, 1996.

[59] L. Gyorgyi, T. Turányi, and R. J. Field, "Mechanistic details of the oscillatory belousov-zhabotinskii reaction," *Journal of physical chemistry*, vol. 94, no. 18, pp. 7162–7170, 1990.

[60] Y.-N. Li, L. Chen, Z.-S. Cai, and X.-z. Zhao, "Experimental study of chaos synchronization in the belousov–zhabotinsky chemical system," *Chaos, Solitons & Fractals*, vol. 22, no. 4, pp. 767–771, 2004.

[61] M. Rivera, G. Martinez Mekler, and P. Parmananda, "Synchronization phenomena for a pair of locally coupled chaotic electrochemical oscillators: A survey," *Chaos: An Interdisciplinary Journal of Nonlinear Science*, vol. 16, no. 3, p. 037105, 2006.

[62] E. Toledo, S. Akselrod, I. Pinhas, and D. Aravot, "Does synchronization reflect a true interaction in the cardiorespiratory system?" *Medical engineering & physics*, vol. 24, no. 1, pp. 45–52, 2002.

[63] M. G. Kitzbichler, M. L. Smith, S. R. Christensen, and E. Bullmore, "Broadband criticality of human brain network synchronization," *PLoS computational biology*, vol. 5, no. 3, p. e1000314, 2009.

[64] C. J. Tessone, M. Cencini, and A. Torcini, "Synchronization of extended chaotic systems with long-range interactions: an analogy to levy-flight spreading of epidemics," *Physical review letters*, vol. 97, no. 22, p. 224101, 2006.

[65] B. Blasius and L. Stone, "Chaos and phase synchronization in ecological systems," *International Journal of Bifurcation and Chaos*, vol. 10, no. 10, pp. 2361–2380, 2000.

[66] N. Basalto, R. Bellotti, F. De Carlo, P. Facchi, and S. Pascazio, "Clustering stock market companies via chaotic map synchronization," *Physica A: Statistical Mechanics and its Applications*, vol. 345, no. 1-2, pp. 196–206, 2005.

[67] V. N. Belykh, I. V. Belykh, and M. Hasler, "Hierarchy and stability of partially synchronous oscillations of diffusively coupled dynamical systems," *Physical Review E*, vol. 62, no. 5, p. 6332, 2000.

[68] M. G. Rosenblum, A. S. Pikovsky, and J. Kurths, "Phase synchronization of chaotic oscillators," *Physical review letters*, vol. 76, no. 11, p. 1804, 1996.

[69] A. A. Eshmawi and E. E. Mahmoud, "Secure communications via complex phase synchronization of pair complex chaotic structures with a similar structure of linear terms with modifying in nonlinear terms," *Alexandria Engineering Journal*, vol. 59, no. 3, pp. 1107–1116, 2020.

[70] W. Liu, J. Xiao, X. Qian, and J. Yang, "Antiphase synchronization in coupled chaotic oscillators," *Physical Review E*, vol. 73, no. 5, p. 057203, 2006.

[71] C.-M. Kim, S. Rim, W.-H. Kye, J.-W. Ryu, and Y.-J. Park, "Anti-synchronization of chaotic oscillators," *Physics Letters A*, vol. 320, no. 1, pp. 39–46, 2003.

[72] V. Astakhov, A. Shabunin, and V. Anishchenko, "Antiphase synchronization in symmetrically coupled self-oscillators," *International Journal of Bifurcation and Chaos*, vol. 10, no. 04, pp. 849–857, 2000.

[73] M. G. Rosenblum, A. S. Pikovsky, and J. Kurths, "From phase to lag synchronization in coupled chaotic oscillators," *Physical Review Letters*, vol. 78, no. 22, p. 4193, 1997.

[74] L. Kocarev and U. Parlitz, "Generalized synchronization, predictability, and equivalence of unidirectionally coupled dynamical systems," *Physical review letters*, vol. 76, no. 11, p. 1816, 1996.

[75] N. F. Rulkov, M. M. Sushchik, L. S. Tsimring, and H. D. Abarbanel, "Generalized synchronization of chaos in directionally coupled chaotic systems," *Physical Review E*, vol. 51, no. 2, p. 980, 1995.

[76] S. Jacquir, S. Binczak, J.-M. Bilbault, V. Kazantsev, and V. Nekorkin, "Synaptic coupling between two electronic neurons," *Nonlinear Dynamics*, vol. 44, no. 1-4, pp. 29–36, 2006.

[77] M. Breakspear, J. R. Terry, and K. J. Friston, "Modulation of excitatory synaptic coupling facilitates synchronization and complex dynamics in a nonlinear model of neuronal dynamics," *Neurocomputing*, vol. 52, pp. 151–158, 2003.

[78] M. J. Tunstall, A. Roberts, and S. R. Soffe, "Modelling inter-segmental coordination of neuronal oscillators: synaptic mechanisms for uni-directional coupling during swimming in xenopus tadpoles," *Journal of computational neuroscience*, vol. 13, no. 2, pp. 143–158, 2002.

[79] Q. Y. Wang, Q. S. Lu, G. R. Chen, and D. H. Guo, "Chaos synchronization of coupled neurons with gap junctions," *Physics Letters A*, vol. 356, no. 1, pp. 17–25, 2006.

[80] E. Padmanaban, R. Banerjee, and S. K. Dana, "Targeting and control of synchronization in chaotic oscillators," *International Journal of Bifurcation and Chaos*, vol. 22, no. 07, p. 1250177, 2012.

[81] D. Sussillo and L. F. Abbott, "Generating coherent patterns of activity from chaotic neural networks," *Neuron*, vol. 63, no. 4, pp. 544–557, 2009.

[82] L. M. Pecora and T. L. Carroll, "Master stability functions for synchronized coupled systems," *Physical review letters*, vol. 80, no. 10, p. 2109, 1998.

[83] Y. Kuramoto, "Chemical oscillations, waves, and turbulence," *Springer Series in Synergetics, Vol. 19*, vol. 40, no. 10, pp. 817–818, 1984.

[84] T. L. Carroll and L. M. Pecora, "Synchronizing chaotic circuits," *IEEE Transactions on circuits and systems*, vol. 38, no. 4, pp. 453–456, 1991.

[85] E. A. Assali, "Predefined-time synchronization of chaotic systems with different dimensions and applications," *Chaos, Solitons & Fractals*, vol. 147, p. 110988, 2021.

[86] R. Guo and Y. Qi, "Partial anti-synchronization in a class of chaotic and hyper-chaotic systems," *IEEE Access*, vol. 9, pp. 46 303–46 312, 2021.

[87] M. Bennett, M. F. Schatz, H. Rockwood, and K. Wiesenfeld, "Huygens's clocks," *Proceedings: Mathematics, Physical and Engineering Sciences*, pp. 563–579, 2002.

[88] J.-b. Liu, C.-f. Ye, S.-j. Zhang, and W.-t. Song, "Anti-phase synchronization in coupled map lattices," *Physics Letters A*, vol. 274, no. 1-2, pp. 27–29, 2000.

[89] I. Grosu, R. Banerjee, P. K. Roy, and S. K. Dana, "Design of coupling for synchronization of chaotic oscillators," *Physical Review E*, vol. 80, no. 1, p. 016212, 2009.

[90] E. E. Mahmoud and B. H. AL-Harthi, "A hyperchaotic detuned laser model with an infinite number of equilibria existing on a plane and its modified complex phase synchronization with time lag," *Chaos, Solitons & Fractals*, vol. 130, p. 109442, 2020.

[91] W. Shammakh, E. E. Mahmoud, and B. S. Kashkari, "Complex modified projective phase synchronization of nonlinear chaotic frameworks with complex variables," *Alexandria Engineering Journal*, vol. 59, no. 3, pp. 1265–1273, 2020.

[92] I. Bashkirtseva, L. Ryashko, and A. N. Pisarchik, "Stochastic transitions between in-phase and anti-phase synchronization in coupled map-based neural

oscillators," *Communications in Nonlinear Science and Numerical Simulation*, vol. 95, p. 105611, 2021.

[93] U. Parlitz, L. Junge, W. Lauterborn, and L. Kocarev, "Experimental observation of phase synchronization," *Physical Review E*, vol. 54, no. 2, p. 2115, 1996.

[94] S. Taherion and Y.-C. Lai, "Experimental observation of lag synchronization in coupled chaotic systems," *International Journal of Bifurcation and Chaos*, vol. 10, no. 11, pp. 2587–2594, 2000.

[95] A. Prasad, J. Kurths, S. K. Dana, and R. Ramaswamy, "Phase-flip bifurcation induced by time delay," *Physical Review E*, vol. 74, no. 3, p. 035204, 2006.

[96] W. S. Sayed and A. G. Radwan, "Generalized switched synchronization and dependent image encryption using dynamically rotating fractional-order chaotic systems," *AEU-International Journal of Electronics and Communications*, vol. 123, p. 153268, 2020.

[97] K. Huang, F. Sorrentino, and M. Hossein-Zadeh, "Experimental observations of synchronization between two bidirectionally coupled physically dissimilar oscillators," *Physical Review E*, vol. 102, no. 4, p. 042215, 2020.

[98] S. Yang and C. Duan, "Generalized synchronization in chaotic systems," *Chaos, Solitons & Fractals*, vol. 9, no. 10, pp. 1703–1707, 1998.

[99] S. Xiang, Y. Han, H. Wang, A. Wen, and Y. Hao, "Zero-lag chaos synchronization properties in a hierarchical tree-type network consisting of mutually coupled semiconductor lasers," *Nonlinear Dynamics*, vol. 99, no. 4, pp. 2893–2906, 2020.

[100] W. Yang, W. Yu, J. Cao, F. E. Alsaadi, and T. Hayat, "Global exponential stability and lag synchronization for delayed memristive fuzzy cohen–grossberg bam neural networks with impulses," *Neural Networks*, vol. 98, pp. 122–153, 2018.

[101] Z. S. Al-Talib and S. F. AL-Azzawi, "Projective synchronization for 4d hyperchaotic system based on adaptive nonlinear control strategy," *Indonesian Journal of Electrical Engineering and Computer Science*, vol. 19, no. 2, pp. 715–722, 2020.

[102] P. Liu, M. Kong, and Z. Zeng, "Projective synchronization analysis of fractional-order neural networks with mixed time delays," *IEEE Transactions on Cybernetics*, 2020.

[103] S. Yang, C. Hu, J. Yu, and H. Jiang, "Projective synchronization in finite-time for fully quaternion-valued memristive networks with fractional-order," *Chaos, Solitons & Fractals*, vol. 147, p. 110911, 2021.

[104] S. Aadhithiyan, R. Raja, Q. Zhu, J. Alzabut, M. Niezabitowski, and C. Lim, "Modified projective synchronization of distributive fractional order complex dynamic networks with model uncertainty via adaptive control," *Chaos, Solitons & Fractals*, vol. 147, p. 110853, 2021.

[105] M. El-Dessoky, E. Alzahrani, and N. Al-Rehily, "Control and adaptive modified function projective synchronization of a new hyperchaotic system," *Alexandria Engineering Journal*, vol. 60, no. 4, pp. 3985–3990, 2021.

[106] G. M. Mahmoud, T. Aboelenen, T. M. Abed-Elhameed, and A. A. Farghaly, "On boundedness and projective synchronization of distributed order neural networks," *Applied Mathematics and Computation*, vol. 404, p. 126198, 2021.

[107] M. Hui, J. Zhang, J. Zhang, H. H.-C. Iu, R. Yao, and L. Bai, "Finite-time projective synchronization of stochastic complex-valued neural networks with probabilistic time-varying delays," *IEEE Access*, vol. 9, pp. 44 784–44 796, 2021.

[108] M. El-Dessoky and M. Khan, "Application of fractional calculus to combined modified function projective synchronization of different systems," *Chaos: An Interdisciplinary Journal of Nonlinear Science*, vol. 29, no. 1, p. 013107, 2019.

[109] A. Khan, P. Trikha, and L. S. Jahanzaib, "Dislocated hybrid synchronization via. tracking control & parameter estimation methods with application," *International Journal of Modelling and Simulation*, pp. 1–11, 2020.

[110] P. Trikha and L. S. Jahanzaib, "Secure communication: using double compound-combination hybrid synchronization," in *Proceedings of International Conference on Artificial Intelligence and Applications*. Springer, 2021, pp. 81–91.

[111] A. Khan and H. Chaudhary, "Hybrid projective combination–combination synchronization in non-identical hyperchaotic systems using adaptive control," *Arabian Journal of Mathematics*, vol. 9, no. 3, pp. 597–611, 2020.

[112] A. Khan and U. Nigar, "Sliding mode disturbance observer control based on adaptive hybrid projective compound combination synchronization in fractional-order chaotic systems," *Journal of Control, Automation and Electrical Systems*, vol. 31, no. 4, pp. 885–899, 2020.

[113] A. Khan and H. Chaudhary, "Adaptive hybrid projective synchronization of hyper-chaotic systems," *Applications and Applied Mathematics: An International Journal (AAM)*, vol. 16, no. 1, p. 7, 2021.

[114] Z. Wang and R. Guo, "Hybrid synchronization problem of a class of chaotic systems by an universal control method," *Symmetry*, vol. 10, no. 11, p. 552, 2018.

[115] M. Dalir and N. Bigdeli, "The design of a new hybrid controller for fractional-order uncertain chaotic systems with unknown time-varying delays," *Applied Soft Computing*, vol. 87, p. 106000, 2020.

[116] W. Jun-Wei, M. Qing-Hua, and Z. Li, "A novel mixed-synchronization phenomenon in coupled chua's circuits via non-fragile linear control," *Chinese Physics B*, vol. 20, no. 8, p. 080506, 2011.

[117] C. Yang, Z. Xiong, and T. Yang, "Finite-time synchronization of coupled inertial memristive neural networks with mixed delays via nonlinear feedback control," *Neural Processing Letters*, pp. 1–18, 2020.

[118] C. Yi, C. Xu, J. Feng, J. Wang, and Y. Zhao, "Pinning synchronization for reaction-diffusion neural networks with delays by mixed impulsive control," *Neurocomputing*, vol. 339, pp. 270–278, 2019.

[119] K. S. Sudheer and M. Sabir, "Hybrid synchronization of hyperchaotic lu system," *Pramana*, vol. 73, no. 4, p. 781, 2009.

[120] P. He, S.-H. Ma, and T. Fan, "Finite-time mixed outer synchronization of complex networks with coupling time-varying delay," *Chaos: An Interdisciplinary Journal of Nonlinear Science*, vol. 22, no. 4, p. 043151, 2012.

[121] M.-C. Ho and Y.-C. Hung, "Synchronization of two different systems by using generalized active control," *Physics Letters A*, vol. 301, no. 5-6, pp. 424–428, 2002.

[122] M. Yassen, "Chaos synchronization between two different chaotic systems using active control," *Chaos, Solitons & Fractals*, vol. 23, no. 1, pp. 131–140, 2005.

[123] E.-W. Bai and K. E. Lonngren, "Synchronization of two lorenz systems using active control," *Chaos, Solitons & Fractals*, vol. 8, no. 1, pp. 51–58, 1997.

[124] S. Agrawal, M. Srivastava, and S. Das, "Synchronization of fractional order chaotic systems using active control method," *Chaos, Solitons & Fractals*, vol. 45, no. 6, pp. 737–752, 2012.

[125] C.-F. Feng, "Projective synchronization between two different time-delayed chaotic systems using active control approach," *Nonlinear Dynamics*, vol. 62, no. 1-2, pp. 453–459, 2010.

[126] G. M. Mahmoud, T. Bountis, and E. E. Mahmoud, "Active control and global synchronization of the complex chen and lü systems," *International Journal of Bifurcation and Chaos*, vol. 17, no. 12, pp. 4295–4308, 2007.

[127] I. Ahmad, A. B. Saaban, A. B. Ibrahim, and M. Shahzad, "Global chaos synchronization of new chaotic system using linear active control," *Complexity*, vol. 21, no. 1, pp. 379–386, 2015.

[128] C. Jiang, A. Zada, M. T. Şenel, and T. Li, "Synchronization of bidirectional n-coupled fractional-order chaotic systems with ring connection based on antisymmetric structure," *Advances in Difference Equations*, vol. 2019, no. 1, pp. 1–16, 2019.

[129] B. Liu, Z. Sun, Y. Luo, and Y. Zhong, "Uniform synchronization for chaotic dynamical systems via event-triggered impulsive control," *Physica A: Statistical Mechanics and its Applications*, vol. 531, p. 121725, 2019.

[130] X. Chen, C. Wang, and J. Qiu, "Synchronization and anti-synchronization of n different coupled chaotic systems with ring connection," *International Journal of Modern Physics C*, vol. 25, no. 05, p. 1440011, 2014.

[131] X. Chen, J. Qiu, Q. Song, and A. Zhang, "Synchronization of coupled chaotic systems with ring connection based on special antisymmetric structure," in *Abstract and Applied Analysis*, vol. 2013. Hindawi, 2013.

[132] C. Jiang, F. Zhang, and T. Li, "Synchronization and antisynchronization of n-coupled fractional-order complex chaotic systems with ring connection," *Mathematical Methods in the Applied Sciences*, vol. 41, no. 7, pp. 2625–2638, 2018.

[133] B.-S. Chen, C.-H. Chiang, and S. K. Nguang, "Robust h_∞ synchronization design of nonlinear coupled network via fuzzy interpolation method," *IEEE Transactions on Circuits and Systems I: Regular Papers*, vol. 58, no. 2, pp. 349–362, 2010.

[134] S.-Y. Li and Z.-M. Ge, "Generalized synchronization of chaotic systems with different orders by fuzzy logic constant controller," *Expert Systems with Applications*, vol. 38, no. 3, pp. 2302–2310, 2011.

[135] X. Chen, J. Cao, J. Qiu, A. Alsaedi, and F. E. Alsaadi, "Adaptive control of multiple chaotic systems with unknown parameters in two different synchronization modes," *Advances in Difference Equations*, vol. 2016, no. 1, p. 231, 2016.

[136] W. Yu, P. DeLellis, G. Chen, M. Di Bernardo, and J. Kurths, "Distributed adaptive control of synchronization in complex networks," *IEEE Transactions on Automatic Control*, vol. 57, no. 8, pp. 2153–2158, 2012.

[137] A. Das and F. L. Lewis, "Cooperative adaptive control for synchronization of second-order systems with unknown nonlinearities," *International Journal of Robust and Nonlinear Control*, vol. 21, no. 13, pp. 1509–1524, 2011.

[138] ——, "Distributed adaptive control for synchronization of unknown nonlinear networked systems," *Automatica*, vol. 46, no. 12, pp. 2014–2021, 2010.

[139] S. Chen and J. Lü, "Synchronization of an uncertain unified chaotic system via adaptive control," *Chaos, Solitons & Fractals*, vol. 14, no. 4, pp. 643–647, 2002.

[140] T.-L. Liao and S.-H. Tsai, "Adaptive synchronization of chaotic systems and its application to secure communications," *Chaos, Solitons & Fractals*, vol. 11, no. 9, pp. 1387–1396, 2000.

[141] J. Cao and J. Lu, "Adaptive synchronization of neural networks with or without time-varying delay," *Chaos: An Interdisciplinary Journal of Nonlinear Science*, vol. 16, no. 1, p. 013133, 2006.

[142] H. Zhang, W. Huang, Z. Wang, and T. Chai, "Adaptive synchronization between two different chaotic systems with unknown parameters," *Physics Letters A*, vol. 350, no. 5-6, pp. 363–366, 2006.

[143] S. Baldi and P. Frasca, "Adaptive synchronization of unknown heterogeneous agents: an adaptive virtual model reference approach," *Journal of the Franklin Institute*, vol. 356, no. 2, pp. 935–955, 2019.

[144] W. Yu, G. Chen, and J. Cao, "Adaptive synchronization of uncertain coupled stochastic complex networks," *Asian Journal of Control*, vol. 13, no. 3, pp. 418–429, 2011.

[145] L. Runzi, W. Yinglan, and D. Shucheng, "Combination synchronization of three classic chaotic systems using active backstepping design," *Chaos: An Interdisciplinary Journal of Nonlinear Science*, vol. 21, no. 4, p. 043114, 2011.

[146] B. Kharabian and H. Mirinejad, "Synchronization of rossler chaotic systems via hybrid adaptive backstepping/sliding mode control," *Results in Control and Optimization*, p. 100020, 2021.

[147] G. Xue, F. Lin, and B. Qin, "Adaptive neural network control of chaotic fractional-order permanent magnet synchronous motors using backstepping technique," *Frontiers in Physics*, vol. 8, p. 106, 2020.

[148] R. Luo, Y. Deng, and Y. Xie, "Neural network backstepping controller design for uncertain permanent magnet synchronous motor drive chaotic systems via command filter," *Frontiers in Physics*, vol. 8, p. 182, 2020.

[149] E. D. Dongmo, K. S. Ojo, P. Woafo, and A. N. Njah, "Difference synchronization of identical and nonidentical chaotic and hyperchaotic systems of different orders using active backstepping design," *Journal of Computational and Nonlinear Dynamics*, vol. 13, no. 5, 2018.

[150] Y.-Y. Hou, B.-Y. Liau, and H.-C. Chen, "Synchronization of unified chaotic systems using sliding mode controller," *Mathematical Problems in Engineering*, vol. 2012, 2012.

[151] Z. Rashidnejad and P. Karimaghaee, "Synchronization of a class of uncertain chaotic systems utilizing a new finite-time fractional adaptive sliding mode control," *Chaos, Solitons & Fractals: X*, vol. 5, p. 100042, 2020.

[152] C. Song, S. Fei, J. Cao, and C. Huang, "Robust synchronization of fractional-order uncertain chaotic systems based on output feedback sliding mode control," *Mathematics*, vol. 7, no. 7, p. 599, 2019.

[153] R.-G. Li and H.-N. Wu, "Secure communication on fractional-order chaotic systems via adaptive sliding mode control with teaching–learning–feedback-based optimization," *Nonlinear Dynamics*, vol. 95, no. 2, pp. 1221–1243, 2019.

[154] O. Mofid, M. Momeni, S. Mobayen, and A. Fekih, "A disturbance-observer-based sliding mode control for the robust synchronization of uncertain delayed chaotic systems: application to data security," *IEEE Access*, vol. 9, pp. 16 546–16 555, 2021.

[155] B. Vaseghi, M. A. Pourmina, and S. Mobayen, "Secure communication in wireless sensor networks based on chaos synchronization using adaptive sliding mode control," *Nonlinear Dynamics*, vol. 89, no. 3, pp. 1689–1704, 2017.

[156] Q. Yao, "Synchronization of second-order chaotic systems with uncertainties and disturbances using fixed-time adaptive sliding mode control," *Chaos, Solitons & Fractals*, vol. 142, p. 110372, 2021.

[157] S. Z. Mirrezapour, A. Zare, and M. Hallaji, "A new fractional sliding mode controller based on nonlinear fractional-order proportional integral derivative controller structure to synchronize fractional-order chaotic systems with uncertainty and disturbances," *Journal of Vibration and Control*, p. 1077546320982453, 2021.

[158] A. Ikhlef and N. Mansouri, "Hyperchaotification and synchronization of chaotic systems," *International Journal of Control Science and Engineering*, vol. 2, no. 4, pp. 69–74, 2012.

[159] M. M. Ibrahim, M. A. Kamran, M. M. N. Mannan, I. H. Jung, and S. Kim, "Lag synchronization of coupled time-delayed fitzhugh–nagumo neural networks via feedback control," *Scientific reports*, vol. 11, no. 1, pp. 1–15, 2021.

[160] D. Xu, Y. Liu, and M. Liu, "Finite-time synchronization of multi-coupling stochastic fuzzy neural networks with mixed delays via feedback control," *Fuzzy Sets and Systems*, vol. 411, pp. 85–104, 2021.

[161] Y. Rao, D. Tong, Q. Chen, W. Zhou, and Y. Xu, "Synchronization of chaotic lure systems with time-delays via quantized output feedback control," *Transactions of the Institute of Measurement and Control*, vol. 43, no. 4, pp. 933–944, 2021.

[162] Y. Chen, Y. Xu, and Q. Lin, "The global finite-time synchronization of a class of chaotic systems via the variable-substitution and feedback control," *IMA Journal of Mathematical Control and Information*, vol. 38, no. 2, pp. 594–621, 2021.

[163] D. Lin, X. Chen, G. Yu, Z. Li, and Y. Xia, "Global exponential synchronization via nonlinear feedback control for delayed inertial memristor-based quaternion-valued neural networks with impulses," *Applied Mathematics and Computation*, vol. 401, p. 126093, 2021.

[164] M. R. Naseh and M. Haeri, "Robust synchronization of chaotic systems using active sliding mode control with minimum control effort," *International Journal of Modern Physics B*, vol. 25, no. 17, pp. 2271–2288, 2011.

[165] A. A. Kekha Javan, A. Shoeibi, A. Zare, N. Hosseini Izadi, M. Jafari, R. Alizadehsani, P. Moridian, A. Mosavi, U. R. Acharya, and S. Nahavandi, "Design of adaptive-robust controller for multi-state synchronization of chaotic systems with unknown and time-varying delays and its application in secure communication," *Sensors*, vol. 21, no. 1, p. 254, 2021.

[166] J.-F. Li, H. Jahanshahi, S. Kacar, Y.-M. Chu, J. Gómez-Aguilar, N. D. Alotaibi, and K. H. Alharbi, "On the variable-order fractional memristor oscillator: Data security applications and synchronization using a type-2 fuzzy disturbance observer-based robust control," *Chaos, Solitons & Fractals*, vol. 145, p. 110681, 2021.

[167] J. Dai, Y. Cao, L. Xiao, H. Tan, and L. Jia, "Design and analysis of a noise-suppression zeroing neural network approach for robust synchronization of chaotic systems," *Neurocomputing*, vol. 426, pp. 299–308, 2021.

[168] K. S. T. Alain, "High-order polynomial observer design for robust adaptive synchronization of uncertain fractional-order chaotic systems," *Journal of Control, Automation and Electrical Systems*, vol. 31, no. 5, pp. 1108–1120, 2020.

[169] R. Solomonoff and A. Rapoport, "Connectivity of random nets," *The bulletin of mathematical biophysics*, vol. 13, no. 2, pp. 107–117, 1951.

[170] A. Rapoport, "Contribution to the theory of random and biased nets," in *Social Networks*. Elsevier, 1977, pp. 389–409.

[171] P. Erdős and A. Rényi, "On the evolution of random graphs," *Publ. Math. Inst. Hung. Acad. Sci*, vol. 5, no. 1, pp. 17–60, 1960.

[172] D. J. Watts and S. H. Strogatz, "Collective dynamics of small-worldnetworks," *nature*, vol. 393, no. 6684, p. 440, 1998.

[173] A.-L. Barabási and E. Bonabeau, "Scale-free networks," *Scientific american*, vol. 288, no. 5, pp. 60–69, 2003.

[174] Y. Kuramoto and D. Battogtokh, "Coexistence of coherence and incoherence in nonlocally coupled phase oscillators," *arXiv preprint cond-mat/0210694*, 2002.

[175] A. Zakharova, M. Kapeller, and E. Schöll, "Chimera death: Symmetry breaking in dynamical networks," *Physical review letters*, vol. 112, no. 15, p. 154101, 2014.

[176] P. ERDdS and A. R&WI, "On random graphs i," *Publ. Math. Debrecen*, vol. 6, pp. 290–297, 1959.

[177] L. A. N. Amaral, A. Scala, M. Barthelemy, and H. E. Stanley, "Classes of small-world networks," *Proceedings of the national academy of sciences*, vol. 97, no. 21, pp. 11 149–11 152, 2000.

[178] A.-L. Barabási, "Scale-free networks: a decade and beyond," *science*, vol. 325, no. 5939, pp. 412–413, 2009.

[179] T. Dahms, "Synchronization in delay-coupled laser networks," Ph.D. dissertation, Ph. D. thesis, Technische Universität Berlin, 2011.

[180] U. Ernst, K. Pawelzik, and T. Geisel, "Delay-induced multistable synchronization of biological oscillators," *Physical review E*, vol. 57, no. 2, p. 2150, 1998.

[181] M. Yalcin, "Cellular neural networks, multi-scroll chaos and synchronization: Theory, applications and implementations." 2005.

[182] P. M. Geffert, *Stochastic Non-Excitable Systems with Time Delay: Modulation of Noise Effects by Time-Delayed Feedback*. Springer, 2015.

[183] C. Edwards and S. Spurgeon, "Sliding mode control: theory and applications," *Journal of Circuits, Systems, and Computers*, 1998.

[184] V. Utkin, J. Guldner, and M. Shijun, *Sliding mode control in electromechanical systems*. CRC press, 1999, vol. 34.

[185] H. Du, X. Yu, M. Z. Chen, and S. Li, "Chattering-free discrete-time sliding mode control," *Automatica*, vol. 68, pp. 87–91, 2016.

[186] M.-L. Tseng and M.-S. Chen, "Chattering reduction of sliding mode control by low-pass filtering the control signal," *Asian Journal of control*, vol. 12, no. 3, pp. 392–398, 2010.

[187] R. E. Skelton, T. Iwasaki, and D. E. Grigoriadis, *A unified algebraic approach to control design*. CRC Press, 1997.

[188] N. Siddique, F. ur Rehman, M. Wasif, W. Abbasi, and Q. Khan, "Parameter estimation and synchronization of vaidyanathan hyperjerk hyper-chaotic system via integral sliding mode control," in *2018 AEIT International Annual Conference*. IEEE, 2018, pp. 1–5.

[189] N. Adhikary and C. Mahanta, "Integral backstepping sliding mode control for underactuated systems: Swing-up and stabilization of the cart–pendulum system," *ISA transactions*, vol. 52, no. 6, pp. 870–880, 2013.

[190] D. Qian, S. Tong, and C. Li, "Observer-based leader-following formation control of uncertain multiple agents by integral sliding mode," *Bulletin of the Polish Academy of Sciences Technical Sciences*, vol. 65, no. 1, pp. 35–44, 2017.

[191] M. Sarfraz and F.-u. Rehman, "Feedback stabilization of nonholonomic drift-free systems using adaptive integral sliding mode control," *Arabian Journal for Science and Engineering*, vol. 42, no. 7, pp. 2787–2797, 2017.

[192] M. Van, S. S. Ge, and H. Ren, "Finite time fault tolerant control for robot manipulators using time delay estimation and continuous nonsingular fast terminal sliding mode control," *IEEE transactions on cybernetics*, vol. 47, no. 7, pp. 1681–1693, 2016.

[193] J. Wang, Q. Zong, R. Su, and B. Tian, "Continuous high order sliding mode controller design for a flexible air-breathing hypersonic vehicle," *ISA transactions*, vol. 53, no. 3, pp. 690–698, 2014.

[194] H. O. Ozer, Y. Hacioglu, and N. Yagiz, "High order sliding mode control with estimation for vehicle active suspensions," *Transactions of the Institute of Measurement and Control*, vol. 40, no. 5, pp. 1457–1470, 2018.

[195] S. Ding and S. Li, "Second-order sliding mode controller design subject to mismatched term," *Automatica*, vol. 77, pp. 388–392, 2017.

[196] A. Levant, "Sliding order and sliding accuracy in sliding mode control," *International journal of control*, vol. 58, no. 6, pp. 1247–1263, 1993.

[197] J. A. Moreno and M. Osorio, "Strict lyapunov functions for the super-twisting algorithm," *IEEE transactions on automatic control*, vol. 57, no. 4, pp. 1035–1040, 2012.

[198] L. Derafa, A. Benallegue, and L. Fridman, "Super twisting control algorithm for the attitude tracking of a four rotors uav," *Journal of the Franklin Institute*, vol. 349, no. 2, pp. 685–699, 2012.

[199] T. Gonzalez, J. A. Moreno, and L. Fridman, "Variable gain super-twisting sliding mode control," *IEEE Transactions on automatic control*, vol. 57, no. 8, pp. 2100–2105, 2011.

[200] F. Valenciaga and P. Puleston, "High-order sliding control for a wind energy conversion system based on a permanent magnet synchronous generator," *IEEE transactions on energy conversion*, vol. 23, no. 3, pp. 860–867, 2008.

[201] W. Abbasi, I. Shah, F. ur Rehman, N. Siddque, and U. Rafique, "Smooth super twisting sliding mode control based stabilization for nonholonomic mechanical systems: A firetruck example," in *2018 AEIT International Annual Conference*. IEEE, 2018, pp. 1–5.

[202] Y. B. Shtessel, I. A. Shkolnikov, and M. D. Brown, "An asymptotic second-order smooth sliding mode control," *Asian journal of control*, vol. 5, no. 4, pp. 498–504, 2003.

[203] S. ud Din, F. ur Rehman, and Q. Khan, "Smooth super-twisting sliding mode control for the class of underactuated systems," *PloS one*, vol. 13, no. 10, p. e0203667, 2018.

[204] V. Utkin and J. Shi, "Integral sliding mode in systems operating under uncertainty conditions," in *Decision and Control, 1996., Proceedings of the 35th IEEE Conference on*, vol. 4. IEEE, 1996, pp. 4591–4596.

[205] D. López-Mancilla, G. López-Cahuich, C. Posadas-Castillo, C. Castañeda, J. García-López, J. Vázquez-Gutiérrez, and E. Tlelo-Cuautle, "Synchronization of complex networks of identical and nonidentical chaotic systems via model-matching control," *Plos one*, vol. 14, no. 5, p. e0216349, 2019.

[206] M. Karabacak and H. I. Eskikurt, "Speed and current regulation of a permanent magnet synchronous motor via nonlinear and adaptive backstepping

control," *Mathematical and Computer Modelling*, vol. 53, no. 9-10, pp. 2015–2030, 2011.

[207] M. Zribi, A. Oteafy, and N. Smaoui, "Controlling chaos in the permanent magnet synchronous motor," *Chaos, Solitons & Fractals*, vol. 41, no. 3, pp. 1266–1276, 2009.

[208] Q. Wei, X.-y. Wang, and X.-P. Hu, "Optimal control for permanent magnet synchronous motor," *Journal of Vibration and Control*, vol. 20, no. 8, pp. 1176–1184, 2014.

[209] Q. Wei, X.-Y. Wang, and X.-P. Hu, "Inverse optimal control for permanent magnet synchronous motor," *Journal of vibration and control*, vol. 21, no. 4, pp. 801–807, 2015.

[210] W. Xing-Yuan and Z. Hao, "Backstepping-based lag synchronization of a complex permanent magnet synchronous motor system," *Chinese Physics B*, vol. 22, no. 4, p. 048902, 2013.

[211] F. Zhang, C. Mu, X. Wang, I. Ahmed, and Y. Shu, "Solution bounds of a new complex pmsm system," *Nonlinear Dynamics*, vol. 74, no. 4, pp. 1041–1051, 2013.

[212] A. Dehkordi, A. Gole, and T. Maguire, "Permanent magnet synchronous machine model for real-time simulation," in *International conference on power systems transients*, 2005.

[213] L. O. Chua and L. Yang, "Cellular neural networks: Theory," *IEEE Transactions on circuits and systems*, vol. 35, no. 10, pp. 1257–1272, 1988.

[214] J. M. Zurada, *Introduction to artificial neural systems*. West publishing company St. Paul, 1992, vol. 8.

[215] G. Liñán, S. Espejo, R. Domínguez-Castro, and A. Rodríguez-Vázquez, "Ace4k: an analog i/o 64× 64 visual microprocessor chip with 7-bit analog accuracy," *International Journal of Circuit Theory and Applications*, vol. 30, no. 2-3, pp. 89–116, 2002.

[216] G. Linan, S. Espejo, R. Dominguez-Castro, and A. Rodríguez-Vázquez, "Architectural and basic circuit considerations for a flexible 128× 128 mixed-signal simd vision chip," *Analog Integrated Circuits and Signal Processing*, vol. 33, no. 2, pp. 179–190, 2002.

[217] T. Roska and Á. Rodríguez-Vázquez, "Toward visual microprocessors," *Proceedings of the IEEE*, vol. 90, no. 7, pp. 1244–1257, 2002.

[218] P. Arena, A. Basile, M. Bucolo, and L. Fortuna, "An object oriented segmentation on analog cnn chip," *IEEE Transactions on Circuits and Systems I: Fundamental Theory and Applications*, vol. 50, no. 7, pp. 837–846, 2003.

[219] J. A. Nossek, G. Seiler, T. Roska, and L. O. Chua, "Cellular neural networks: Theory and circuit design," *International Journal of Circuit Theory and Applications*, vol. 20, no. 5, pp. 533–553, 1992.

[220] T. Roska, A. Zarandy, and C. Rekeczky, "Cellular neural networks," in *Nonlinear and Distributed Circuits*. CRC Press, 2005, pp. 7–1.

[221] L. O. Chua and T. Roska, *Cellular neural networks and visual computing: foundations and applications*. Cambridge university press, 2002.

[222] N. Sengor, M. Yalcin, Y. Cakir, M. Ucer, C. Guzelis, F. Pekergin, and O. Morgul, "An application of cellular neural network maximum clique problem," in *1998 Fifth IEEE International Workshop on Cellular Neural Networks and their Applications. Proceedings (Cat. No. 98TH8359)*. IEEE, 1998, pp. 208–211.

[223] S. Duan, X. Hu, Z. Dong, L. Wang, and P. Mazumder, "Memristor-based cellular nonlinear/neural network: design, analysis, and applications," *IEEE transactions on neural networks and learning systems*, vol. 26, no. 6, pp. 1202–1213, 2014.

[224] G. Manganaro, P. Arena, and L. Fortuna, *Cellular neural networks: chaos, complexity and VLSI processing*. Springer Science & Business Media, 2012, vol. 1.

[225] A. Baştürk and E. Günay, "Efficient edge detection in digital images using a cellular neural network optimized by differential evolution algorithm," *Expert Systems with Applications*, vol. 36, no. 2, pp. 2645–2650, 2009.

[226] H.-C. Chen, Y.-C. Hung, C.-K. Chen, T.-L. Liao, and C.-K. Chen, "Image-processing algorithms realized by discrete-time cellular neural networks and their circuit implementations," *Chaos, Solitons & Fractals*, vol. 29, no. 5, pp. 1100–1108, 2006.

[227] H. Li, X. Liao, C. Li, H. Huang, and C. Li, "Edge detection of noisy images based on cellular neural networks," *Communications in Nonlinear Science and Numerical Simulation*, vol. 16, no. 9, pp. 3746–3759, 2011.

[228] X. Hu, G. Feng, S. Duan, and L. Liu, "A memristive multilayer cellular neural network with applications to image processing," *IEEE transactions on neural networks and learning systems*, vol. 28, no. 8, pp. 1889–1901, 2016.

[229] E. Bilotta, P. Pantano, and S. Vena, "Speeding up cellular neural network processing ability by embodying memristors," *IEEE transactions on neural networks and learning systems*, vol. 28, no. 5, pp. 1228–1232, 2016.

[230] K. Ratnavelu, M. Kalpana, P. Balasubramaniam, K. Wong, and P. Raveendran, "Image encryption method based on chaotic fuzzy cellular neural networks," *Signal Processing*, vol. 140, pp. 87–96, 2017.

[231] P. Arena, R. Caponetto, L. Fortuna, and D. Porto, "Bifurcation and chaos in noninteger order cellular neural networks," *International Journal of Bifurcation and Chaos*, vol. 8, no. 07, pp. 1527–1539, 1998.

[232] S. Vaidyathan, "Hybrid chaos synchronization of 3-cells cellular neural network attractors via adaptive control method," *International Journal of PharmTech Research*, vol. 8, no. 8, pp. 61–73, 2015.